6GNTN

D3.5 REPORT ON 3D MULTI LAYERED NTN ARCHITECTURE

Revision: v.1.0

Work package	3
Task	Task 3.1
Due date	31/12/2023
Submission date	28/03/2024
Deliverable lead	DLR
Version	1.0
Authors	Sandro Scalise, Juraj Poliak and Samuele Raffa (DLR) Madivanane Nadarassin, Nicolas Chuberre (TAS-F) Russell Hills (TAS-UK) Ji Lianghai (QCOM) Eduardo Medeiros and Per-Erik Eriksson (ERIS) Fanny Parzysz, Olivier Bouchet and Olivier Le Moult (ORA) Sebastian Euler (ERIF)
Reviewers	Alessandro Vanelli-Coralli, Carla Amatetti (UNIBO) Xavier Artiga (CTTC)
Abstract	This deliverable presents a first iteration of the NTN topology (type of UEs, type of NTN nodes and envisaged communication links), a preliminary network sizing via link budget analysis and some initial considerations of the most promising NTN architecture and functional split options suiting the user cases identified in D2.1.
Keywords	NTN Topology, NTN Nodes, Link Budgets, Functional Architecture, Functional Split

Document Revision History

Version	Date	Description of change	List of contributor(s)
V0.1	29/12/2023	Table of Content	Sandro Scalise (DLR)
V0.2	16/01/2024	First draft Section 2.2.2 and Section 3.4	Juraj Poliak and Samuele Raffa (DLR) Ji Lianghai (QCOM)
V0.3	05/02/2024	Revised Document Structure after GA	Sandro Scalise (DLR)
V0.4	29/02/2024	First stable versions of Chapters 1 and 3	Sandro Scalise (DLR) Russel Hills (TAS-UK) Ji Lianghai (QCOM) Eduardo Medeiros and Per-Erik Eriksson (ERIS)
V0.5	14/03/2024	First stable versions of Chapter 2 CCTC QA review of Chapters 1 and 3 taken into account QCOM revision of Chapter 1 and Chapter 3	Sando Scalise, Juraj Poliak and Samuele Raffa (DLR) Madivanane Nadarassin (TAS-F) Ji Lianghai (QCOM)
V0.6	15/03/2024	ERIS/ERIF revision of Chapter 1 and Chapter 3	Sandro Scalise (DLR) Eduardo Medeiros and Per-Erik Eriksson (ERIS) Sebastian Euler (ERIF)
V0.9	25/03/2024	All comments to the previous version taken into account Revision of Chapter 2 Executive Summary and Conclusion updated	Sandro Scalise and Juraj Poliak (DLR) Madivanane Nadarassin (TAS-F)
V1.0	28/03/2024	UNIBO QA review taken into account Editorial cleaning	Sandro Scalise (DLR) Alessandro Vanelli-Coralli (UniBo)

DISCLAIMER

COPYRIGHT NOTICE

Project co-funded by the European Commission in the Horizon Europe Programme		
Nature of the deliverable:	R	
Dissemination Level		
PU	*Public, fully open, e.g., web (Deliverables flagged as public will be automatically published in CORDIS project's page)*	✓
SEN	*Sensitive, limited under the conditions of the Grant Agreement*	
Classified R-UE/ EU-R	*EU RESTRICTED under the Commission Decision No2015/ 444*	
Classified C-UE/ EU-C	*EU CONFIDENTIAL under the Commission Decision No2015/ 444*	
Classified S-UE/ EU-S	*EU SECRET under the Commission Decision No2015/ 444*	

* R: Document, report (excluding the periodic and final reports)

DEM: Demonstrator, pilot, prototype, plan designs

DEC: Websites, patents filing, press & media actions, videos, etc.

DATA: Data sets, microdata, etc.

DMP: Data management plan

ETHICS: Deliverables related to ethics issues.

SECURITY: Deliverables related to security issues

OTHER: Software, technical diagram, algorithms, models, etc.

EXECUTIVE SUMMARY

The goal of this deliverable is to provide an initial version of the 6G-NTN network topology, carry out an initial sizing of the communication links and perform a preliminary analysis of the required Radio Access Network (RAN), Core network (CN) functions, and the corresponding split options to be implemented in space to meet the 6G-NTN Use Cases (UC) requirements.

It is worth emphasizing that this deliverable supersedes D3.1, so in case of any conflicting information, the content in D3.5 prevails over D3.1.

In this deliverable, firstly, the main elements of the 6G-NTN system have been identified and characterized, namely:

- User Equipment (UEs), classified according to their usage type and to the type and capabilities of the Front Ends they will have.

- Network nodes, further divided into deterministic (satellites) and flexible/opportunistic such as High-Altitude Platforms (HAPs) or special heavy drones.

- Communication links between the above elements, namely service links, inter-node links (INL) or inter-satellite links (ISL), and feeder links.

A three-layer architecture made of HAPs as opportunistic/flexible nodes to locally improve the capacity and/or the coverage, two Low Earth Orbit (LEO) constellations with altitude between 400 km and 800 km for C-band and Q/V band connectivity, and an overlay layer of three GEO satellites have been retained. The focus has been put on the LEO constellations, where 2 possible configurations have been identified, namely:

- A **conventional architecture**, where all LEO satellites of the two envisaged constellations are identical and incudes the payload for service links in C or Q/V-band, optical as well as RF inter-satellite links, and feeder links to connect to the ground stations.

    For this architecture, the analysis based on the 6G-NTN UCs shows that different functional split options might be best suited for different UCs and, therefore, a "one size fits all" approach is not ideal. Therefore, a novel concept called "Adaptive Functional Split" has been proposed. How this flexibility could be implemented and especially the impact on 6G standardization shall be subject of further analysis.

- A **distributed architecture** in which we distinguish between "service satellite" including only the payload for service links in C or Q/V-band and optical inter-satellite links. Clusters of 4 service satellites are connected via the aforementioned optical inter-satellite links to a feeder satellite. "Feeder satellites" are connected to each other and to the HAPs and GEOs via optical and RF inter-satellite links and to the ground via the feeder link, but do not directly connect to any user equipment.

    The rationale behind the distributed architecture is to maximise the service link throughput by using almost all available power and mass in the service satellites. Conversely, feeder satellites should have enough available power and mass to implement all necessary RAN and eventually CN functionalities in space. In the remaining part of the project, the two solutions will be analysed and compared in more details (power/mass budgets as well as cost assessment are ongoing).

    According to this design philosophy, it is proposed to implement a functional split in which only the RU and the low PHY are placed in the service satellites, whereas all the rest of the DU, CU and if necessary CN functionalities are located in the feeder satellites.

Last not least, link budgets and throughput estimations **focusing on LEO satellites** have been performed, leading to the following initial conclusions:

- LEO C-Band satellites can support 15.2 and 4.8 Gbps aggregate throughput in the service uplink and downlink respectively.

- For LEO Q/V-band satellites, the figures are 48 and 18 Gbps respectively. Note that all service link budgets calculations consider so far 5G New Radio (NR) systems. Improvements in the spectral efficiency arising from the work described in D4.1 '*Report on unified and data driven air interface for 6G-NTN*' will be considered in later deliverables.

- The requirements for the optical ISL depend on several points such as the adopted functional split, the routing algorithms, the number of ground stations and the % of traffic which might be processed on board each satellite. Nevertheless, 100 Gbps appears as a reasonable figure in terms of required optical power and telescope size, which is also compatible with ongoing industrial developments.

- The sizing of the feeder link is less critical, since the number of ground stations could be increased and/or their capabilities improved e.g. by using larger antennas.

In general, the link budget and throughput analysis has shown so far that no major bottleneck in the LEO constellation shall be expected. A detailed performance assessment and related optimization will be performed in the follow of the project.

The structure of this deliverables is as follows:

- Chapter 1 presents the main elements of the 6G-NTN network, namely the type of terminals, the type of non-terrestrial nodes and the radio links between them. Here the concepts of conventional vs. distributed LEO constellations are also presented.

- Chapter 2 contains the preliminary link budget analysis for the LEO constellations given the network topology, types of terminals, and considered communication links discussed in the previous chapter. A summary is provided for the sake of convenience in Section 2.4.4 for the reader who is not interested in the many and lengthy link budget calculations and related assumptions.

- Chapter 3 analyses the different functional split options for the LEO constellations.

TABLE OF CONTENTS

LIST OF FIGURES

LIST OF TABLES

ABBREVIATIONS

5G	Fifth Generation	**DN**	Data Network
6G	Sixth Generation	**DP-QPSK**	Dual Polarisation Quaternary Phase Shift Keying
ABFN	Analog Beam-Forming Network	**DBFN**	Digital Beam-Forming Network
ACM	Adaptive Coding and Modulation	**DU**	Distributed Unit
AF	Application Function	**E2E or e2e**	End to end
AMF	Access and Mobility Management Function	**EOC**	Edge of Coverage
AP	Access Point	**ETN**	Edge Transport Node
AR	Augmented Reality	**FDD**	Frequency Division Duplex
ARQ	Automatic Repeat reQuest	**FE or F/E**	Front End
AS	Access Stratum	**FFT**	Fast Fourier Transform
ATN	Aggregation Transport Node	**FiWi**	Fiber Wireless
AUSF	Authentication Server Function	**FL**	Feeder Link
AWGN	Additive White Gaussian Noise	**FSO**	Free Space Optic
BBU	Base Band Unit	**GA**	General Assembly
BER	Bit Error Rate	**GEO**	Geostationary Earth Orbit
CN	Core Network	**gNB**	Next Generation Node B
COC	Center of Coverage	**GS**	Ground Station
COTS	Commercial Off-The-Shelf	**GSO**	Geo-Synchronous Orbit
CP	Control Plane or Cyclic Prefix	**GUI**	Graphical User Interface
CU	Central Unit	**GW**	Gateway

DAC	Digital to Analog Converter	**SINR or SNIR**		Signal to Noise plus Interference Ratio
DL	Downlink	**HAP**		High Altitude Platform
EIRP	Equivalent Isotropic Radiated Power	**DRA**		Direct Radiating Array
HARQ	Hybrid Automatic Repeat reQuest	**MAC**		Medium Access Control
HIBS	HAP station as IMT Base Station	**MEO**		Medium Earth Orbit
HMD	Head Mounted Display	**MIMO**		Multiple-Input Multiple-Output
HO	Handover	**NAS**		Non-Access Stratum
IEEE	Institute of Electrical and Electronics Engineers	**NF**		Noise Figure or Network Function
IFFT	Inverse Fast Fourier Transform	**NGSO**		Non-Geo-Synchronous Orbit
IMT	International Mobile Telecommunications	**NR**		New Radio
INL	Inter-Node Link	**NTN**		Non-Terrestrial Networks
IoT	Internet of Things	**OADM**		Optical Add/Drop Multiplexer
IP	Internet Protocol	**OCC**		Optical Camera Communication
IRIS[2]	Infrastructure for Resilience, Interconnectivity and Security by Satellite	**OFDM**		Orthogonal Frequency Division Multiplexing
ISL	Inter-Satellite Link	**OISL**		Optical ISL
ITU	International Telecommunication Union	**OLT**		Optical Line Terminal
LAN	Local Area Network	**ONU**		Optical Network Unit
LCT	Laser Communication Terminal	**OWC**		Optical Wireless Communication
LED	Light-Emitting Diode	**PCB**		Printed Circuit Board
LEO	Low Earth Orbit	**PCF**		Policy Control Function
LiFi	Light Fidelity	**PDCP**		Packet Data Convergence Protocol

LoS	Line of Sight	**PDU**	Protocol Data Unit
Lx	Layer x of the OSI Protocol Stack (x = 1...7)	**PHY**	Physical Layer
MCS	Modulation and Coding Scheme	**LDPC**	Low Density Parity Check
PoC	Proof of Concept	**TDM**	Time Division Multiplexing
PON	Passive Optical Network	**TDMA**	Time Division Multiple Access
POS	Passive Optical Splitter	**TN**	Terrestrial Network
PPDR	Public Protection and Disaster Relief	**TX**	Transmission / Transmitter
PRB	Physical Resource Block	**U2U**	User Equipment to User Equipment
PSK	Phase Shift Keying	**UC**	Use Case
QAM	Quadrature Amplitude Modulation	**IAB**	Integrated Access and Backahul
QPSK	Quaternary Phase Shift Keying	**UDM**	Unified Data Management
RAN	Radio Access Network	**UE**	User Equipment
RF	Radio Frequency	**UHD**	Ultra-High Definition
RLC	Radio Link Control	**UL**	Uplink
RNC	Radio Network Controller	**UP**	User Plane
RNTI	Radio Network Temporary Identifier	**UPF**	User Plan Function
RRC	Radio Resource Control	**Uu**	Interface between UE and RAN
RTT	Round Trip Time	**CPA**	Coarse Pointing Assembly
RU	Radio Unit	**VLEO**	Very Lowe Earth Orbit
RX	Reception / Receiver	**VR**	Virtual Reality
SaaS	Software as a Service	**WDM**	Wavelength Division Multiplexer
SCS	Sub-Carrier Spacing	**BW**	Bandwidth
SDA	Space Development Agency	**FOV**	Field of View

SDAP	Service Data Adaptation Protocol	**WLAN**	Wireless Local Area Network
SFP	Small Factor Pluggable	**W-PON**	Wireless Passive Optical Network
SL	Service Link or Side Link	**Xn**	Network interface between NG-RAN nodes
SMF	Session Management Function	**ZED**	Zero Energy Device
SNR	Signal to Noise Ratio	**MTU**	Maximum Transfer Unit
SSPA	Solid State Power Amplifier	**TWTA**	Travelling Wave Tube Amplifier
TCP	Transmission Control Protocol	**AFS**	Adaptive Functional Split
TDD	Time Division Duplex	**ADC**	Analog to Digital Converter
VSAT	Very Small Aperture Terminal		

1   6G-NTN NETWORK TOPOLOGY

Deliverable D3.5 is the second version of the '*Report on 3D multi layered NTN architecture'*. Two further versions of this deliverable are planned in the course of the project at the end of the second and third project years respectively.

The architecture presented in this document is the outcome of an intense design activity, in which many different options have been analysed in terms of terminal and payload capabilities, as well as potential orbits to be considered, following a holistic approach and leading to the configuration presented in this chapter, which foresees two different options as far as the LEO constellation is concerned. The results from Tasks 2.1, 2.2, 2.3, reported in the corresponding deliverables, have also been taken into consideration.

The proposed architecture will be further analyzed and, if necessary, refined in the next issues of this deliverable throughout the project lifetime, taking also into account the progress of the ongoing initiative IRIS[2] (Infrastructure for Resilience, Interconnectivity and Security by Satellite) of the European Commission, which at the time of writing is still at the stage of best and final offer submission. Furthermore, preliminary inputs from Task 2.5 on the availability of frequency bands have been considered, as well as input from other ongoing WP3 tasks regarding UE antennas, payload dimensioning, and LEO constellation sizing.

As already presented in the project proposal, the underpinning concept of 6G-NTN is a 3D multi-layered architecture illustrated in Figure 1. The "3D" characteristic stems from the full integration of the non-terrestrial component with the terrestrial one, while the "multi-layered" feature is related to the integration of different layers consisting of communication nodes, i.e., satellites or HAPs flying at different and multiple altitudes. The flying nodes are interconnected by inter-node links (INL). We identify as horizontal links connections among nodes of the same constellation, e.g., LEO to LEO, and vertical links connections among nodes of different constellations, e.g., LEO to GEO. The differentiation between horizontal and vertical links plays a significant role in the definition of the architecture interfaces as the characteristics (e.g., delay, availability, etc) of the links change significantly.
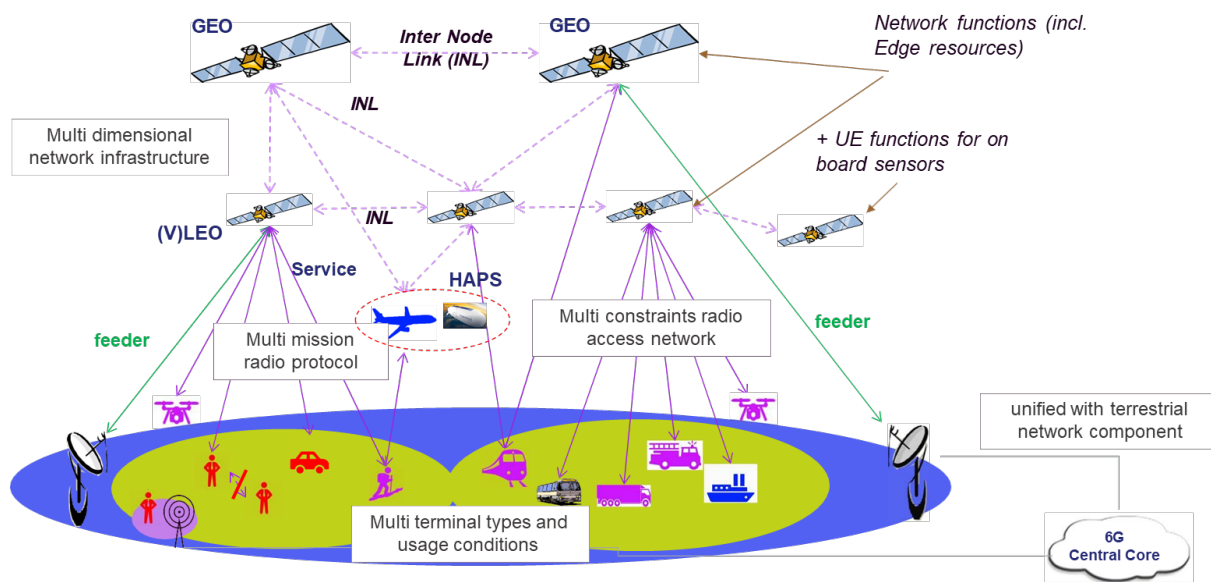
FIGURE 1: 6G-NTN 3D NETWORK CONCEPT.

The rest of this chapter presents the main elements of the 6G-NTN network, namely the type of terminals, here after referred to as User Equipment (UE), the type of non-terrestrial nodes (HAPs and satellites at different altitudes), and the radio links between them.

1.1 TYPE OF USER EQUIPMENT

The following set of UEs was defined in D2.2 [5], Section 4:

- Handheld
  - Consumer
  - Professional
- Drone-based
  - Light (and dismountable)
    - o Max size 10x10x2 cm including antenna
    - o Max weight 200-300 g
    - o Max power consumption 10 mW / 1 W in idle / connected mode.
  - Heavy
    - o Max size 20x20 cm including antenna
    - o Max weight < 1 kg
    - o Max power consumption 100 mW / 10 W in ideal idle / connected mode.
- Mounted UEs
  - Automotive
  - Airborne (planes, helicopters, HAPs)
  - Vessel, train or bus-mounted

Furthermore, each type of terminal will typically have many Radio Frequency Front-Ends (RF FEs) to operate in different frequency bands, including Terrestrial Network (TN) and Non-Terrestrial Network (NTN) bands, and with different characteristics in terms of Noise Figure (NF), transmit power, and maximum antenna gain. The types of RF FEs considered so far are presented in Table 1. Insights on antenna design for UEs will be reported in D3.2 '*Report on terminals*' and might influence the final figures to be considered.

TABLE 1: RF-FE TAXONOMY FOR 6G-NTN UE

Frequency Band	Remarks	NF [dB]	Max TX Power [dBm]	Max Antenna Gain [dBi]	RF-FE Acronym
Non-Terrestrial Frequency Bands					
C (see also Figure 3)	Non-directive (hemispherical) antenna	9	23	-3	C_NTN_1
		7	26	-3	C_NTN_2
		7	26	0	C_NTN_3
Q/V (see also Figure 3)	Directive antenna	5	34	28	QV_NTN_1
		5	37	32	QV_NTN_2
Terrestrial Cellular Bands					

< 3 GHz and permitted for HIBS	The gNB in this case is on board a HAP				HIBS_TN_1
< 3 GHz and permitted for aerial use		9	23	-3	AERO_TN_1
Permitted for general use					CELL_TN_1

Accordingly, the mapping between the types of UEs and the available RF FEs has been defined and reported in Table 2. Please note that aerial platforms such as HAPs could have a double role in the 6G-NTN network since they can act both as UEs as well as Non-Terrestrial Nodes. Different class of aerial nodes are envisaged and will be detailed furthermore in D3.3 '*Report on software defined payload and its scalability*'.

TABLE 2: MAPPING BETWEEN UE TYPES AND RF FE

UE Type	Available RF FEs			
	Non-Terrestrial		Terrestrial	
	Non-Directive	Directive	gNB in HAP	gNB on ground
Handheld Consumer	C_NTN_1		HIBS_TN_1	CELL_TN_1
Handheld Professional	C_NTN_2		HIBS_TN_1	CELL_TN_1
Automotive	C_NTN_3	QV_NTN_1	HIBS_TN_1	CELL_TN_1
Light Drone	C_NTN_1 or C_NTN_2	QV_NTN_1	HIBS_TN_1	AERO_TN_1
Heavy Drone	C_NTN_3	QV_NTN_2	HIBS_TN_1	
Airborne		QV_NTN_1 or QV_NTN_2		
Vessel / Train / Bus	C_NTN_3	QV_NTN_2	HIBS_TN_1	CELL_TN_1

1.2 TYPE OF NON-TERRESTRIAL NODES

Non-Terrestrial or flying nodes are basically HAPs or special heavy drones as well as satellites in different orbits. Satellites can be either placed in a geosynchronous orbit (GSO), meaning they rotate around the Earth with a period equal to one sidereal day (and with an average angular speed equal to that of the Earth), or in lower orbits with a period lower than one sidereal day, i.e., with an angular speed faster than that of the Earth.

The 6G-NTN topology considers two types of non-terrestrial nodes, namely deterministic nodes with a fixed and predictable orbit (both GSO and NGSO) and flexible nodes, namely HAPs or special heavy drones, which might or might not be present or not at different points in time and at different locations to extend coverage or enhance the network capacity. The latter are supposed to be deployed "opportunistically" depending on specific needs but are not meant to be a permanent infrastructure with global coverage.

The detailed payload and antenna design for non-terrestrial nodes will be carried out in D3.3 '*Report on software defined payload and its scalability*'.

1.2.1 Deterministic Non-Terrestrial Nodes

Deterministic nodes are basically satellites at different orbits. The 3D 6G-NTN network foresees different layers, namely:

➲ **An upper GSO layer made of 3 satellites in geostationary orbits (GEO)**. This is a special type of circular geosynchronous orbit with 0° inclination and an altitude of approximately. 35.786 km. GEO satellites fly onfly in an equatorial plane with a constant angular speed equal to that of the Earth. Thus, for a user located on the Earth surface they appear as fixed in the sky, which means no tracking antenna capabilities are needed for fixed terminals. Three such satellites can provide almost global coverage, excluding polar regions from where the satellites are are not visible (i.e. close to or below the horizon). The actual coverage is determined by the minimum elevation, i.e., the minimum angle with which the satellite is visible over the local horizon of a user located on the Earth surface, as shown in Figure 2. Inclined GSO orbits are not further considered since one of the main advantages of GEO, namely no need for tracking antennas, is lost in such case, whereas link budgets remain tight, and delay stays high.

The GSO role is expected to have mostly a complementary role with respect to NGSO, focusing on:

- broadcast & multicast mission especially targeting fixed ground stations located e.g. at the edge of coverage, which is however not the primary focus of the 6G-NTN project

- broadband access that is less performant in terms of data rate and delay compared to the one of NGSO and shall therefore be considered either as backup or as complementary capacity in case of hotspots (assuming dual steer/connectivity between GSO and NGSO links)

- non-delay sensitive traffic offloading from the NGSO network thanks for to the presence of inter-satellite links between NGSO and GSO layers.

- providing essential control and management planes functionalities to the NGSO fleet in case of unavailability of the feeder links / ground segment. This should allow resilient and autonomous operation (eventually with reduced capabilities) of the network even in presence of major disruption of the ground infrastructure.

- Ensure resilience and links recovery in case e.g. of failure of the lower constellations.

Subsequent issues of this deliverables will address the interworking between the GSO layer and the NGSO one as well as end-to-end and protocol integration aspects with the TN. Nevertheless, no detailed GSO payload design will be carried out in Task 3.3, where the focus will remain on the design of the NGSO constellation.

(c)2020 Satellite Signals www.satsig.net/maps/geostationary-satellite-elevation-map.htm
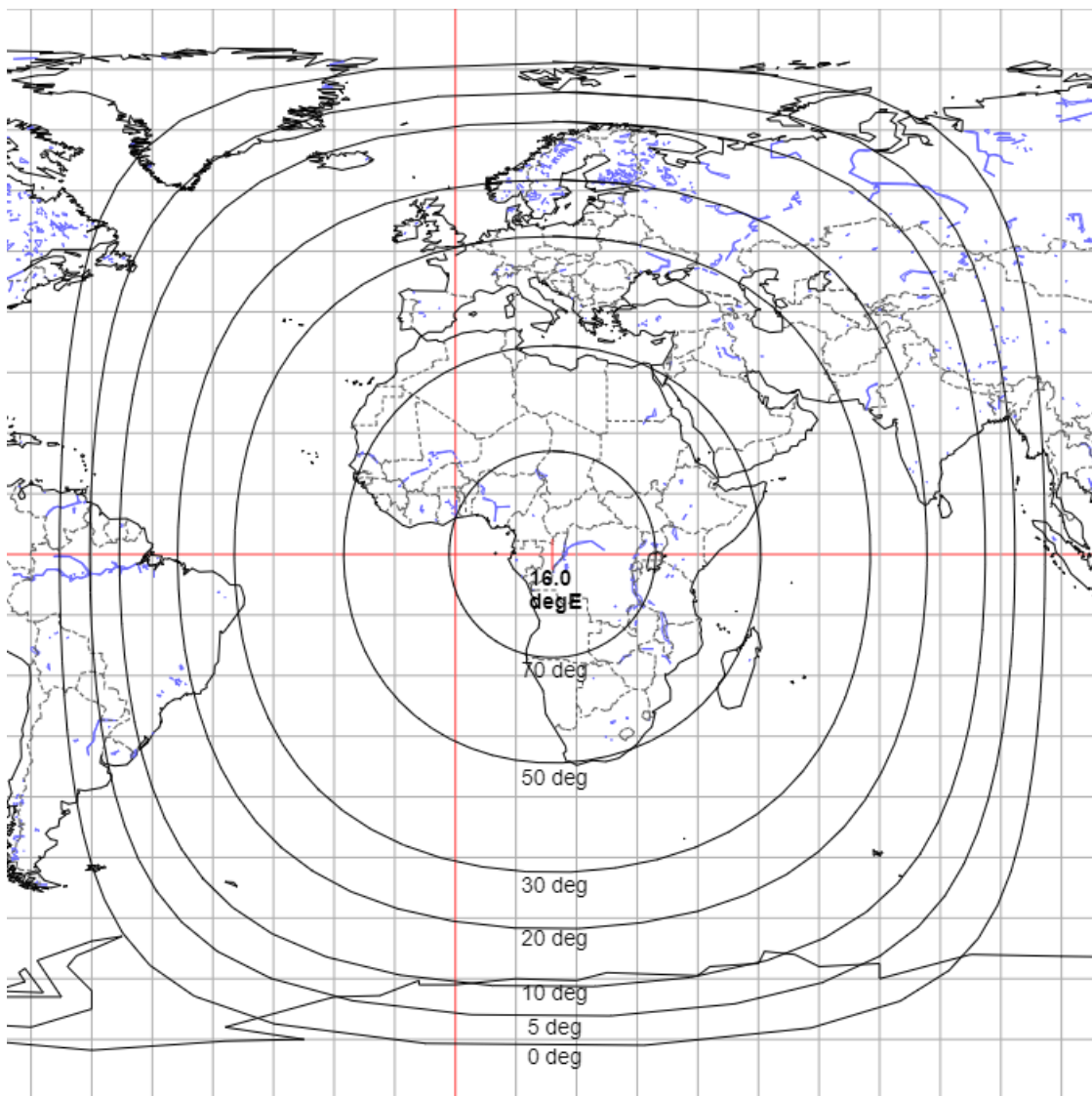
FIGURE 2: EXEMPLARY COVERAGE OF A GEO SATELLITE FOR DIFFERENT MINIMUM ELEVATION ANGLES.

➲ **A lower layer made on NGSO satellites**, where LEO encompasses Earth-centered circular orbits with an altitude of 2.000 km or less, thus rotating around the Earth much faster than the Earth rotates around its axis. The main role of NGSO satellites is to provide broadband access to handhelds and to VSAT-like UEs (see also Table 2). This has been so far the focus of WP 3 and more specifically of Task 3.1. A summary of the initial constellation sizing which is still ongoing in Tasks 3.3 and 3.4 at the time of writing is provided for the sake of completeness in Section 1.4.

➲ Medium Earth Orbit (MEO) satellites, flying typically at an altitude around 10.000 km, will not be initially considered in order to limit the number of possible architectural options to be analyzed. At a later stage in the project, it will be assessed whether the introduction of one additional layer between GSO and LEO could bring benefits justifying the remarkable increase in cost and especially complexity. Alternatively, a MEO layer could be considered as alternative to the GSO one to increase synergies with the expected solution for the IRIS[2] (Infrastructure for Resilience, Interconnectivity and Security by Satellite) system of the European Commission.

1.2.2 Flexible NTN Nodes

Flexible nodes are basically HAPs and/or special heavy drones which might be temporarily deployed to provide additional capacity to specific areas. Remarkable examples are, for instance, disaster areas where no terrestrial infrastructure is available or areas where a sudden capacity increase is envisaged for a limited period of time, such as e.g., large concerts or sport events both within cities but also in remote locations. Note that **it is not foreseen to have a permanent network of such nodes, rather they will be opportunistically deployed when and where needed**.

1.3 OVERVIEW OF COMMUNICATION LINKS

The following type of communication links are considered in the 6G-NTN architecture:

- **Feeder Links (FLs)** connecting deterministic or flexible nodes to a Ground Station (GS) / Gateway (GW) on ground. GSs typically have large antennas and less stringent power limitations compared to UEs, therefore FLs have typically a very high availability in the range of 99.5% thanks to a number of advanced fading countermeasures such as power control, Adaptive Coding and Modulation (ACM), predictive handover, etc. Still, the available data rate might vary in case of deep fading events caused e.g., by rain. FLs might be both Downlinks (DLs) – Space to Earth and Uplinks (ULs) – Earth to Space.

- **Inter-Node Links (INLs)** connecting non-terrestrial nodes. When both nodes are satellites, the term **Inter-Satellite Links (ISLs)** can be also used. When the link is realized using optical communication technologies, it will be named **Optical Inter-Satellite Link (OSIL)**. Otherwise, it is implicitly assumed that conventional RF technologies are used.

- **Service Links (SLs)** connecting deterministic or flexible nodes to a UE on ground or mounted in a drone, plane or HAP (see Table 2). Also, SLs might be both Downlinks (DLs) – Space to Earth and Uplinks (ULs) – Earth to Space.

An overview of the communication links of the 6G-NTN network is shown in Figure 3, including also the relevant frequency bands identified in D2.5 *'Report on Regulatory requirements'*.
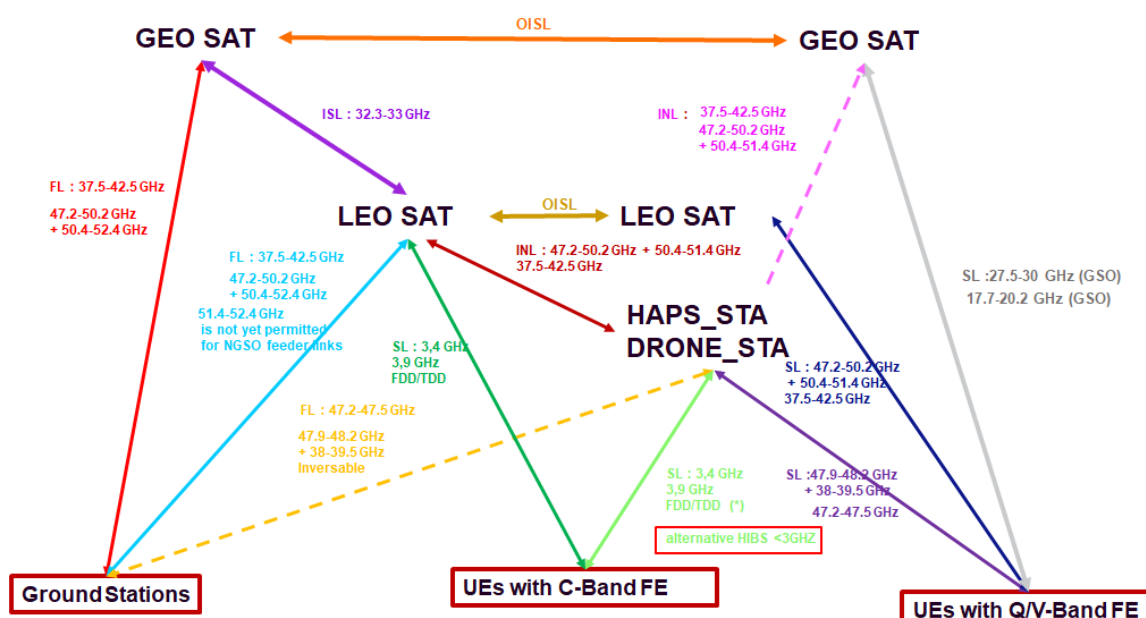
FIGURE 3: OVERVIEW OF RELEVANT COMMUNICATION LINKS AND FREQUENCY BANDS.SERVICE LINKS

HAPs and (heavy) drones are marked with the "_STA" to denote they are meant as flying base stations and not as UEs.

Service links will be either in C-band with hemispherical / omnidirectional antennas or in Q/V band with highly directive antennas, as also reported in Table 1 and Table 2. For C-band links, FDD is assumed as baseline, but the feasibility of TDD will be investigated in WP4. For the Q/V-band links, FDD is the most logical approach, since the uplink and downlink are in separated frequency bands. Given the risk of not having C-band availability for HAPs due to regulatory issues, connectivity in lower frequency bands < 3 GHz is retained as backup option.

It is worth emphasizing that Figure 3 also shows for the sake of completeness service links in Ka-band between UEs and GEO satellites. These are meant for the aforementioned legacy broadcast & multicast mission targeting fixed ground stations located e.g. at the edge of coverage, which will be assumed to be part of the 6G-NTN system but not further analysed in the project and assumed to be largely based on state-of-the-art / available equipment and technologies. This mission will however affect the sizing of the GEO satellites in terms of mass and power budget.

On the contrary, backup complementary connectivity via GEO satellites in Q/V-band, although not shown in Figure 3, is also supposed to be part of the final 6G-NTN network and will be further investigated in the rest of the project.

1.3.1 Inter-Node Links

Five different types of INLs are potentially envisaged, namely:

1. Links between HAPs and LEO satellites, to be realized with optical technology. Since HAPs are mostly envisaged as standalone flexible network nodes not necessarily in visibility of a ground station, all HAPs shall be able to connect to the LEO constellation.

2. Links between HAPs and GEOs, to be realized also with optical technology. Due to the very large distance, their technical feasibility and meaningfulness given the achievable data rate shall be subject of future trade-off analysis.

3. Links between LEOs and GEOs, to be realized in Ka-band using state-of-the-art / available equipment and available frequency allocation. Whether all LEO satellites will be equipped with ISL capabilities towards GEO or only a subset, it's subject of further trade-off analysis in the rest of the project. Eventually, optical technology might be used instead of the legacy RF solution if the data rate turns out to be not sufficient.

4. Links between LEO satellites, to be realized with optical technology.

5. Links between GEO satellites, to be realized also with optical technology. Due to the very large distance (close to 90.000 km assuming 3 GEOs equally spaced), their technical feasibility and meaningfulness given the achievable data rate shall be subject of future trade-off analysis.

In summary**: LEO-GEO in Ka-band, LEO-LEO with optical technology and HAP-LEO with optical technology are retained as baseline, GEO-GEO and HAP-GEO both with optical technology shall be subject of further analysis.**

1.3.2 Feeder Links

All feeder links are supposed to be in Q/V-band. Although other frequencies may be considered, the Q/V band is the preferred choice, given the bandwidth available and the crowding of the spectrum. At present, they are mainly used as feeder links for GEO missions. Moreover, the beams are directive so that interference management with the other system will be less constraining to manage.

HAPs will have feeder links only if they are in visibility of a ground station. The sizing of the ground network in terms of number of placements of the ground stations will be however driven by the need of the LEO constellation(s), so HAPs connectivity to a ground station will be merely opportunistic. In other words, no dedicated ground stations for HAPs will be considered, but HAPs can use any LEO ground station which is in visibility. Otherwise, they need to relay the traffic via the LEO network.

1.4 SUMMARY OF ONGOING LEO CONSTELLATION DESIGN

To achieve global coverage a certain number of satellites is required, typically grouped into a number of orbital planes with the same inclination but intersecting the equatorial plane at different positions. From the point of view of a user located on the Earth surface, satellites are moving (thus a non-negligible Doppler effect is present, although mostly deterministic) and frequent satellite handovers take place whenever a satellite is about to set and a new one is raising on the horizon. The design of a NGSO constellation is a complex exercise subject to many tradeoffs between many parameters such as altitude, number and inclination of the orbital planes, overall number and size of satellites, coverage on ground, and, last but not least, also the number of required ground stations, which will be reported in D3.3 '*Report on Software defined payload and its scalability*' and D3.4 '*Report on VLEO space segment*' and their updated versions. For the time being, the working assumption is to consider LEO constellations with an **altitude of 600 km**.

Two different architectural design are being addressed in detail in Task 3.4 and will be also considered for the functional architecture in Chapter 3, hereafter referred to as **conventional and distributed architectures** respectively.

1.4.1 Conventional Architecture

In the **conventional architecture** as the one sketched in Figure 1, **all LEO satellites of the constellation are identical** and shall include:

- service links with multibeam coverage

- 4 bidirectional laser terminals for the ISL, connecting the two adjacent satellites in the same orbital plane and the 2 nearest satellites in the two adjacent orbital planes (standard configuration). Please note that an additional laser terminal might be needed to connect to HAPs as detailed in section 1.3 and for redundancy purposes.

- 2 feeder links as a minimum (for redundancy and/or seamless ground station handover)

- a Ka-band payload for the ISL to the GEO satellites, which might be eventually be present only in some LEO satellites (not considered in this study)

- all required RAN and eventually Core Network functionalities

A preliminary constellation sizing is shown in Table 3 showing the required number of satellites and orbital planes to have single or double satellite visibility for two different minimum elevation angles. The selected reference constellation is identified in bold. At the time of writing the working assumption is to have 2 of such constellations in nearly polar orbit, one for C-band connectivity and another one for Q/V-band connectivity. The total number of LEO satellites for the 6G-NTN network is therefore twice the one reported in Table 3.

TABLE 3: EXAMPLE OF LEO CONSTELLATION SIZING AT 600KM ALTITUDE.

Minimum number of Visible Satellites	Minimum User Elevation 30°			Minimum User Elevation 45°		
	Satellites per plane	Number of planes	Total number of satellites	Satellites per plane	Number of planes	Total number of satellites
1 (with minimum 10s handover duration)	28	17	476	**47**	**27**	**1269**
2	57	16	912	89	26	2314

1.4.2 Distributed Architecture

In the **distributed architecture**, the **satellites of the constellation are not all identical**. Specifically, we distinguish between **service satellites** and **feeder satellites**.

As shown in Figure 4, service satellites are mainly devoted to provide connectivity to the UEs but they don't have feeder links. Most of the available payload mass and power is thus devoted to maximize the service up- and downlink capacity, so these satellites will connect via ISLs to the feeder satellites but will have neither feeder links nor ISLs among them.

On the other hand, feeder satellites do not have direct link to the UEs, but they implement the full transport network in space using ISLs and feeder links and providing additional processing capabilities in space to implement RAN and if needed Core Network and Edge Computing functionalities.

Although from Figure 4 one might infer that service satellites are flying lower than feeder satellites, this is only a logical representation. As a matter of fact, the current ongoing constellation design in Task 3.4 foresees the same altitude for all satellites and the following parameters (further details in D3.4 '*Report on VLEO space segment*'):

- 600km altitude
- 45° min user elevation
- Near-polar inclination (~87°) in order to provide global coverage
- Minimum of 1 satellite always visible
- Minimum 10 s of overlap between 2 satellites for a user on ground to allow handover from one satellite to another
- Each feeder satellite nominally serves 4 service satellites in each of the C and Q/V constellations
- 1269 service satellites total (27 planes, 47 satellites per plane)
- 336 feeder satellites total (14 planes, 24 satellites per plane)

A polar orbit allows global coverage with a minimum number of satellites, although this does create excess capacity over the poles where the orbital planes cross. Reducing the inclination by a few degrees maintains global coverage with a minimal change in the number of satellites,

while significantly increasing the separation between satellites at the poles to simplify management of the constellation with regards to potential collisions.

The number of feeder satellites is larger than 318 (~1269/4) as might be expected. This is because each feeder satellite serves two service satellites in two adjacent planes – as there are an odd number of service satellites per plane, there will be one feeder satellite in each plane that only serves two service satellite. Also, there is an odd number of service satellite planes, meaning there will be plane of feeder satellites that only serve one service plane, and therefore only serve two service satellites (assuming the relative geometry of service and feeder satellites is kept constant). As not all feeder satellites are fully utilised, slightly more satellites are required.

The overall resulting LEO constellation is sketched in Figure 5, where red stars are service satellites, green stars are feeder satellites, magenta links are the ISL between service and feeder satellites and cyan links are the ISL between feeder satellites.

Service satellites will implement the service links in either C or Q/V-band with multibeam coverage and shall have at least two bidirectional laser terminals, one to connect to the nearest feeder satellite plus a second one for hot redundancy. The constellation configuration described above provides global coverage with a single satellite visible at all times, but does not consider the frequency band. To provide both C-band and Q/V-band global coverage, and assuming service satellites can provide only C- or Q/V-band (not both due to size constraints), it is assumed that there effectively will be two independent service constellations of 1269 satellites each – one for C-band and one for Q/V-band. These will each provide global coverage in their respective bands, and as it is currently assumed they will both have the same configuration (altitude, inclination etc), then both constellations can co-orbit in a 'fixed' formation (ignoring the periodic variation in one orbit). This fixed formation allows both the C- and Q/V-band constellations to be served by the same feeder constellation, with each feeder satellite serving 4 satellites from each of the C- and Q/V-band constellations.

Feeder satellites will implement up to 4 feeder links (for redundancy and/or seamless ground station handover) and up to 13-14 bidirectional laser terminals:

- 4 to connect to the C-band service satellites
- 4 to connect to the Q/V-band service satellites
- 4 to connect to other feeder satellites (2 in plane and 2 inter-plane)
- 1-2 additional laser terminals might be needed to connect to HAPs as detailed in section 1.3 and for redundancy purposes.

Moreover, a Ka-band payload for the ISL link to the GEO satellites shall be considered, which might be eventually be present only in a reduced number of feeder satellites

The advantages of this architectural solution are manifold, namely:

- **it allows higher service link throughput,** since no resources have to be provisioned for feeder link and ISL and all available power can be devoted to the service link.
- **it offers better scalability and flexibility**, since the feeder satellites are totally agnostic regarding which spectrum and bandwidth is used for the service links. As long as the ISL and feeder links capacity does not become the bottleneck, new service satellites (more powerful and/or operating in a different frequency bands) could be progressively and seamlessly added.

Basically, through the distributed architecture the service links are completely decoupled from the transport network in space. Although this concept is not new, so far it has been considered mostly at academic level. As a matter of fact, all existing constellations including e.g. Starlink

(if we exclude the fact that different generations are coexisting in space) adopts a conventional design where all satellites are (functionally) identical. **For the first time in the 6G-NTN projects, a detailed constellation, payload and functional architecture design for this distributed solution will be proposed.**

On the other hand, this solution requires ca 15% more satellites and additional payload design and accommodation. This will be analyzed in the cost assessment to be performed in the remaining part of the project.
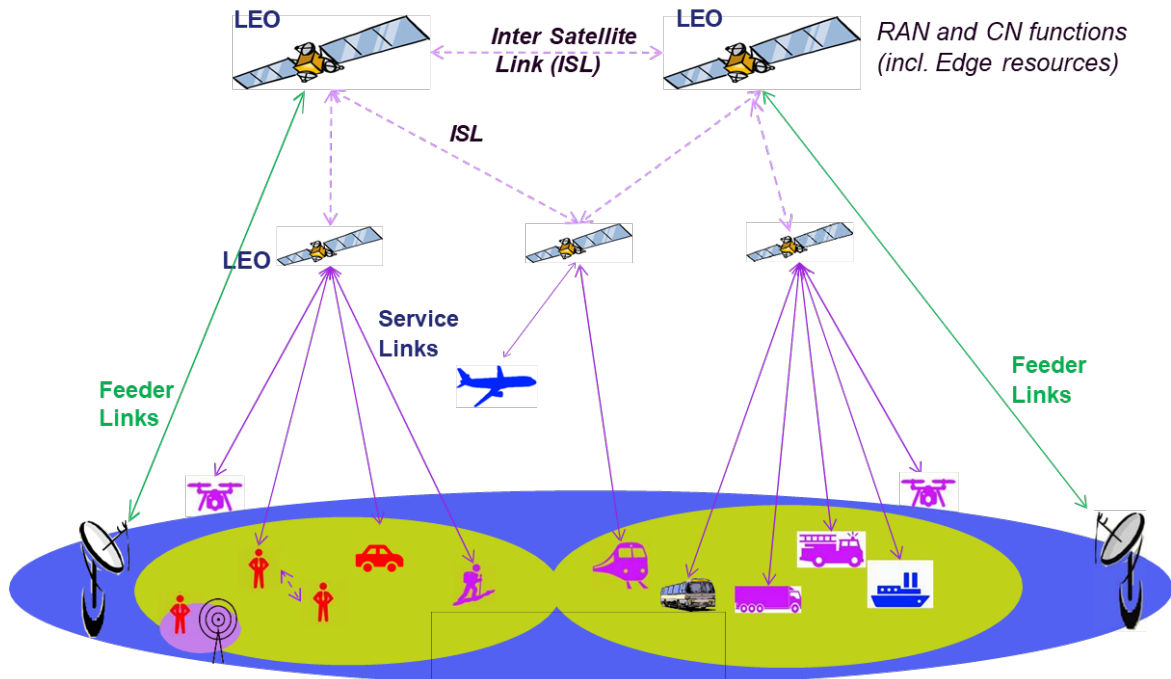
FIGURE 4: LEO CONSTELLATION (DISTRIBUTED ARCHITECTURE).
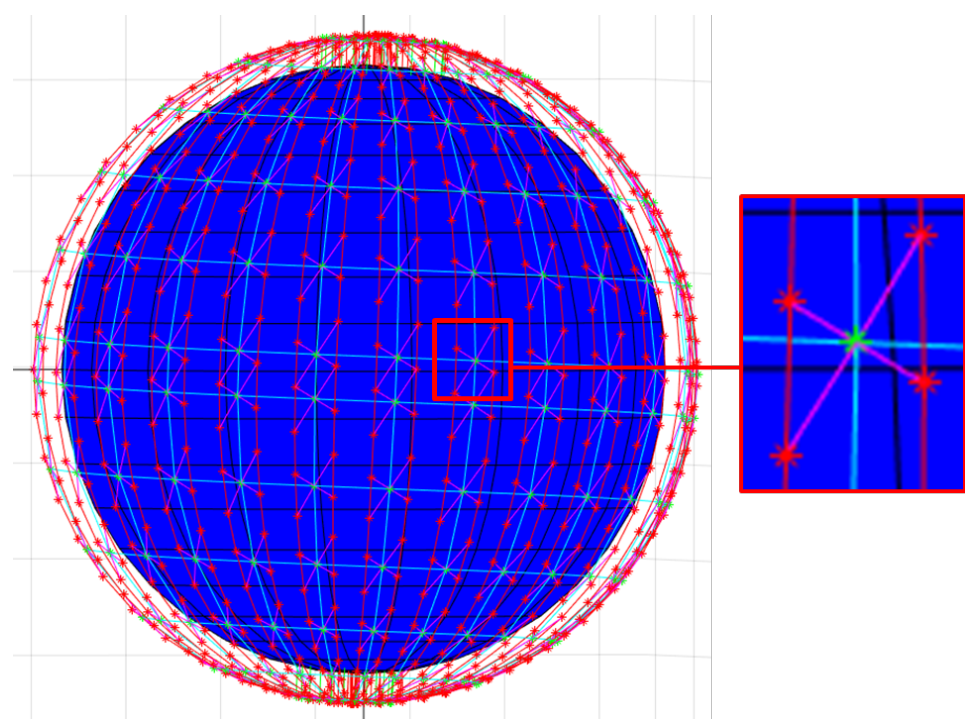
FIGURE 5: SERVICE AND FEEDER SATELLITES CONSTELLATION.

2   INITIAL 6G-NTN NETWORK SIZING

This chapter contains the preliminary link budget analysis for the LEO constellation given the network topology, types of terminals, and considered communication links discussed in the previous chapter. **A summary is provided for the sake of convenience in Section 2.4.4 for the reader who is not interested in the many and lengthy link budget calculations and related assumptions.**

2.1   SERVICE LINK BUDGETS

This section reports the achievable rate for both C-band and Q/V-band assuming different fading depths, elevation angles and 5G NR. This will be updated in the next issues taking into account the results of WP4 on waveform improvements.

For C-band, the UE rate is in the order of hundreds of kbps, whereas for Q/V-band, UE rate in the order of 1-10 Mbps can be achieved.

The objective of this chapter is to give first the hypothesis taken at this stage on the design of the constellation C and Q/V for first the estimation of the performance of the system in term of throughput (global capacity by satellite). The detailed trade-off and the definition of the solution will be given in D3.3 'Report on Software defined payload and its scalability'. These results remain preliminary and are based on also preliminary hypothesis. The purpose is to evaluate the maximum throughput that each satellite will have to handle. Il will allow to define/design the interlinks (OISL, ISL …etc) and also the evaluation of the processing capacity on board. These parameters could evolve with the reflexion during this study taking into account the feedback on each part of the system (link and payloads). This feedback is needed to adjust the sizing of payloads and network elements to ensure that, in the long term, all elements are sized with the same or at least shared constraints. It's a tricky task, since all the elements are interrelated and interdependent, which means that initial choices have to be somewhat realistic. Realistic, with a vision of the technologies available and sufficiently mature by 2030. Technology in the space domain is difficult to anticipate, given that the market is still uncertain, and is therefore essentially driven by huge terrestrial technologies.

2.1.1   C-Band

2.1.1.1   Coverage

The constellation shall cover 98% of the earth surface (sea and ground) and satellite will be placed in a polar orbit in order to achieve global coverage.

The constellation can be optimized with a wide tilt angle to minimize the number of satellites. This implies some restrictions and, above all, a reduction in pole coverage. A polar constellation with a slight inclination to ensure maximum coverage have been selected even of a number of satellites coverage superpose at the poles. This disadvantageous feature will be used to mute off a number of payloads in order to ensure a efficient thermal control.

A trade-off performed on several parameters allow to define a best compromise solution, details will be given in D3.3 'Report on Software defined payload and its scalability'.

Each satellite ensures a coverage of minimum elevation angle of 45° which represent 499 cells of 45 km arranged in a hexagonal lattice as shown in Figure 6.

45 km
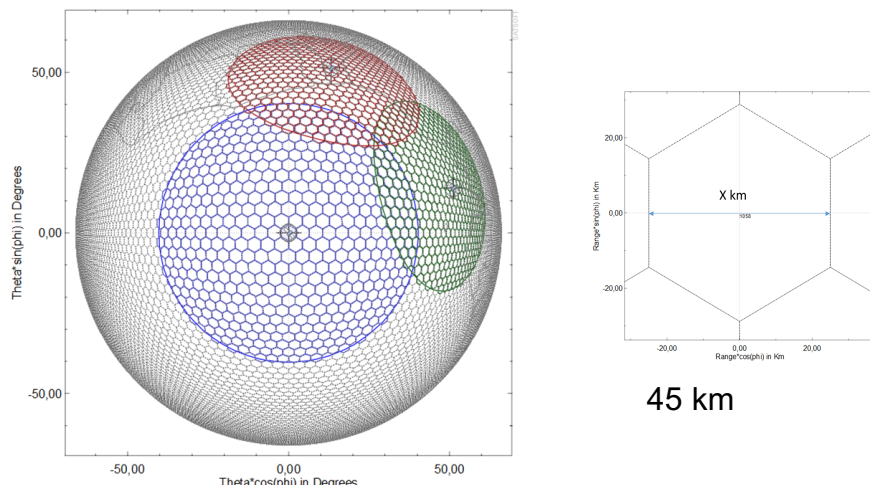
FIGURE 6: VIEW OF SATELLITE COVERAGE / CELL SIZE

2.1.1.2   C-Band Payload Characteristics

A detailed payload sizing is ongoing in T3.3 and will be reported in D3.3 '*Report on Software defined payload and its scalability*'. The main parameters relevant to the calculations and figures presented in this chapter are :

- EIRP density is taken as 28 dBW/MHz per beam

- 100 active beams are taken as a nominal value which represent 20% of the beam on the coverage.

- A bandwidth of 100 MHz is taken for the link budget

2.1.1.3   C-band UE Characteristic

With respect to the types of RF-FE presented in Table 1, a worst-case assumption is taken here, considering a noise figure NF = 9 dB, an antenna gain taking into account only the scan losses and a TX power of 23 dBm.

2.1.1.4   C-Band Numerology

The considered C-band numerology is show in Table 4.

TABLE 4: NUMEROLOGY C-BAND

ID	Frequency Range				Used Frequency		Channel Bandwidth		PRB					
	UL		DL		UL	DL	UL	DL	UL	DL	# carriers	SCS BW	PRB BW	# PRB
	Fmin (GHz)	Fmax (GHz)	Fmin (GHz)	Fmax (GHz)	GHz	GHz	MHz	MHz	kHz	kHz	-	kHz	kHz	-
C1	3.2	3.3	3.9	4	3.9	3.4	100	100	360	360	12	30	360	273

2.1.1.5   Summary of the Data for Satellite and UE

The data for the satellite definition and the UE definition are summarised in the table below.

TABLE 5: UE AND SATELLITE DEFINITION C-BAND

UE	Parameter	Unit	Value
	Band Name	-	C
RX (downlink)	Downlink Frequency	(GHz)	3.40
	Antenna Size	(m)	0.05
	Number of ER	-	1
	Antenna Noise Figure (NF)	(dB)	9.00
	Antenna gain (NADIR)	(dBi)	2.28
	Antenna gain (45°)	(dBi)	1.23
	Antenna gain (30°)	(dBi)	-0.73
	G/T (NADIR)	dB/K	-31.34
	G/T (45°)	dB/K	-32.39
	G/T(30°)	dB/K	-34.35
SCS PRB	SCS	kHz	30
	Downlink BW	MHz	100
	Nb Downlink PRBs	-	273
	Uplink BW	MHz	100
	Nb Uplink PRBs	-	273
TX (uplink)	Uplink Frequency	(GHz)	3.90
	Antenna Size	(m)	0.05
	Number of ER	-	1
	Antenna gain (NADIR)	(dBi)	3.47
	Antenna gain (45°)	(dBi)	2.42
	Antenna gain (30°)	(dBi)	0.46
	Antenna transmit power	dBW	-7
	Antenna transmit power	W	0.20
	UE DEFINITION		

SATELLITE	Parameter	Unit	Value
	Satellite	-	LEO-600
	Altitude	km	600
	Band Name	-	C
	Nb spots total	-	499
	Nb active spots during 1ms timeslot	-	100
	Cell diameter	km	45
TX (downlink)	Downlink Frequency	GHz	3.40
	Antenna Size	m	1.95
	Number of ER	-	1056
	Antenna gain (NADIR)	dBi	34.86
	Antenna gain (El 45°)	dBi	33.81
	Antenna gain (El 30°)	dBi	31.85
	EIRP density	dBW/MHz	28.00
RX (uplink)	Uplink Frequency	GHz	3.90
	Antenna Size	m	1.95
	Number of ER	-	1056
	Antenna gain (NADIR)	dBi	36.05
	Antenna gain (45°)	dBi	35.01
	Antenna gain (30°)	dBi	33.04
SCS PRB	SCS	kHz	30
	Downlink BW	MHz	100
	Nb Downlink PRBs	-	273
	Uplink BW	MHz	100
	Nb Uplink PRBs	-	273
C/I	Downlink (Sat TX)	dB	12
	Uplink (Sat RX)	dB	12
	SATELLITE DEFINITION		

2.1.1.6   Uplink Budget: Max Throughput

The table below gives the computed data in term of capacity resulting from link budget. The presented throughput figures correspond to the following scenarios:

1) The objective is to evaluate the max throughput achievable by a user. In other word what the satellite could offer in term of maximum throughput for a single user located at nadir, transmitting at maximum power (23 dBm) and using the maximum possible number of PRBs. A UE could achieve a maximum of 7 Mbps of uplink throughput in this scenario.
2) The objective is to evaluate the throughput achievable by a user using only 1 PRB and transmitting at maximum power. Users are on a cell around the nadir and 100 cells are active. The aggregate peak throughput is 19.5 Gbits in this scenario.
3) The objective is to evaluate the throughput achievable by a user using only 1 PRB and transmitting at maximum power. Users are on a cell around the edge of coverage and 100 cells are active. The aggregate min throughput is 13.4 Gbits in this scenario.
4) The objective is to evaluate the throughput achievable by a user using only 1 PRB and transmitting at maximum power. Users are distributed between nadir (30%) and edge (70%) and 100 cells are active. The aggregate average throughput is 15.2 Gbits in this scenario.
5) The objective is to evaluate the max throughput achievable by a user in light indoor scenario (10 dB additional attenuation). In other word what the satellite could achieve in term of maximum throughput for a user located at nadir, transmitting at maximum power (23 dBm) and using the maximum possible number of PRBs. A UE could achieve a maximum of 750 kbps of uplink throughput in this scenario.
6) The objective is to evaluate the instantaneous throughput over 100 cells (active beams) with 100 users uniformly distributed between nadir (30%) and edge (70%). This figure could be scaled according to the number of real users by cell and by applying the beam hopping scheme of 1/5.

TABLE 6: C-BAND UPLINK THROUGHPUT AT 99.5% AVAILABILITY

UPLINK	unity		Remark	nb of user	nb PRB per user nadir	at 45°
1) PEAK Throughput Achievable per an user						
Peak throughput	Mbits/s	**7.065**	1 user per cell, nadir	1	91	
peak Spectral density	bits/s/Hz	0.2156	1 user per cell, nadir	1	91	
peak troughput/km^2	kbits/s/km^2	4.03	Dp_up/ cell surface	1		
2) PEAK Throughput Achievable by the satellite						
Peak throughput 1PRB at nadir	Mbits/s	**0.715**	1 user per cell, nadir	1	1	
peak Spectral density 1PRB at nadir	bits/s/Hz	1.9874	1 user per cell, nadir	1	1	
Aggregated peak throughput on a nadir cell	Mbits/s	195.2	273 users on a cell at nadir	273	1	
Aggregate Max throughput 1PRB per user all beams	Gbits/s	**19.5**	273 user per cell nadir, 100 beams around nadir	27300	1	
3) MIN Throughput Achievable by the satellite						
Peak throughput 1PRB at edge	Mbits/s	**0.489**	1 user per cell, edge	1	1	
peak Spectral density 1PRB at edge	bits/s/Hz	1.3585	1 user per cell, edge	1	1	
Aggregated peak throughput on a edge cell	Mbits/s	133.5	273 users on a cell at edge	273	1	
Aggregate throughput 1PRB/user all beams	Gbits/s	**13.4**	273 user per cell edge, 100 beams at the edge	27300	1	
4) AVERAGE Throughput Achievable by the satellite						
Average Aggregate throughput 1PRB/user in 1 beam	Mbits/s	**152.1**	max user 273 per cell, nadir to edge, best conditions			
Average Aggregate throughput 1PRB/user all beams	Gbits/s	**15.2**	273 user per cell, cell distributed from nadir to edge	27300	1	
average throughput/Km^2	kbits/s/km2	**86.7**				
5) PEAK Throughput Achievable per an user (indoor)						
Peak throughput (indoor)	Mbits/s	**0.749**	1 user per cell, nadir, 10dB atten max PRB	1	6	
peak Spectral density	bits/s/Hz	0.347	1 user per cell, nadir, 10dB atten max PRB	1	6	
Peak throughput 1PRB	Mbits/s	0.389	1 user per cell, nadir, 10dB atten	1	1	
peak Spectral density 1PRB	bits/s/Hz	1.081736	1 user per cell, nadir, 10dB atten	1	1	
6) AVERAGE Throughput Achievable per an user						
average Peak thoughput	Mbits/s	**3.26**	1 user per cell, nadir to edge, best conditions	1	91	21
average spectral density	bits/s/Hz	0.22	1 user per cell, nadir to edge, best conditions	1	91	21
aggregated peak throughput	Mbits/s	326.06	100 users on 100 beams	100	91	21
average throughput/Km^2	kbits/s/km^2	1.86		100	91	21

For the uplink, the throughput to take in consideration for the dimensioning of the inter satellite links is 15.2 Gbps. This value corresponds to a probable maximum throughput experienced and will be consolidated with more realistic traffic pattern. According to this maximum reference throughput, the user requirements and an estimated activity factor taken from D2.3 [6], we can evaluate the characteristics of the service offer as in the table below.

TABLE 7: SERVICE PERFORMANCE EVALUATION C-BAND RX

Need /users	Mbps	2.00
Activity factor	%	0.01
per user (need)	Kbps	0.20
number users per cell	per cell	760267
surface cell	km^2	1753.70
density	users per Km^2	434

2.1.1.7 Downlink Budget: Max Throughput

The table below gives the computed data in term of capacity resulting from link budget. The presented throughput figures correspond to the following scenarios:

0) The objective is to evaluate the max throughput achievable in downlink to a user located at nadir and assuming all power of the satellite is concentrated on one beam only.

1) The objective is to evaluate the max throughput achievable in downlink to a user at nadir and power distributed over 100 beams. In this case, 100 beams are active, the cells covered are around the nadir, and only one user is present in each cell. The satellite is in nominal mode of operation and the cells to cover are around nadir. This case could occur

exceptionally in area where the coverage of the users is really concentrated in a 1/5 of the total satellite coverage.

2) The objective is to evaluate the max throughput achievable in downlink to a user at edge of coverage and power distributed over 100 beams. This case is the worst-case scenario, the users are distributed near the edge of the coverage

3) The objective is to evaluate the average throughput achievable in downlink to a user from nadir to edge and power distributed over 100 beams. This case is the more probable scenario, the users are distributed over the coverage and a suitable beam hopping process will ensure an appropriate management of the throughput by covering at each slot a sub-selected cell over the total cells by a first analysis of the area. AI and deep learning process at term to optimize the beam hopping process could also be envisaged.

4) The objective is to evaluate the max throughput achievable by a user in indoor condition (10 dB additional attenuation) at nadir

5) The objective is to evaluate the case where 1 PRB is given to each user and all power distributed over the 273 PRB (full band) and compute the aggregated throughput reached

6) The objective is to evaluate the case where there are 100 active cell, 1 user per cell with full power of the beam on one PRB.

TABLE 8: C-BAND DOWNLINK THROUGHPUT AT 99.5% AVAILABILITY

DOWNLINK	unity		remark 1	nb users	nb PRB		remark 2
					Nadir	EL 45°	
1) PEAK Throughput Achievable per an user							
Peak throughput	Mbits/s	158.64	1 user per cell, nadir, best conditions	1	273		all Power on one cell
peak Spectral density	bits/s/Hz	1.6461	1 user per cell, nadir, best conditions	1	273		all Power on one cell
peak troughput/km^2	kbits/s/km^2	90.5	Dp_up/ cell surface	1			
2) PEAK Throughput Achievable per an user							
Peak throughput nadir cell	Mbits/s	86.83	1 user per cell, 100 cells, best conditions, nadir	1	273		Power on 100 cells (20% of coverage cell)
Peak Spectral density nadir cell	bits/s/Hz	0.8835	1 user per cell, 100 cells, best conditions, nadir	1	273		Power on 100 cells (20% of coverage cell)
Peak troughput/km^2 nadir cell	kbits/s/km^2	49.5	Dpm_down/ cell surface	1	273		
aggregated Peak throughput nadir cells	Gbits/s	8.68		100	273		
3) PEAK Throughput Achievable per an user							
Peak throughput edge cell	Mbits/s	31.86	1 user per cell, 100 cells, best conditions edge	1		273	Power on 100 cells (20% of coverage cell)
Peak Spectral density edge cell	bits/s/Hz	0.3242	1 user per cell, 100 cells, best conditions edge	1		273	Power on 100 cells (20% of coverage cell)
Peak troughput/km^2 edge cell	kbits/s/km^2	18.2	Dpm_down/ cell surface	100		273	
aggregated Peak throughput edge cells	Gbits/s	3.19					
4)Avergage Throughput Achievable per an user							
average Peak throughput distributed	Mbits/s	48.35	1 user per cell, 100 cells, best conditions, nadir to edge	1	273		Power on 100 cells (20% of coverage cell)
average peak Spectral density	bits/s/Hz	0.4920	1 user per cell, 100 cells, best conditions, nadir to edge	1	273		Power on 100 cells (20% of coverage cell)
average peak troughput/km^2	kbits/s/km^2	27.6	Dpm_down/ cell surface	1			
aggregated throughput	Gbits/s	4.84		100	273	273	100 cells distributed over the coverage
5) PEAK Throughput Achievable per an user (indoor)							
Peak throughput (indoor)	Mbits/s	138.56	1 user per cell, nadir, 10dB atten	1	273		all Power on one cell/max PRB
peak Spectral density	bits/s/Hz	1.458	1 user per cell, nadir, 10dB atten	1	273		all Power on one cell/max PRB
6) Throughput 1 PRB per user							
Average Throughput 1 PRB per user	Mbits/s	0.32	1 PRB per users/ 100 beams	27300	1	1	Power on 8 cells (1.6% of coverage cell)
Average spectral efficiency	bits/s/Hz	0.88	1 PRB per users/100 beams	27300	1	1	Power on 8 cells (1.6% of coverage cell)
Aggregated throughput	Gbits/s	8.68	1 PRB per users/100 beams	27300	1	1	Power on 8 cells (1.6% of coverage cell)
7) Throughput ALL power in 1 PRB 1 user							
Average Throughput 1 PRB per user	Mbits/s	0.593	in one beam (taken near nadir)	100	1	1	power on 1 PRB 1 user per cell
Average spectral efficiency	bits/s/Hz	1.64613	in on beam (taken near nadir)	100	1	1	power on 1 PRB 1 user per cell
Aggregated throughput	Mbits/s	59.30	in one beam (taken near nadir)	100	1	1	power on 1 PRB 1 user per cell

For the downlink, the throughput to take in consideration for the dimensioning of the inter satellite links is 4.8 Gbps. This value corresponds to a probable maximum throughput experienced and will be consolidated with more realistic traffic pattern. According to this maximum reference throughput, the user requirements and an estimated activity factor, we can evaluate the characteristics of the service offer as in the table below.

TABLE 9: SERVICE PERFORMANCE EVALUATION C-BAND TX

Need per user (objective)	Mbps	20
activity factor	%	0.5
per user (need)	Kbps	100.00
nb of users	per cell	484
surface cell	Km^2	1753.70
density	users /Km^2	0.27572

2.1.2 Q/V-Band

2.1.2.1 Coverage

The definition of satellite coverage for Q/V band is the result of an ongoing trade-off in Task 3.3 taking into account all the dimensioning parameters. As technical maturity in Q/V is more difficult to assess, several assumptions have been made to define the satellite antenna and UE antenna solutions. Satellite coverage has an impact on constellation size, while cell size is linked to antenna aperture size. The results converge towards a payload solution comprising several DRA antennas of limited size and beams-generating capacity. Reflections are underway to see the technological advances that would make it possible to move from ABFN or DBFN. The definition of cells is also constrained by the ability to keep the satellite stable, so as not to make pointing errors and ensure good cell performance. For this reason, we chose not to dimension very small cells. The choice was made to keep the same coverage and cell definition as for C-band, which means we only need one "cell definition" in 6G-NTN.

Therefore the coverage is the same as the C-Band coverage shown in Figure 6 with 45° maximum elevation and 499 cells of 45km in a hexagonal lattice. Taking the same coverage will allow to have only one cell definition on earth.

2.1.2.2 Q/V-Band Payload Characteristics

A detailed payload sizing is ongoing in T3.3 and will be reported in D3.3 '*Report on Software defined payload and its scalability*'. The main parameters relevant to the calculations and figures presented in this chapter are :

- EIRP flux is taken as 18.2 dBW/MHz per beam

- Two classes of payloads are considered: one with 8 active beams (baseline), another one with 4 active beams (backup)

- The payload is constituted of 7 antennas, each one generates 4 or 8 actives beams

- The bandwidth of each antenna is 400 MHz

2.1.2.3 Q/V-Band UE Characteristic

With respect to the types of RF-FE presented in Table 1, an "average terminal" with a noise figure NF = 5 dB, an antenna gain of 30 dBi and a TX power of 34 dBm has been assumed

2.1.2.4 Q/V-Band Numerology

The considered Q/V-band numerology is show in Table 10

TABLE 10: NUMEROLOGY Q/V-BAND

ID	Frequency Range				Used Frequency		Channel Bandwidth		PRB					
	UL		DL		UL	DL	UL	DL	UL	DL	# carriers	SCS BW	PRB BW	# PRB
	Fmin (GHz)	Fmax (GHz)	Fmin (GHz)	Fmax (GHz)	GHz	GHz	MHz	MHz	kHz	kHz	-	kHz	kHz	-
Q-V2	47.2	50.4	37.5	40.5	50	40	400	400	1440	1440	12	120	5760	264

2.1.2.5 Summary of the Data for Satellite and UE

The data for the satellite definition and the UE definition are summarised in the table below.

TABLE 11: UE AND SATELLITE DEFINITION Q/V-BAND

UE	Parameter	Unit	Value
	Band Name	-	Q-V
RX (downlink)	Downlink Frequency	GHz	40.00
	Antenna Size	m	0.1
	Number of ER	-	379
	Antenna Noise Figure (NF)	dB	4.00
	Antenna gain (NADIR)	dBi	30.45
	Antenna gain (45°)	dBi	29.41
	Antenna gain (30°)	dBi	27.44
	G/T (NADIR)	dB/K	2.14
	G/T (45°)	dB/K	1.09
	G/T(30°)	dB/K	-0.87
SCS PRB	SCS	kHz	120
	Downlink BW	MHz	400
	Nb Downlink PRBs	-	264
	Uplink BW	MHz	400
	Nb Uplink PRBs	-	264
TX (uplink)	Uplink Frequency	GHz	50.00
	Antenna Size	m	0.08
	Number of ER	-	379
	Antenna gain (NADIR)	dBi	29.95
	Antenna gain (45°)	dBi	28.91
	Antenna gain (30°)	dBi	26.94
	Antenna transmit power	dBW	4
	Antenna transmit power	W	2.51

UE definition

SATELLITE	Parameter	Unit	Value
	Satellite	-	LEO-600
	Altitude	km	600
	Band Name	-	Q-V
	Cell diameter	km	45
TX (downlink)	Downlink Frequency	GHz	40.00
	Antenna Size	m	0.13
	Number of ER	-	512
	Antenna gain (NADIR)	dBi	33.00
	Antenna gain (El 45°)	dBi	31.95
	Antenna gain (El 30°)	dBi	29.99
	EIRP density	dBW/MHz	18.20
RX (uplink)	Uplink Frequency	GHz	50.00
	Antenna Size	m	0.10563913
	Number of ER	-	512
	Antenna gain (NADIR)	dBi	33.00
	Antenna gain (45°)	dBi	31.95
	Antenna gain (30°)	dBi	29.99
	G/T (NADIR)	dB/K	4.68
	G/T (45°)	dB/K	3.63
	G/T(30°)	dB/K	1.67
SCS PRB	SCS	kHz	120
	Downlink BW	MHz	400
	Nb Downlink PRBs	-	264
	Uplink BW	MHz	400
	Nb Uplink PRBs	-	264

Satellite definition

2.1.2.6 Uplink Budget: Max Throughput

Table 12 gives the computed data in term of capacity resulting from link budget. The presented throughput figures correspond to the scenarios already described in section 2.1.1.6. In addition, scenarios 7) and 8) report the aggregated throughput taking into account the 7 antennas and 8 / 4 active beams per antenna respectively.

For the uplink, the throughput to take in consideration for the dimensioning of the inter satellite links is 48 / 24 Gbps for 8 / 4 active beams per antenna respectively. These values correspond to a probable maximum throughput experienced and will be consolidated with more realistic traffic pattern. According to this maximum reference throughput, the user requirements and an estimated activity factor, we can evaluate the characteristics of the service offer as in Table 13.

2.1.2.7 Downlink Budget: Max Throughput

Table 14 gives the computed data in term of capacity resulting from link budget. The presented throughput figures correspond to the scenarios already described in section 2.1.1.7. In

addition, scenario 7) is meant to show the limitation on throughput if all the power is put on one PRB with 8 active beams. Scenarios 8) and 9) report the aggregated throughput taking into account the 7 antennas and 8 / 4 active beams per antenna respectively.

For the downlink, the throughput to take in consideration for the dimensioning of the inter satellite links is 17.7 / 8.9 Gbps for 8 / 4 active beams per antenna respectively. These values correspond to a probable maximum throughput experienced and will be consolidated with more realistic traffic pattern. According to this maximum reference throughput, the user requirements and an estimated activity factor, we can evaluate the characteristics of the service offer as in Table 15.

TABLE 12: V-BAND UPLINK THROUGHPUT AT 99.5% AVAILABILITY

UPLINK	unity		remark 1		nb PRB	
				nb user	nadir	45°
1) PEAK Throughput Achievable per an user						
Peak throughput	Mbits/s	80.190	1 user per cell, nadir	1	264	
peak Spectral density	bits/s/Hz	0.2110	1 user per cell, nadir	1	264	
peak troughput/km^2	kbits/s/km^2	45.73	Dp_up/ cell surface	1	264	
2) PEAK Throughput Achievable by the satellite						
Peak throughput 1PRB at nadir	Mbits/s	3.54	1 user per cell, nadir	1	1	
peak Spectral density 1PRB at nadir	bits/s/Hz	2.46	1 user per cell, nadir	1	1	
Aggregated peak throughput on a nadir cell	Mbits/s	934.56	264 users on a cell at nadir	264	1	
Aggregate Max throughput 1PRB per user all beams	Gbits/s	7.48	264 user per cell nadir, 8 beams around nadir	2112	1	
3) PEAK Throughput Achievable by the satellite						
Peak throughput 1PRB at edge	Mbits/s	3.12	1 user per cell, edge	1	1	
peak Spectral density 1PRB at edge	bits/s/Hz	2.17	1 user per cell, edge	1	1	
Aggregated peak throughput on a edge cell	Mbits/s	823.42	264 users on a cell at edge	264	1	
Aggregate Max throughput 1PRB per user all beams	Gbits/s	6.59	264 user per cell nadir, 8 beams at edge	2112	1	
4) AVERAGE Throughput Achievable by the satellite						
Average Aggregate throughput 1PRB/user in 1 beam	Mbits/s	856.50	264 user in one beam	264	1	
Average Aggregate throughput 1PRB/user all beams	Gbits/s	6.85	264 per cell, 8 beams nadir to edge,	2112	1	
average throughput/Km^2	kbits/s/km2	488.39	264 user per cell, cell distributed from nadir to edge	264	1	
5) PEAK Throughput Achievable per an user (indoor)						
Peak throughput (indoor)	Mbits/s	8.340	1 user per cell, nadir, 10dB atten	1	21	
peak Spectral density	bits/s/Hz	0.2759	1 user per cell, nadir, 10dB atten	1	21	
Peak throughput 1PRB	Mbits/s	2.480	1 user per cell, nadir, 10dB atten	1	1	
peak Spectral density 1PRB	bits/s/Hz	1.7220	1 user per cell, nadir, 10dB atten	1	1	
6) AVERAGE Throughput Achievable per an user						
average Peak thoughput	Mbits/s	37.2437	1 user per cell, nadir to edge, best conditions	1	264	62
average spectral density	bits/s/Hz	0.2110	1 user per cell, nadir to edge, best conditions	1	264	62
aggregated peak throughput	Mbits/s	3.7244	8 users on 8 beams	8	264	62
average throughput/Km^2	kbits/s/km2	21.2372		8	264	62
7) AGGREGATED MAX throughput 7 antenna /8 beams	Gbits/s	47.96	56 beams, 264 users per beam	14784	1	1
8) AGGREGATED MAX throughput 7 antenna /4 beams	Gbits/s	23.98	28 beams, 264 users per beam	2.114	1	1

TABLE 13: SERVICE PERFORMANCE EVALUATION V-BAND RX

UPLINK		
8 beams per antenna		
Need per user	125	Mbps
activity factor	2	%
real need	2.5	Mbps
nb users per cell	343	
surface cell	1753.70	km^2
density	0.20	user/km^2
active surface %	1.60	%
4 beams per antenna		
Need per user	125	Mbps
activity factor	2	%
real need	2.5	Mbps
nb users per cell	343	
surface cell	1753.70	km^2
density	0.20	user/km^2
active surface %	0.80	%

TABLE 14: Q-BAND DOWNLINK THROUGHPUT AT 99.5% AVAILABILITY

DOWNLINK	unity		remark 1	nb users	nb PRB		remark 2
					Nadir	EL 45°	
1) PEAK Throughput Achievable per an user							
Peak throughput	Mbits/s	596.7	1 user per cell, nadir, best conditions	1	264		all Power on one cell
peak Spectral density	bits/s/Hz	1.5696	1 user per cell, nadir, best conditions	1	264		all Power on one cell
peak troughput/km^2	kbits/s/km^2	340.3	Dp_up/ cell surface	1			
2) PEAK Throughput Achievable per an user							
Peak throughput nadir cell	Mbits/s	414.01	1 user per cell, 8 cells, best conditions, nadir	1	264		Power on 8 cells (1.6% of coverage cell)
Peak Spectral density nadir cell	bits/s/Hz	1.0890	1 user per cell, 8 cells, best conditions, nadir	1	264		Power on 8 cells (1.6% of coverage cell)
Peak troughput/km^2 nadir cell	kbits/s/km^2	236.1	Dpm_down/ cell surface	1	264		
aggregated Peak throughput nadir cells	Gbits/s	3.31	1 user per cell, 8 cells, best conditions, nadir	8	264		
3) PEAK Throughput Achievable per an user							
Peak throughput edge cell	Mbits/s	273.39	1 user per cell, 8 cells, best conditions edge	1		264	Power on 100 cells (1.6% of coverage cell)
Peak Spectral density edge cell	bits/s/Hz	0.7191	1 user per cell, 8 cells, best conditions edge	1		264	Power on 100 cells (1.6% of coverage cell)
Peak troughput/km^2 edge cell	kbits/s/km^2	155.9	Dpm_down/ cell surface	8		264	
aggregated Peak throughput edge cells	Gbits/s	2.19					
4)Avergage Throughput Achievable per an user							
average Peak throughput distributed	Mbits/s	315.57	1 user per cell, 8 cells, best conditions, nadir t	1	264		Power on 8 cells (1.6% of coverage cell)
average peak Spectral density	bits/s/Hz	0.8301	1 user per cell, 8 cells, best conditions, nadir t	1	264		Power on 8 cells (1.6% of coverage cell)
average peak troughput/km^2	kbits/s/km^2	179.9	Dpm_down/ cell surface	1			
aggregated throughput	Gbits/s	2.52		8	264	264	8 cells distributed over the coverage
5) PEAK Throughput Achievable per an user (indoor)							
Peak throughput (indoor)	Mbits/s	117.52	1 user per cell, nadir, 10dB atten	1	264		all Power on one cell
peak Spectral density	bits/s/Hz	0.3091	1 user per cell, nadir, 10dB atten	1	264		all Power on one cell
6) Throughput 1 PRB per user							
Average Throughput 1 PRB per user	Mbits/s	1.57	1 PRB per users/ 8 beams	2112	1	1	Power on 8 cells (1.6% of coverage cell)
Average spectral efficiency	bits/s/Hz	1.09	1 PRB per users/8 beams	2112	1	1	Power on 8 cells (1.6% of coverage cell)
Aggregated throughput	Gbits/s	3.32	1 PRB per users/8 beams	2112	1	1	Power on 8 cells (1.6% of coverage cell)
7) Throughput ALL power in 1 PRB 1 user							
Average Throughput 1 PRB per user	Mbits/s	2.55	in one beam (taken near nadir)	8	1	1	power on 1 PRB 1 user per cell
Average spectral efficiency	bits/s/Hz	1.77	in on beam (taken near nadir)	8	1	1	power on 1 PRB 1 user per cell
Aggregated throughput	Mbits/s	20.40	in one beam (taken near nadir)	8	1	1	power on 1 PRB 1 user per cell
8) AGGREGATED MAX throughput 7 antenna /8 beams	Gbits/s	17.67	56 beams, 264 users per beam	1848	1	1	
9) AGGREGATED MAX throughput 7 antenna /4 beams	Gbits/s	8.84	28 beams, 264 users per beam	924	1	1	

TABLE 15: SERVICE PERFORMANCE EVALUATION Q-BAND TX

DOWNLINK		
8 beams per antenna		
Need per user (objective)	250	Mbps
activity factor	2	%
per user (need)	5.00	Mbps
nb of users	83	per cell
surface cell	1753.70	Km^2
density	0.05	users /Km^2
4 beams per antenna		
Need per user (objective)	250	Mbps
activity factor	2	%
per user (need)	5.00	Mbps
nb of users	83	per cell
surface cell	1753.70	Km^2
density	0.024	users /Km^2

2.2 INTER-NODE LINK BUDGETS

2.2.1 Inter-Orbit Link Budgets

The inter-orbit links constitute the inter-node links between LEO and GEO satellites, HAPs and LEO satellites, and HAPs and GEO satellites. The inter-orbit link budgets have been calculated in accordance with the antenna sizing performed by Thales Alenia Space France for the corresponding radio frequency (RF) bands, resulting in the preliminary definition of the antenna parameters for Equivalent Isotropic Radiated Power (EIRP) and Gain to Noise Temperature (G/T). For HAP-LEO and HAP-GEO links, also a solution based on optical technology have been analysed. The achievable data rates for each of the inter-node links between HAP, LEO and GEO are presented below.

2.2.1.1 LEO-GEO Link Budgets

This link is ensured by antenna in Ka band in dedicated ISL ITU defined band as shown in the table below.

TABLE 16: POSSIBLE FREQUENCY BAND FOR ISL GEO-LEO

BANDS			ITU FREQUENCY BAND FOR ISL
GHz	GHz	BW	
22.55	23.55	1	used by Iridium (23.18-23,38) and GSO data Relay systems with LEO
32.3	33	0.7	
54.25	56.9	2.65	Only for GSO-GSO links pfd limitation at 1000 km above earth surface of -147 dBW/m^2/100MHz
56.9	57	0.1	Only for GSO-GSO and HEO-LEO links pfd limitation at 1000 km above earth surface of -147 dBW/m^2/100MHz
57	58.2	1.2	Only for GSO-GSO links pfd limitation at 1000 km above earth surface of -147 dBW/m^2/100MHz
59	59.3	0.3	Only for GSO-GSO links pfd limitation at 1000 km above earth surface of -147 dBW/m^2/100MHz
59.3	66	6.7	
66	71	5	Potential identification for terrestrial 5G
116	122.25	6.25	Only for GSO-GSO links pfd limitation at 1000 km above earth surface of -148 dBW/m^2/MHz
122.25	123	0.75	
130	134	4	
167	174.8	7.8	
174.8	182	7.2	Only for GSO-GSO links pfd limitation at 1000 km above earth surface of -144 dBW/m^2/MHz

The two selected frequency bands are in Ka band 22.55-23.55 GHz and 32.3-33 GHz. The first band are used by a constellation and need to be coordinated.

The two Ka bands are used for full duplex operation. However, it is possible to use only one band, but this requires a great deal of filtering between the TX and RX parts, which complicates the design of the front-ends. Using both bands, as shown in the diagram below, offers the advantage of increased bandwidth and greater flexibility, but requires the development of amplifier components working in both bands. The balance sheet is based on this second choice. In the event of identified constraints, we can always return to work only with one frequency band.
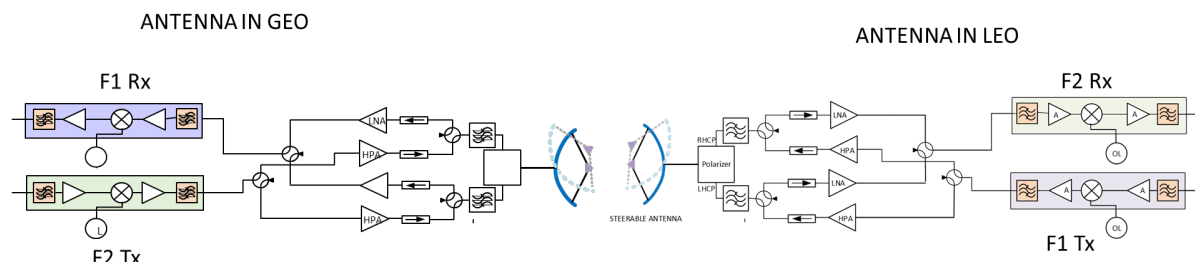
FIGURE 7: ISL ARCHITECTURE FRONT-ENDS FOR GEO-LEO LINK

ISL sizing will depend on the platform capacity and the desired flow rate. The table and chart below give the values for 2 cases of 300 mm and 700 m mechanically steerable cassegrain antennas. The tables give some typical performances for the two links in F1 and F2 frequency band for the two antenna sizes. The bandwidth and the amplifier power have also an impact on the achievable throughput. The purpose at this stage is to give some typical values in term of throughput. Only a precise budget will allow to define (power available, target in throughput) a best solution.

300 mm	ANTENNA		F1	F2
	Diameter	mm	300.00	300.00
	Frequency	GHz	23.1	32.7
	Directivity	dBi	35.2	38.3
	Feeder losses	dB	1.4	1.6
	GAIN	dBi	33.8	36.7
	EIRP	dBW	51.6	49.8
	G/T	dB.K^{-1}	8.5	10.7

700 mm	ANTENNA		F1	F2
	Diameter	mm	700	700
	Frequency	GHz	23.1	32.7
	Directivity	dBi	42.6	45.4
	Feeder losses	dB	1.4	1.6
	GAIN	dBi	41.2	43.8
	EIRP	dBW	58.9	56.8
	G/T	dB.K^{-1}	17.7	15.9
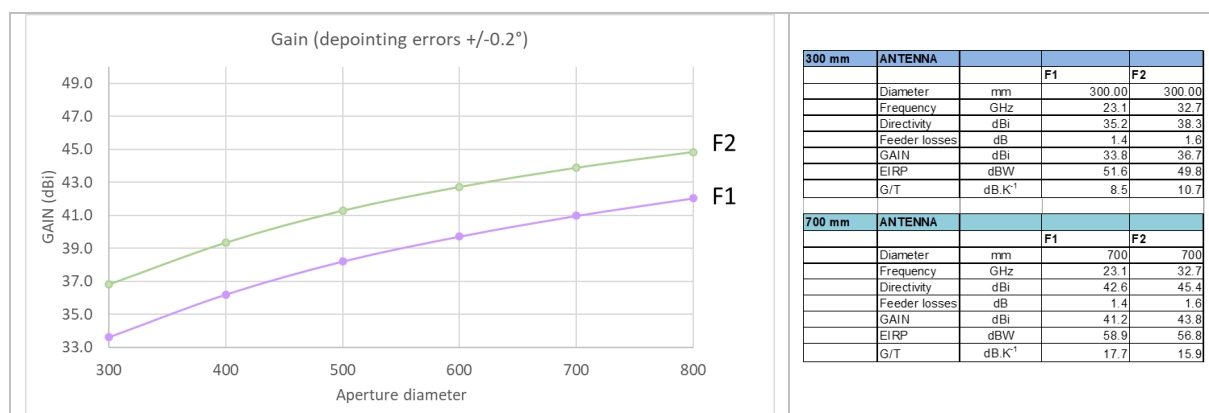
FIGURE 8: ANTENNA PERFORMANCES VERSUS APERTURE

The link budgets for the link in F1 or F2 frequency band of the inter-node link between a LEO and a GEO satellite are presented in Figure 9 and Figure 10. The architecture

The link is realized in the Ka band between 32.3 GHz and 33 GHz with 200 MHz spacing between the downlink and the uplink. The proposed architecture is based on the use of both bands. For a bandwidth of 100 MHz are of the order of 250 Mbps. It is possible to increase this throughput to a certain extent, as shown by the curves in Figure 9 (b) and Figure 10 (b). Working with two bands gives more flexibility than working with a single band, where spacing is required between the downlink and uplink bands. Depending on requirements, an

architecture shall be chosen that meets the needs. The impact in term of power consumption, mass and volume could limit the accommodation on the satellite platform.

Tx20 Rx20		
BW available	**1**	**GHz**
Carrier BW	100.000	MHz
gain	41.15	
Frequency	23.05	GHz
Power SSPA	40	W
Power SSPA	16.02059991	dBW
EIRP Tx20	57.2	dBW
C/Im up	15.0	dB
Distance between sat	40000.0	km
Free space loss	-211.7	dB
link margin	0.50	dB
G/T	**15.9**	dB/K
C/No up	89.9	dBHz
C/I uplink	27	dB
C/N uplink	10.1	dB
C/(N+I) uplink	8.35	dB
DVB-S2X rate	**245.84**	Mb/s

(a)

(b)
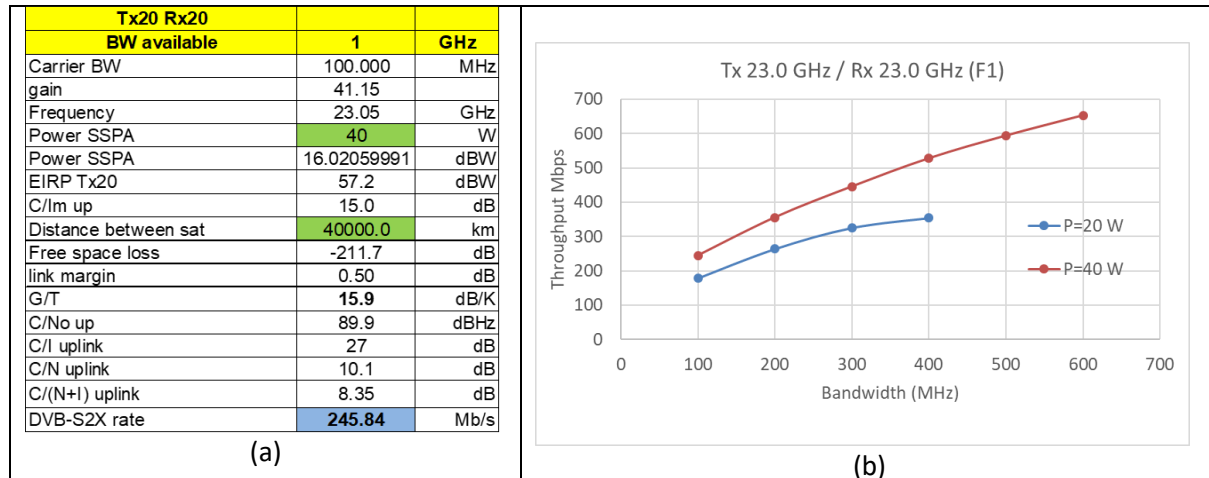
FIGURE 9: THROUGHPUT PERFORMANCES KA LOWER BAND 23 (ANTENNA APERTURE 700 MM)

| Tx 30 Rx 30		
BW available	**0.7**	**GHz**
Carrier BW	100.000	MHz
Gain	43.80	
Frequency	32.67	GHz
Puissance SSPA	40.00	W
power SSPA	16.02	dBW
EIRP Tx30	**59.8**	dBW
C/Im up	15.0	dB
Distance between sat	40000.0	km
Free space loss	-214.8	dB
link margin	0.50	dB
G/T	**17.7**	dB/K
C/No up	91.4	dBHz
C/I uplink	27	dB
C/N uplink	11.6	dB
C/(N+I) uplink	9.39	dB
DVB-S2X rate	**274.57**	Mb/s

(a)

(b)
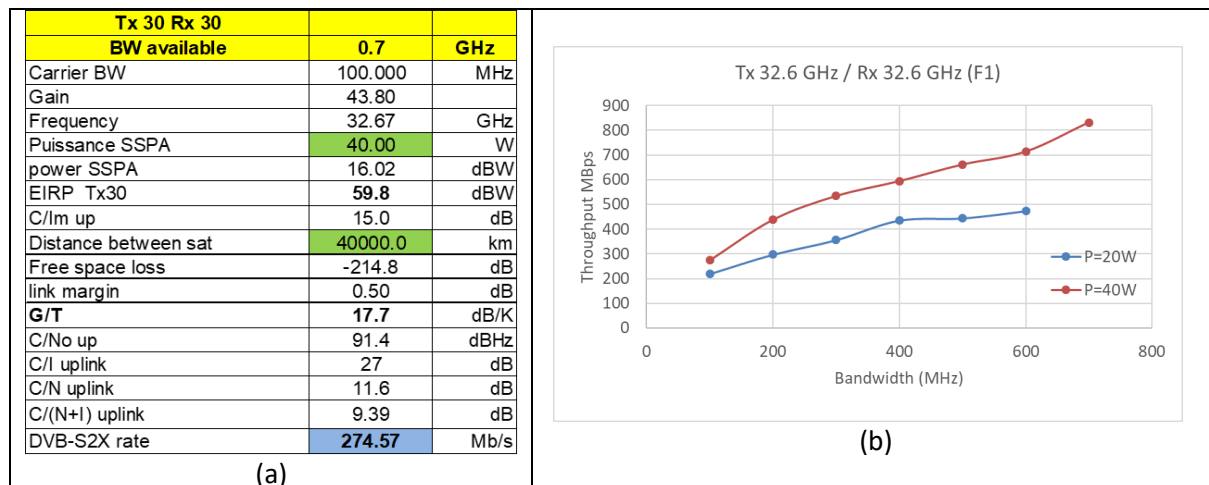
FIGURE 10: THROUGHPUT PERFORMANCES KA UPPER BAND 32 (ANTENNA APERTURE 700 MM)

2.2.1.2 HAP-LEO Link Budgets – RF Technology

The budget in that case is similar to a feeder link between a LEO satellite and a ground station in term of frequency bands (Q/V) except that the antenna on a HAP is constrained by power consumption, mass and volume. For the moment, several options are available: either a small cassegrain-type reflector antenna, or a Q/V active antenna (1 or 2 beams). It's too early to fix a design, as it also depends on the type of HAP, which are diverse and have more or less significant carrying capacities according to the orientations taken by the manufacturers. In our case, it is assumed a small, mechanically pointed antenna with a diameter reduced to 300 mm. The corresponding antenna parameters for the LEO satellite and the HAPs are reported in the table below.

TABLE 17: HAP AND LEO ANTENNAS PARAMETERS

Antenna	HAPS diameter 300 mm			
TX		GAIN	38.3	dBi
	50 GHz	EIRP	46.8	dBW
RX		GAIN	37.1	dBi
	40 GHz	G/T	10.3	dB/K
FEEDER	satellite Diameter 700 mm			
TX		GAIN	43.9	dBi
	40 GHz	EIRP	52.7	dBW
RX		GAIN	46.2	dBi
	50 GHz	G/T	12.7	dB/K

The assumptions made for the antennas are slightly optimistic, and it has been assumed that they can be installed on the both satellite and HAPs. This gives us an idea of the dimension of the antenna and consequently the associated payloads and the achievable data rate. Subsequently, it will allow to give some guidelines in adjusting the design of the payloads to the right needs. The tables below give the link budget for uplink and downlink for the internodes HAP-LEO for two cases of the elevation angle: 90° (best case) and 10° (worst case). The links are realized in the Q/V band, where the downlink is between 37.5 GHz and 42.5 GHz (bandwidth 5 GHz) and the uplink is between 47.2 GHz and 50.2 GHz (bandwidth 3 GHz), as well as 50.4 GHz and 51.4 GHz.

For the downlink, the full bandwidth 5 GHz is considered for the link and the throughput is between 1 Gbps and 7.8 Gbps.

For the uplink, the power limitation does not allow to close the link budget at low elevation angle with a 3000 MHz bandwidth. Nevertheless, the throughput is between 300 Mbps and 5.2 Gbps.

With this configuration, it should be noted that atmospheric losses will be limited, as HAP are flying at an altitude protected from attenuation due to rain and the real throughput to ensure is not yet evaluated.

TABLE 18: HAP-LEO LINK BUDGET PARAMETERS

	Parameter	Unit	Value
	Band Name	-	Q-V
	Downlink Frequency	GHz	40.00
	Uplink Frequency	GHz	50.00
Constellation	Selection for Feeder Link	-	Upper constellation
	Reference - Number of satellite	-	1269
	Reference - Altitude	km	600
	Reference - Elevation Min	°	10
	Upper - Number of satellite	-	336
	Upper - Altitude /Haps altitude	km	580
	Upper - Elevation Min	°	10
	Selected - Number of satellite	-	336
	Selected - Altitude	km	580
	Selected - Elevation Min	°	10
Satellite	Satellite Antenna Gain Tx	dBi	43.90
	Satellite EIRP	dBW	52.70
	Satellite Antenna Gain Rx	dBi	46.20
	Satellite G/T	dB/K	12.70
HAPS	Gateway Antenna Gain Tx	dBi	38.30
	Gateway EIRP	dBW	46.80
	Gateway Antenna Gain Rx	dBi	37.10
	Gateway G/T	dB/K	10.30
C/I	Downlink (Sat TX)	dB	14
	Uplink (SatRX)	dB	14

TABLE 19: LEO-HAP DOWNLINK BUDGET

		Unit	Downlink SAT --> GW	Downlink SAT --> GW (NADIR)
GLOBAL	Band Name	-	Q-V	Q-V
	Downlink Frequency	**GHz**	**40.00**	**40.00**
	Useful Bandwidth	MHz	5000.00	5000.00
SATELLITE - TX	EIRP	dBW	52.70	52.70
	Satellite altitude	km	580.00	580.00
HAPS - RX	Elevation angle to satellite (seen from UE)	°	10.00	90.00
	Slant Range	km	1885.46	580.00
	Antenna view angle	°	64.51	0.00
	Figure of Merit: G/T	dB/K	10.30	10.30
	Polarisation mismatch loss	dB	0.00	0.00
	Effective G/T	**dB/K**	**10.30**	**10.30**
LOSSES	**Free space propagation**	**dB**	**190.00**	**179.76**
	Atmospheric loss	**dB**	**8.36**	**0.63**
	Shadowing margins	**dB**	**0.00**	**0.00**
	Body loss	dB	0.00	0.00
RESULTS	**Obtained C/N**	**dB**	**-3.82**	**11.10**
	Spectral Efficiency	bits/s/Hz	0.1922	1.5696
	UE Rate	**Mbits/s**	**961.04**	**7847.81**

TABLE 20: HAP-LEO UPLINK BUDGETS

		Unit	Uplink HAPS --> SAT	Uplink HAPS --> SAT (NADIR)
GLOBAL	Band Name	-	Q-V	Q-V
	Uplink Frequency	**GHz**	**50.00**	**50.00**
	Useful Bandwidth	MHz	1000.00	3000.00
HAPS - TX	Elevation angle to satellite	°	10.00	90.00
	Slant Range	km	1885.46	580.00
	Antenna view angle	°	64.51	0.00
	Polarisation mismatch loss	dB	0.00	0.00
	EIRP	**dBW**	**46.80**	**46.80**
SATELLITE - RX	Satellite altitude	km	580.00	580.00
	Figure of merit (G/T)	**dB/K**	**12.70**	**12.70**
LOSSES	**Free space propagation**	**dB**	**191.94**	**181.70**
	Atmospheric loss	**dB**	**9.81**	**2.07**
	Shadowing margins	**dB**	**0.00**	**0.00**
RESULTS	**Obtained C/N**	**dB**	**-3.72**	**8.23**
	Spectral Efficiency	bits/s/Hz	0.2759	1.7227
	UE Rate	**Mbit/s**	**275.940**	**5168.070**

2.2.1.3 HAP-LEO Link Budgets – Optical Technology

The link budgets for the downlink and the uplink of the inter-node link between a HAP and a LEO satellite are presented in Table 21 for three cases of the altitude: 400 km, 600 km and 800 km and for link ranges at two elevation extremes: zenith (90° elevation) and horizon (0° elevation). The latter is physically not doable and is provided for reference purposed only. The link is realized in the optical C-Band (around 1550 nm wavelength). **It is shown that, depending on the link range, data rates of up to 100 Gbps are achievable in both the downlink and the uplink. Especially for higher altitude LEO cases, the link is limited to certain minimum elevation angle to achieve positive link margin. However, even at low elevations and higher LEO altitude, 10 Gbps links are feasible**.

TABLE 21: HAP-LEO OPTICAL LINK BUDGETS

HAP-LEO	DL	UL	DL	UL	DL	UL
Tx altitude [km]	400	20	600	20	800	20
Rx altitude [km]	20	400	20	600	20	800
Tx aperture [mm]	80	30	80	30	80	30
Rx aperture [mm]	30	80	30	80	30	80

Tx power [dBm]		30		30		30
Link range @zenith [km]		380		580		780
Link range @horizon [km]		2238		2785		3254
Atmospheric absorption [dB]				1		
Pointing loss [dB]				3		
Link Margin @10G [dB]		4.5 to 19.89		2.59 to 16.22		1.24 to 13.65
Link Margin @100G [dB]		-5.5 to 9.89		-7.41 to 6.22		-8.76 to 3.65

The following plots illustrate the achievable link capacity as a function of link elevations for various uplink transmit optical powers.

Although optical technology appears superior in terms of data rate, other factors have to be taken into account in order to make a final selection, for instance the effect of the HAP movement onto the pointing performance as well as the power and mass budget considering that the Q/V antenna could be the same used also for the feeder link. Therefore, the final selection will be done in the next issue of this deliverable.
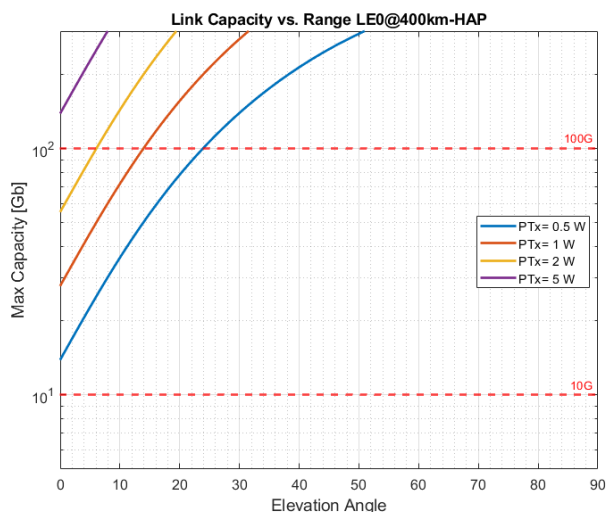

*FIGURE 11: DOWNLINK CAPACITY FOR LEO-HAP LINKS AT 400KM LEO ALTITUDE.*
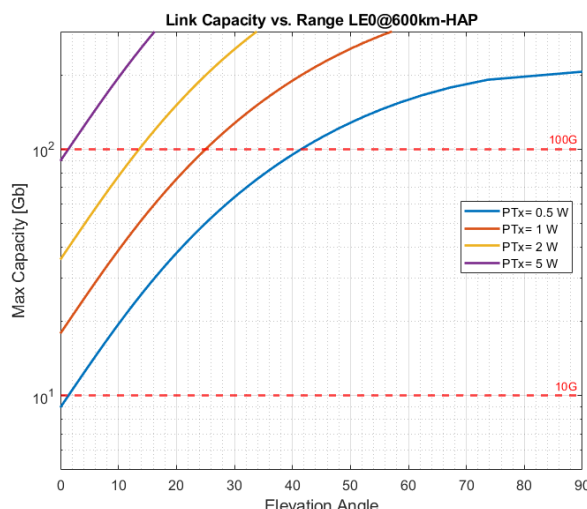
*FIGURE 12: DOWNLINK CAPACITY FOR LEO-HAP LINKS AT 600KM LEO ALTITUDE.*
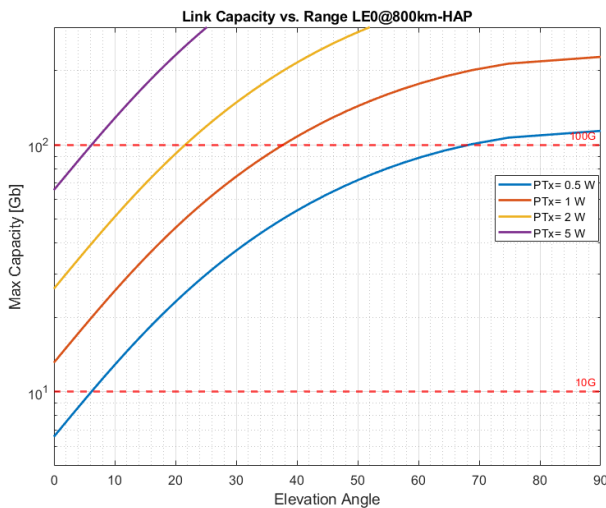
FIGURE 13: DOWNLINK CAPACITY FOR LEO-HAP LINKS AT 800KM LEO ALTITUDE.

2.2.1.4 HAP-GEO Link Budgets – RF Technology

In this case, the results contained in D3.1 has shown that the date rate achievable with RF technology is too low (kbps range). Therefore, only optical technology is considered.

2.2.1.5 HAP-LEO Link Budgets – Optical Technology

The optical link budgets for the downlink and the uplink of the inter-node link between a HAP and a GEO satellite are presented in Table 22. The link is operated at optical C-Band (around 1550 nm wavelength) able to achieve data rates of 10 Gbps with small, but positive link margin. In order to accommodate this link budget, 80 mm terminal aperture at HAP and 250 mm terminal aperture at GEO along with increased transmit power of 2 W would be required. **Whether it's worth to keep the HAP-GEO links, it will be subject of further analysis.**

TABLE 22: HAP-GEO OPTICAL LINK BUDGETS

HAP-GEO	DL	UL
Tx altitude [km]	35768	20
Rx altitude [km]	20	35768
Tx aperture [mm]	250	80
Rx aperture [mm]	80	250
Tx power [dBm]		33
Atmospheric absorption [dB]	1	
Pointing loss [dB]	3	
Link range @zenith [km]	35768	
Link range @horizon [km]	41647	
Link Margin @10G [dB]	0.51 to 1.84	
Link Margin @100G [dB]	-9.49 to -8.16	

The following figure shows the achievable link capacity as a function of link elevations for various uplink transmit optical powers.
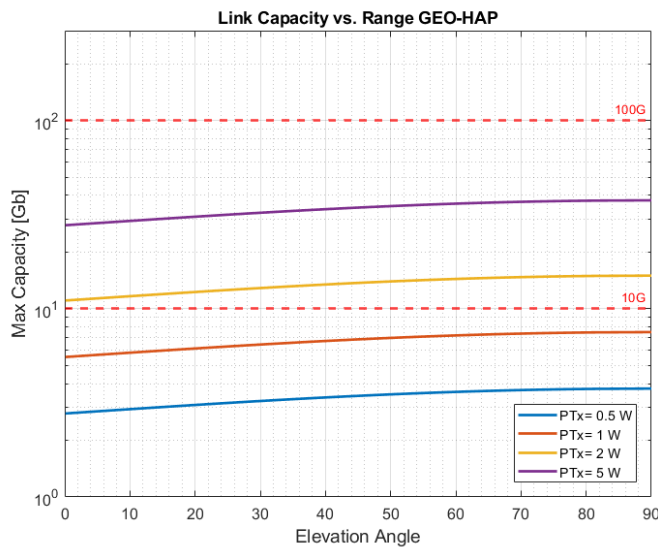
FIGURE 14: DOWNLINK CAPACITY FOR GEO-HAP LINKS.

2.2.2 Intra-Orbit Link Budgets

Optical inter-satellite links (OISL) provide a reliable and high-throughput communication link between two satellites. Different scenarios are investigated, namely:

1. LEO-LEO OISL at various altitudes (400 km, 600 km and 800 km) for a conventional constellation design such as the one presented in Section 1.4.1

2. GEO-GEO OISL assuming three equally spaced GEO satellites on the equatorial belt

3. OISL between service and feeder LEO satellites for the distributed constellation presented in 1.4.2

4. OISL between feeder satellites for the distributed constellation presented in 1.4.2

Note that for intra-plane OISL (Scenario 1), Doppler rates, pointing angles rates as well as fast link switching mechanisms can be neglected lowering such the implementation effort. Inter-plane OISL (Scenarios 2-4) considerations are further discussed in Section 2.2.2.3.

In the following we are presenting link budgets for the individual scenarios including justification for choice of system and channel parameters. The following system parameters are used to define the scenarios:

➲ Link distance

➲ Size (diameter) of the TX and RX apertures

➲ TX power launched from the communications system

➲ Detector sensitivity in photons per bit that defines the required minimum received optical power at given data rate and BER.

Coherent modulation format for both link directions was assumed. This is assumed to be valid for bitrates of 10 Gbps and beyond, where non-coherent modulations (such as on-off keying or pulse-position modulation) require significant implementation effort compared to lower bitrates whilst being inferior in terms of sensitivity and overall performance when compared to coherent (e.g., PSK and QAM) formats. State-of-art coherent communications systems with DP-QPSK modulation, pre-amplification and robust coding are capable of achieving

sensitivities as low as 5 photons per bit (10ppb value used in calculations below to allow for certain implementation margin).

In-line with the current state-of-art development in space optical terminals (based e.g. on SDA recommendation [74]), we neglect interference between individual links. Low divergence of the transmitted beam (<1 mrad) in combination with narrow field-of-view (FOV) of individual terminals (~few mrad) ensures stable tracking. During acquisition, identification of the individual terminals is ensured during link (switchover) planning (based on the ephemeris) and using complementary wavelength bands for transmission and reception that can be planned considering also link geometry on-orbit. Additional strategies, such as link identification via tracking system or at link layer could be considered.

In general, channel is modelled as loss-less AWGN (Additive White Gaussian Noise) channel absent of non-linearities. Losses are considered constant and described as follows:

- Free-space propagation is modelled as free-space loss due to link distance and wavelength

- TX and RX Gains are those inherent to the telescope size. The different values reflect the fact that whilst reception occurs over the entire aperture, the transmitted beam must be smaller than the mechanical size of the telescope to avoid diffraction effects (by a factor of $2^{1/2}$)

- Optical losses at the transmitter and receiver are due to imperfect transmission and reflection properties of the optics

Furthermore, we use optical system properties such as:

- RX splitting loss to model the loss due to splitting part of the optical power used for the tracking of the optical terminals

- RX coupling loss models the limited performance of the optical fibre-coupling subsystem

- Last, we assumed 4dB coding gain provided by a low-complexity channel code.

2.2.2.1　LEO-LEO Link Budgets

Orbital parameters of a LEO-LEO link are as follows:

TABLE 23: ORBITAL PARAMETERS LEO (ALL VALUES IN KM)

Altitude	ISL Range (in-plane)	ISL Range (adjacent plane)
400	1059	1074
600	1567	1572
800	2065	2039

TABLE 24: LINK BUDGET LEO OISL WITH 30MM APERTURE

Parameter	Units	LEO-LEO at 400 km	LEO-LEO at 600 km	LEO-LEO at 800 km
Link Distance	km	1070	1570	2060
Tx Aperture	cm	0.03		
Rx Aperture	cm	0.03		

Parameter	Units			
Tx Power	dBm	**37.0**		
Tx Gain	dB	92.6		
Tx Optical Loss	dB	-0.7		
Tx Pointing Loss	dB	-2.0		
Free Space Loss	dB	-258.8	-262.1	-264.5
Rx Gain	dB	95.7		
Rx Optical Loss	dB	-1.5		
Coding Gain	dB	4.0		
Rx Splitting Loss	dB	-1.0		
Rx Coupling Loss	dB	-3.0		
Received optical power	dBm	-41.7	-45.0	-47.4
Effective received optical power*	dBm	-37.7	-41.0	-43.4
Detector Sensitivity	PPB	10		
Req. Power at 10G	dBm	-49.0		
Link Margin at 10G	dB	**11.3**	**8.0**	**5.6**
Req. Power at 100G	dBm	-39.0		
Link Margin at 100G	dB	**1.3**	**-2.0**	**-4.4**

* the effective optical power considers coding gain w.r.t the (nominal) received optical power.

From the provided link budgets for 30 mm aperture we can observe that whilst 10G OISL is feasible, 100G OISL is only feasible for lowest altitudes (400 km). By increasing the aperture size to 80 mm (e.g., TESAT SCOT-80 optical terminal [7]), the 100G OISL is feasible even with one tenth of the optical power (500 mW) compared to the case with small aperture.

TABLE 25: LINK BUDGET LEO OISL WITH 80MM APERTURE.
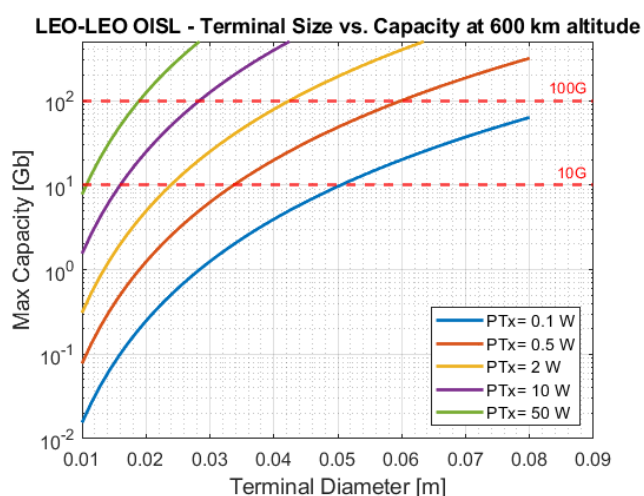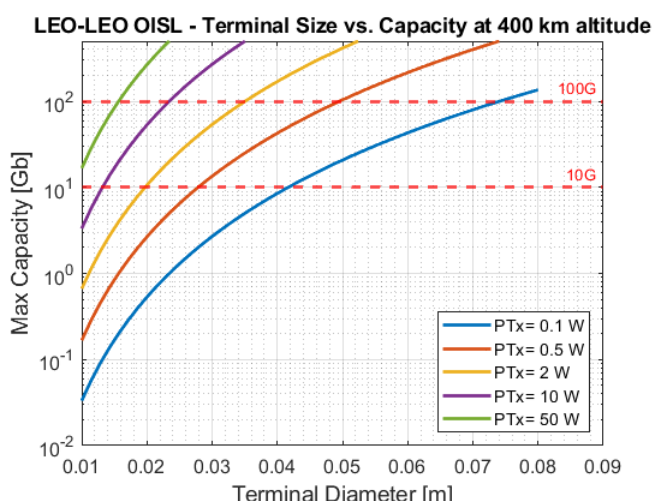
Parameter	Units	LEO-LEO at 400 km	LEO-LEO at 600 km	LEO-LEO at 800 km
Link Distance	km	1070	1570	2060
Tx Aperture	m	**0.08**		
Rx Aperture	m	**0.08**		
Tx Power	dBm	**27.0**		
Tx Gain	dB	101.2		
Tx Optical Loss	dB	-0.7		
Tx Pointing Loss	dB	-2.0		
Free Space Loss	dB	-258.8	-262.1	-264.5
Rx Gain	dB	104.2		
Rx Optical Loss	dB	-1.5		

Coding Gain	dB	4.0		
Rx Splitting Loss	dB	-1.0		
Rx Coupling Loss	dB	-3.0		
Received optical power	dBm	-34.6	-37.9	-40.3
Effective received optical power*	dBm	-30.6	-33.9	-36.3
Detector Sensitivity	PPB	10		
Req. Power at 10G	dBm	-49.0		
Link Margin at 10G	dB	18.4	15.1	12.7
Req. Power at 100G	dBm	-39.0		
Link Margin at 100G	dB	8.4	5.1	2.7

* the effective optical power considers coding gain w.r.t the (nominal) received optical power.

The dependency of the achievable capacity in Gbps on the optical terminal aperture diameter with launch (transmit) power as parameter is also shown in following graphs (reported as Figure 15) for 400km, 600km and 800km LEO OISL scenarios.
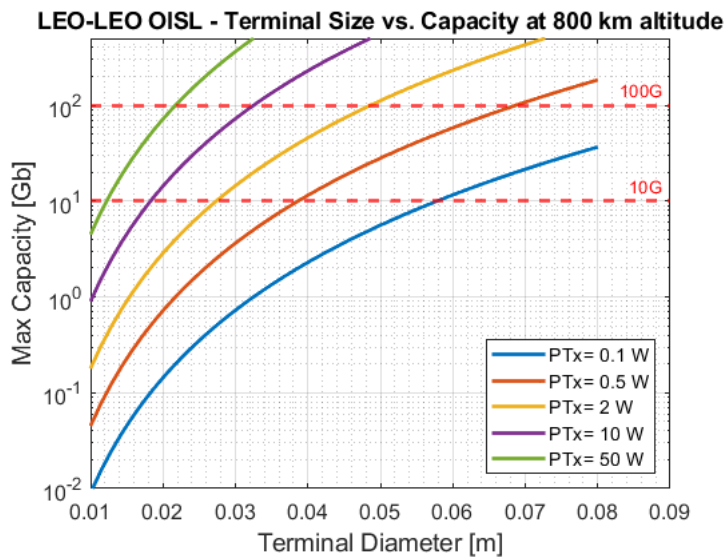
FIGURE 15: CAPACITY ASSESSMENT IN GBPS OF A LEO OISL AS A FUNCTION OF THE USED TERMINAL DIAMETER FOR VARIOUS TRANSMITTED OPTICAL POWER LEVELS AND DIFFERENT ALTITUDES

2.2.2.2 GEO-GEO Link Budgets

Assuming 70 mm aperture (e.g., SmartLCT), the link budget for 70,000 km GEO OISL cannot be closed. In order to reach 10G GEO OISL, the optical power would need to be increased to 100W (50dBm) – such technology is not yet available for space applications, but is currently under development in an ESA contract.

Alternatively, the aperture size would need to be increased to 250 mm (such as 260 mm telescope on the recently-launched TELEO demonstration on-board BADR-8 satellite [8]) to enable 100G GEO-GEO OISL. The dependency of the achievable capacity for various terminal aperture sizes and launch (transmit) powers is also illustrated in Figure 16.

TABLE 26: LINK BUDGET GEO OISL FOR TWO DIFFERENT APERTURE SIZES

Parameter	Units	GEO-GEO	GEO-GEO
Link Distance	km	70000	
Tx Aperture	m	0.07	0.25
Rx Aperture	m	0.07	0.25
Tx Power	dBm	37.0	
Tx Gain	dB	100.0	111.1
Tx Optical Loss	dB	-0.7	
Tx Pointing Loss	dB	-2.0	
Free Space Loss	dB	-295.1	
Rx Gain	dB	103.0	114.1
Rx Optical Loss	dB	-1.5	
Coding Gain	dB	4.0	
Rx Splitting Loss	dB	-1.0	
Rx Coupling Loss	dB	-3.0	

Total Transmission	dBm	-63.3	-41.1
Effective Power	dBm	-59.3	-37.1
Detector Sensitivity	PPB	10	
Req. Power at 10G	dBm	-49.0	
Link Margin at 10G	dB	**-10.3**	**11.9**
Req. Power at 100G	dBm	-39.0	
Link Margin at 100G	dB	**-20.3**	**1.9**
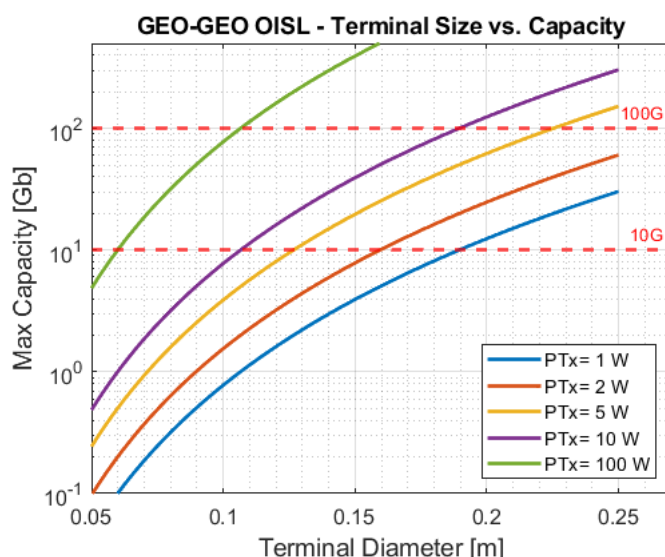
FIGURE 16: CAPACITY ASSESSMENT IN GBPS OF A GEO OISL AS A FUNCTION OF THE USED TERMINAL DIAMETER FOR VARIOUS TRANSMITTED OPTICAL POWER LEVELS.

2.2.2.3 Service-Feeder OISL

Last, we consider Service-Feeder scenario. For the sake of the analysis we first consider symmetrical nodes (i.e. same TX and RX sizes). This allows us to investigate the changing link geometry as can be seen in Figure 17. However, one may want to scale the aperture sizes to close the link budget for a given target data rate.

Link distance variation in this scenario is relatively small and causes only minimal changes in physical RTT (UE → Service Satellite → Feeder Satellite and back) at most approx. 15-20%. Azimuth and elevation graphs show that nearly hemispherical coarse pointing assembly (CPA) would be required, but at given (very small) angular rates and considered terminal sizes, such CPA realizations are commercially available.

Considering maximum link distance of 820 km and following link capacity considerations in Section 2.2.2.1, capacity estimations for asymmetrical system realizations i.e. for different service and feeder satellite optical terminal sizes were analyzed for 10 Gbps and 100 Gbps link capacities in Figure 18 at the top and bottom, respectively.
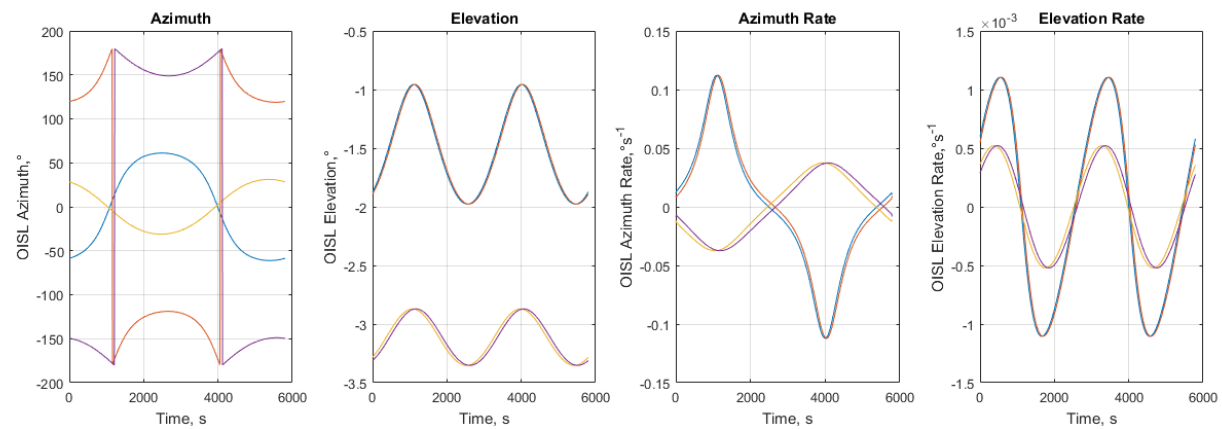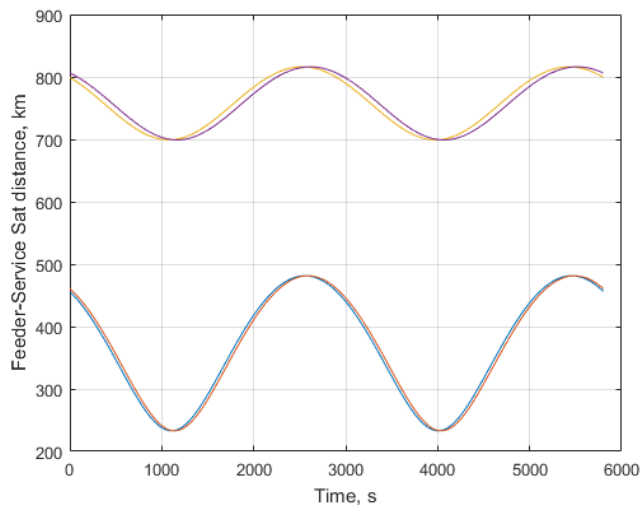
FIGURE 17: LINK DISTANCE (TOP) AND AZIMUTH AND ELEVATION ANGLES AND RATES (BOTTOM) IN SERVICE-FEEDER OISL SCENARIO.
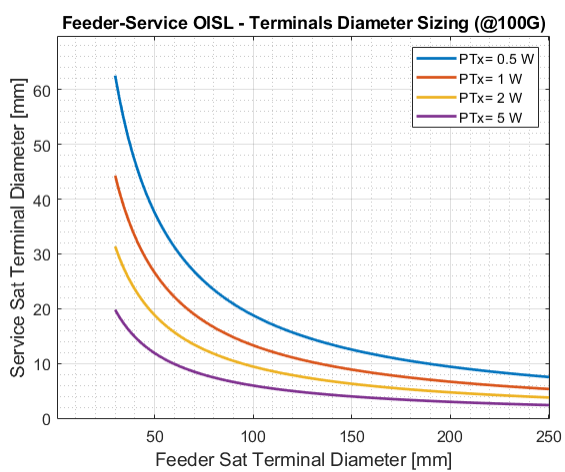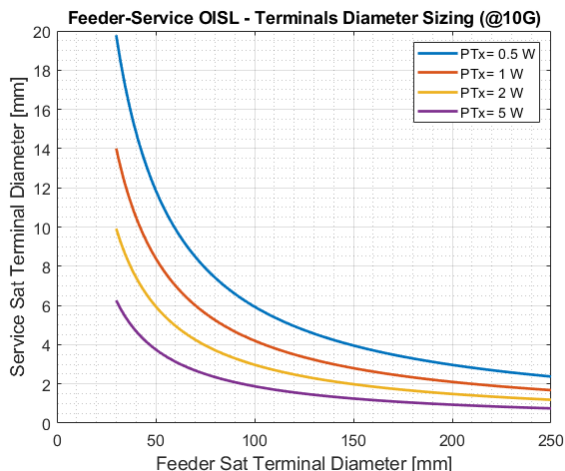
FIGURE 18: TERMINAL SIZING FOR SERVICE AND FEEDER SATELLITE OPTICAL TERMINALS FOR VARIOUS (FEEDER) TRANSMIT POWERS AT 10GBPS (TOP) AND 100GBPS (BOTTOM).

2.2.2.4 Feeder-Feeder OISL

For Feeder-Feeder OISL, the situation varies, whether intra-plane or inter-plane OISLs are considered. Figure 19 shows nearly constant link distance of approx. 1850 km for intra-plane OISL, but significant variation for inter-plane OISL. In such scenario, adaptive data rates or modulation formats or transmit power (or a combination of these) can be used to optimize the available resources at the cost of reduced link capacity or achievable link distance (and so coverage).

In Figure 19 one can also observe somewhat reduced field-of-regard, which allows for more flexibility in the optical terminal placement on the spacecraft, for instance at positions that would provide partially obscuration by other payloads, antennas or solar panels. More critically, angular (particularly azimuth) rates at link switchovers would not allow for an instantaneous switchover around polar regions. Gaps in order of lower tens of seconds are expected as angular rates up to approx. 5 deg/s are more realistic. This only includes physical link re-acquisition and omits the additional delay caused by data and link layers.

Finally, Figure 20 shows the nominal link capacity as a function of terminal diameter and for different values of the optical power.
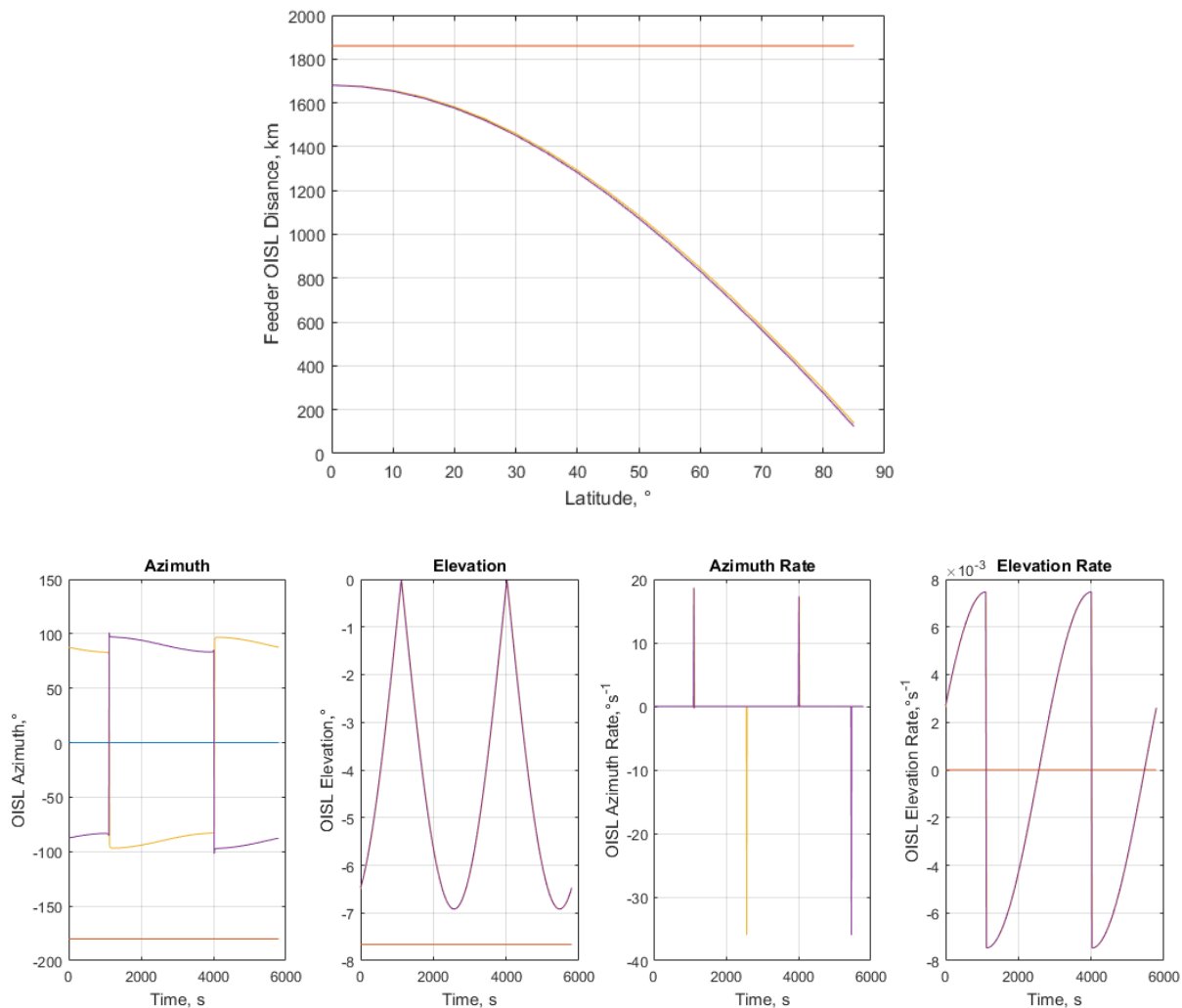
FIGURE 19: TOP: FEEDER-FEEDER OISL DISTANCE ANALYSIS FOR INTRA-PLANE (YELLOW) AND INTER-PLANE (RED) OISL. BOTTOM: AZIMUTH AND ELEVATION ANGLES AND RATES.
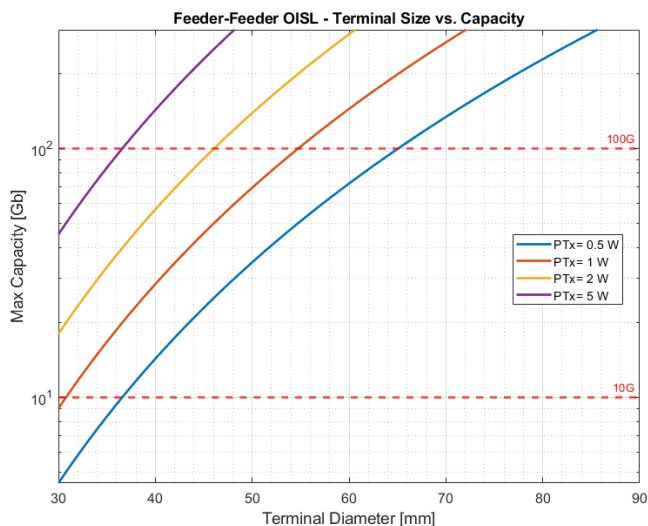

FIGURE 20: CAPACITY ASSESSMENT IN GBPS OF A FEEDER-FEEDER OISL AS A FUNCTION OF THE USED TERMINAL DIAMETER FOR VARIOUS TRANSMITTED OPTICAL POWER LEVELS.

To overcome the aforementioned problem an alternative (diagonal) configuration is being considered in T3.4, as shown in Figure 21 (vs. rightmost picture of Figure 5). A slightly longer however more constant link distances for both inter-plane and intra-plane OISLs can be achieved, with max. distance of approx. 2040 km. For this distance, capacity assessment was also carried out and is shown in Figure 22. As discussed at the beginning of Section 2.2.2, relatively small angles between individual links is considered to not cause any interference.
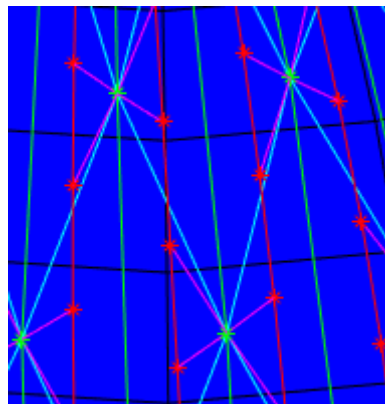

FIGURE 21: DISTRIBUTION OF FEEDER (GREEN) AND SERVICE (RED) SATELLITES ON ORBIT WITH SERVICE-FEEDER OISL (MAGENTA) AND FEEDER-FEEDER OISL (CYAN).
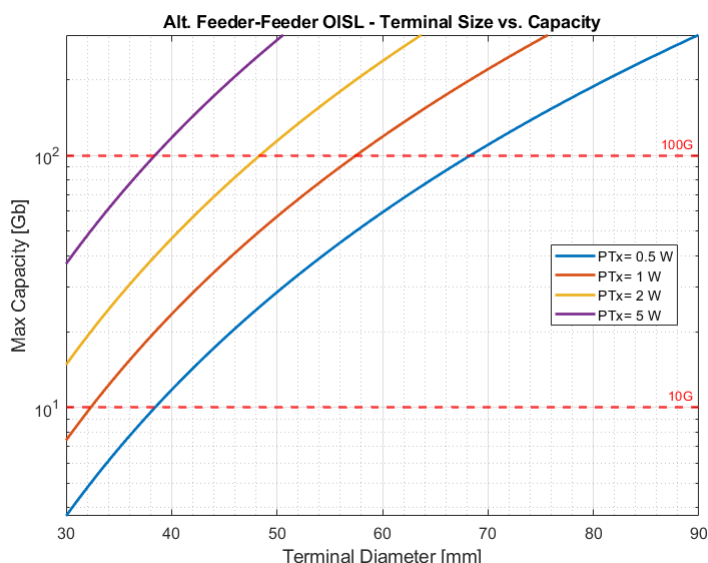

FIGURE 22: CAPACITY ASSESSMENT IN GBPS OF AN ALTERNATIVE FEEDER-FEEDER OISL AS A FUNCTION OF THE USED TERMINAL DIAMETER FOR VARIOUS TRANSMITTED OPTICAL POWER LEVELS.

2.2.2.5 Size, Weight and Power Requirements for Optical Terminals

Size, Weight and Power (SWaP) for given datarates is an essential consideration in an overall technical budget of the payload. For LEO terminal, DLR OSIRISv3 and NASA T-BIRD developments were considered as a baseline to establish a reasonable SWaP estimate for 10G and 100G LEO terminals with 30mm and 80mm apertures, respectively.

TABLE 27: SWAP ESTIMATE FOR OPTICAL TERMINALS. WHERE * INDICATES ASSUMPTION OF COTS COHERENT 100G TRANSCEIVER UPGRADE.

	OSIRISv3 / TOSIRS [75]	T-BIRD [9]	LEO 6G-NTN	LEO 6G-NTN
Size [U / mm3]	*150x200x280*	*100x200x300*	*~100x200x200*	*~100x200x300*
Weigt [kg]	*~10**	*<3*	13	20+
Power [W]	*~150**	*100*	75 to 130	100-200
Aperture [mm]	*30*	*22-23*	**30**	**80**
Data rate	*1G*	*200G*	**10G**	**100G**

2.3 FEEDER LINKS

The feeder link budgets for LEO satellites assumes 99.5% availability, clear sky conditions and a ground station located in Toulouse.

In order to estimate the capacity of the feeder links, we need to define the size of the antennas and realistic parameters for estimating the achievable throughput. The aim is not to perform a sensitivity analysis, but to make reasonable assumptions on what will be achievable in the near future (2030), even if it means adjusting the design for optimization raisons. The table below summarise the characteristics of the space and ground antennas and the parameters used for the link budget calculation.

TABLE 28: ANTENNA PERFORMANCES GROUND STATION AND FEEDER SATELLITE

GATEWAY	earth		Diameter 9.3 m	
TX		GAIN	67.9	dBi
	50 GHz	EIRP	87.0	dBW
RX		GAIN	68.4	dBi
	40 GHz	G/T	40.7	dB.K^{-1}

FEEDER	satellite	diameter 700 mm		
TX		GAIN	43.9	dBi
	40 GHz	EIRP	52.7	dBW
RX		GAIN	46.2	dBi
	50 GHz	G/T	12.7	dB.K^{-1}

TABLE 29: PARAMETERS FOR LINK BUDGET COMPUTATION

	Parameter	Unit	Value
	Band Name	-	Q-V
	Downlink Frequency	GHz	40.00
	Uplink Frequency	GHz	50.00
Constellation	Selection for Feeder Link	-	Upper constellation
	Reference - Number of satellite	-	1380
	Reference - Altitude	km	600
	Reference - Elevation Min	°	10
	Upper - Number of satellite	-	196
	Upper - Altitude	km	600
	Upper - Elevation Min	°	10
	Selected - Number of satellite	-	196
	Selected - Altitude	km	600
	Selected - Elevation Min	°	10
Satellite	Satellite Antenna Gain Tx	dBi	43.90
	Satellite EIRP	dBW	52.70
	Satellite Antenna Gain Rx	dBi	46.20
	Satellite G/T	dB/K	12.70
Gateway	Gateway Antenna Gain Tx	dBi	67.90
	Gateway EIRP	dBW	87.00
	Gateway Antenna Gain Rx	dBi	68.40
	Gateway G/T	dB/K	40.70
C/I	Downlink (Sat TX)	dB	18
	Uplink (SatRX)	dB	18

2.3.1 Uplink and Downlink Budgets

The link budget is driven by the C/I of the link. This value is a hypothesis taken and will depend on the interference environment. In other words, it depends on the number of stations and their distribution. Nevertheless, these antennas are very large compared to the working wavelength, which suggests that the C/I value is achievable. However, in the budget we have limited ourselves to spectral efficiency, which leaves room for strong attenuation and availability, especially in tropical areas.

In all tables, the throughput has been calculated by limiting the spectral efficiency in NR to 2.7140 bits/s/Hz in uplink and 1.39 bits/s/Hz in downlink. It is possible to work at higher spectral efficiencies, which would enable access to higher throughput if needed. Simulations are currently underway to estimate the spectral efficiency of NR for high C/N. It is also possible to provide the link using DVB-S2x with higher data rates, and to reach flow rates 2 or 3 times higher than the values reported above. There are several possible ways to investigate, bearing in mind that the system will have to be optimized in terms of deployment cost, which also presupposes optimal dimensioning of the ground stations (antenna size/power/number).

As a consequence, and for starting the dimensioning of number of ground station, the value fixed to evaluate each feeder link are shown in the table below. These are target values rather than values to be optimized, and it will be necessary to guarantee them to a certain extent by playing on the design elements of NF antennas in the amplification chain, SSPA or TWTA, antenna surface, as well as pointing errors. The sensitivity of the link to handover and overhead have not been evaluated.

TABLE 30: UPLINK BUDGET

		Unit	Uplink GW --> SAT (NADIR)
GLOBAL	Band Name	-	Q-V
	Uplink Frequency	**GHz**	**50.00**
	Useful Bandwidth	MHz	3000.00
GATEWAY - TX	Elevation angle to satellite	°	90.00
	Slant Range	km	600.00
	Antenna view angle	°	0.00
	Polarisation mismatch loss	dB	0.00
	EIRP	**dBW**	**87.00**
SATELLITE - RX	Satellite altitude	km	600.00
	Figure of merit (G/T)	**dB/K**	**12.70**
LOSSES	**Free space propagation**	**dB**	**181.99**
	Propagation losses computation	-	Computation [RD1] & [RD2]
	UE location	-	Toulouse
	Weather condition	-	Clear Sky
	Atmospheric loss	**dB**	**2.07**
	Shadowing margins	**dB**	**0.00**
INTERMEDIATE RESULT	C/No	dBHz	144.2
	C/N	dB	49.5
	C/Io	dBHz	112.77
	C/I	dB	18.00
	C/(No+Io)	dBHz	112.77
	Overall C/(No+Io) (including Global Losses)	dBHz	112.77
RESULTS	**Obtained C/N**	**dB**	**18.00**
	Spectral Efficiency	bits/s/Hz	2.7140
	UE Rate	**Mbit/s**	**8142.120**

TABLE 31: DOWNLINK BUDGET

		Unit	Downlink SAT --> GW (NADIR)
GLOBAL	Band Name	-	Q-V
	Downlink Frequency	**GHz**	**40.00**
	Useful Bandwidth	MHz	5000.00
SATELLITE - TX	**EIRP**	**dBW**	**52.70**
	Satellite altitude	km	600.00
GATEWAY - RX	Elevation angle to satellite (seen from UE)	°	90.00
	Slant Range	km	600.00
	Antenna view angle	°	0.00
	Figure of Merit: G/T	dB/K	40.70
	Polarisation mismatch loss	dB	0.00
	Effective G/T	**dB/K**	**40.70**
LOSSES	**Free space propagation**	**dB**	**180.05**
	Propagation losses computation	-	Computation [RD1] & [RD2]
	UE location	-	Toulouse
	Weather condition	-	Clear Sky
	Atmospheric loss	**dB**	**0.63**
INTERMEDIATE RESULTS	C/No	dBHz	141.31
	C/N	dB	44.32
	C/Io	dBHz	114.99
	C/I	dB	18.00
	C/(No+Io)	dBHz	114.98
	Overall C/(No+Io) (including Global Losses)	dBHz	114.98
RESULTS	**Obtained C/N**	**dB**	**17.99**
	Spectral Efficiency	bits/s/Hz	1.3901
	UE Rate	**Mbits/s**	**6950.73**

TABLE 32: CAPACITY FEEDER/GATEWAYS LINKS

FEEDER	(double polarization)	
	Tx	Rx
	Gbps	Gbps
	13.9	**16.3**

2.4 PRELIMINARY THROUGHPUT/CAPACITY ESTIMATION

This chapter provides an initial throughput/capacity estimation for a LEO multi-beam satellite. More precisely, we estimate the achievable aggregate data rates of the C- and Q/V band service links of a LEO multi-beam satellite. For this, we assume that the satellite is power-limited with a maximum downlink beam usage up to 20% in C band and up to 12% in Q/V band. Furthermore, we assume a geographically uniform distribution of the users and traffic load. In such a scenario the available spectrum is only partially used in each of the satellite beams so that inter beam interference is avoided.

For user uplinks, a LEO satellite could in principle support a higher beam usage and thus higher aggregated data rates than for user downlinks, but many applications are characterized by higher or similar data rates in the downlink and might not need higher data rates in the uplink.

2.4.1 Throughput/Capacity Estimation for C-Band

The following parameters have been assumed for the C-band service links of a LEO multi-beam satellite:

- Beam size: 45 km hexagonal lattice
- Number of beams: 499 beams (EL 45°)
- Geographically uniform distribution of users and traffic load
- Uplink and downlink beam usage: 5%, 10% and 20%
- Frequency reuse / interference avoidance: achieved with low uplink and downlink beam usage
- Available bandwidth: 100 MHz up, 100 MHz down (FDD)
- Number of PRBs: 273 up, 273 down
- PRB bandwidth: 360 kHz
- Total bandwidth of all PRBs: 95.04 MHz up, 95.04 MHz down

7) Table 33 summarizes the performances of the service link detailed in The objective is to evaluate the max throughput achievable by a user. In other word what the satellite could offer in term of maximum throughput for a single user located at nadir, transmitting at maximum power (23 dBm) and using the maximum possible number of PRBs. A UE could achieve a maximum of 7 Mbps of uplink throughput in this scenario.

8) The objective is to evaluate the throughput achievable by a user using only 1 PRB and transmitting at maximum power. Users are on a cell around the nadir and 100 cells are active. The aggregate peak throughput is 19.5 Gbits in this scenario.

9) The objective is to evaluate the throughput achievable by a user using only 1 PRB and transmitting at maximum power. Users are on a cell around the edge of coverage and 100 cells are active. The aggregate min throughput is 13.4 Gbits in this scenario.

10) The objective is to evaluate the throughput achievable by a user using only 1 PRB and transmitting at maximum power. Users are distributed between nadir (30%) and edge (70%) and 100 cells are active. The aggregate average throughput is 15.2 Gbits in this scenario.

11) The objective is to evaluate the max throughput achievable by a user in light indoor scenario (10 dB additional attenuation). In other word what the satellite could achieve in term of maximum throughput for a user located at nadir, transmitting at maximum power (23 dBm) and using the maximum possible number of PRBs. A UE could achieve a maximum of 750 kbps of uplink throughput in this scenario.

12) The objective is to evaluate the instantaneous throughput over 100 cells (active beams) with 100 users uniformly distributed between nadir (30%) and edge (70%). This figure could be scaled according to the number of real users by cell and by applying the beam hopping scheme of 1/5.

Table 6 and Table 8. The table gives the number of cells that the satellite shall cover due to the superposition of the coverage (imposed by handover constraints) and also due to the polar orbit. The effective number of cells to cover is reduced and less than 499 cells.

The total throughput of the constellation has been computed taking into account the fact that the satellite can cover only 25, 50 or 100 cells simultaneously for a given EIRP flux density per beam. If the number of cells is larger than these values then a beam-hopping process is used to share the available capacity.

By taking into account the hypothesis of

Table 32 and Table 33 and Figure 23, the aggregated throughput of the constellation has been evaluated together with the number of feeders/gateways needed for the overall constellation. The number of feeder satellite is 336 in the concept of distributed constellation presented in Section 1.4.2, two feeder links per satellite (for handover and redundancy) shall fulfil the need.

TABLE 33: CAPACITY OF THE C-BAND LINK FOR 100 ACTIVES BEAMS

USER link						
		nb active cells		**Tx**		**Rx**
			Gbps		Gbps	
Throughput	for	100	4.8			15.2
			Gbps		Gbps	
Throughput	per cell	1	0.048			0.152
Activity factor		30%				
hypothesis service type						
	Mesh	%	10%			
	Star	%	90%			
HANDOVER	2 sat in visibility	second	10			
	% of cell to cover by 2 sat		10%			
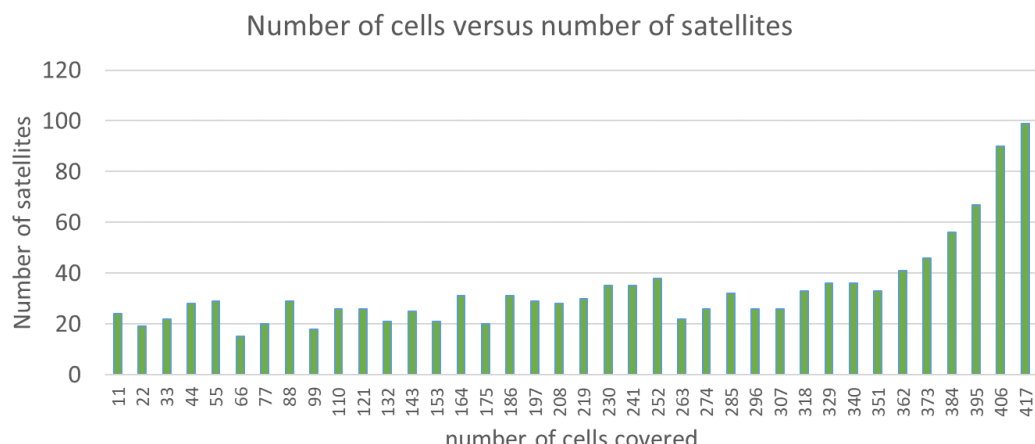
FIGURE 23: NUMBER OF CELLS VERSUS NUMBER OF SATELLITES

TABLE 34: AGGREGATED CONSTELLATION THROUGHPUT / NUMBER OF FEEDERS/GATEWAYS NEEDED

	Aggregated throughput		nb of feeder	
nb active beams	Tx	Rx	Tx	Rx
28 dBW/MHz per beam	Gbps	Gbps		
25	451	1429	29	79
50	885	2801	57	155
100	1693	5361	110	296

2.4.2

2.4.3 Throughput/Capacity Estimation for Q/V-Band

The following parameters have been assumed for the Q/V-band service links of a LEO multi-beam satellite:

- Beam size: 45 km

- Number of beams: 499 beams (EL 45°)

- Geographically uniform distribution of users and traffic load

- Beam usage: 28 and 56 beams 5,6% and 11,2%

- Frequency reuse / interference avoidance: achieved with low uplink and downlink beam usage

- Available bandwidth: 400 MHz up, 400 MHz down

- Number of PRBs: 264 up, 264 down

- PRB bandwidth: 1440 kHz

- Total bandwidth of all PRBs: 380.16 MHz up, 380.16 MHz down

The table below summarizes the value found in the analysis of the performances of the antenna in Q/V band. The values take the maximum data rate of each satellite. A hypothesis has been taken in the service mesh and star and need to be consolidated. Moreover, an activity factor of 30% have be taken to evaluate the maximum throughput that the constellation shall handle. All these values shall be reviewed with and more consolidated approach and investigation on what is the

TABLE 35: CAPACITY OF THE QV-LINK FOR 56 ACTIVES BEAMS

USER						
		nb cell		**Tx**		**Rx**
			Gbps		Gbps	
throughput	for	56	17.68			48
			Gbps		Gbps	
throughput	per cell	1	0.32			0.86
activity factor		30%				
hypothesis srevice type						
	Mesh	%	10%			
	Star	%	90%			
HANDOVER	2 sat in visibility	second	10			
	% of cell to cover by 2 sat		10%			

With these parameters we get a maximum aggregate data rate of 48 Gbps in the uplink beams and of 17.68 Gbps in the downlink beams (per satellite) with 56 actives beams.

Due to the higher spectral efficiency in the uplink, the aggregate data rate in the uplinks is higher than in the downlinks. Since these higher uplink data rates might be not needed for most of the applications, the transmit power and uplink spectral efficiency of the Q/V band user terminals could be reduced to achieve similar data rates in the uplinks than in the downlinks.

By taking into account the hypothesis of

Table 32, Table 33 and Figure 23, the aggregated throughput of the constellation has been evaluated together with the number of feeders/gateways needed for the overall constellation. The number of LEO Link satellite is 336 in the concept of in the concept of distributed constellation presented in Section 1.4.2, three feeder links per satellite (for handover and redundancy) shall fulfil the needs.

TABLE 36: AGGREGATED CONSTELLATION THROUGHPUT / NUMBER OF FEEDERS/GATEWAYS NEEDED

	Aggregated throughput		nb of feeder	
nb active beams	**Tx**	**Rx**	**Tx**	**Rx**
18.2 dBW/MHz per beam	Gbps	Gbps		
28	2984	8002	215	492
56	5835	15225	420	935

2.4.4 Summary of Links Capacity

A calculation of the maximum throughput that can be carried by the various links is shown in the figure below. This is a preliminary dimensioning to estimate the areas of work: system dimensioning, identification of blocking points (bottlenecks) and orientation of the subsequent design effort.
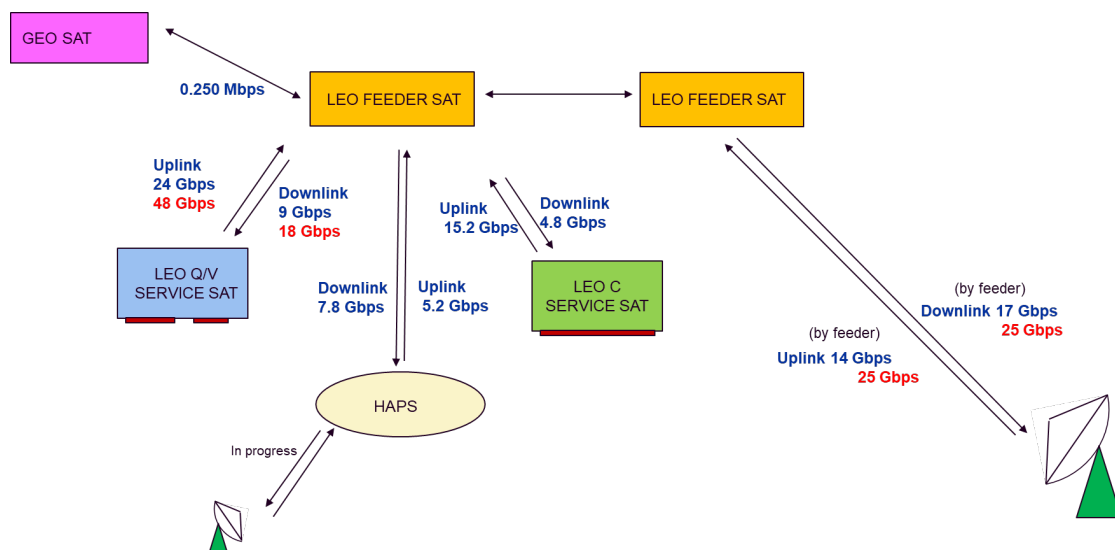
FIGURE 24: SUMMARY OF LINKS CAPACITY

The following comments are in order:

➲ The aggregate throughput of the LEO services satellites has been estimated for a given consumption/dissipation capacity taking into account the service link budgets from section 2.1. These figures could evolve in the rest of project taking into account cost/volume/mass constraints. Moreover, depending on the functional split architecture (discussed in the next chapter), there might be a bandwidth expansion factor to be considered (see section 3.2.1) → **OISL at 100 Gbps shall be considered as baseline here**.

➲ For HAP-LEO links no aggregate throughput deriving from the service link budgets is available yet, so Figure 24: Summary of Links capacityFigure 24 reports the result of the link budget with RF technology presented in section 2.2.1.2. Alternatively, a 10 Gbps optical link could be used.

- The requirements for the optical ISL between feeder satellites depend on several points such as:

    - the adopted functional split
    - the routing algorithms
    - the number of ground stations
    - the % of traffic which might be processed on board each satellite

    → **OISL at 100 Gbps seems a reasonable baseline, but further and more detailed analysis through simulations need to be performed to consolidate this assumption.**

- Similar considerations apply to the feeder links, where in additional it shall be taken into account whether or not each country requires to have at least one gateway (e.g. for security reasons) and the necessity to have at least two feeders per satellite to ensure handover. However the feeder links can be optimized in terms of throughput according to the needs by adding more ground stations or increasing each ground station capability, so this part of the space network is not considered a potential bottleneck.

3 INITIAL 6G-NTN FUNCTIONAL ARCHITECTURE

Throughout this chapter we will assume 5G terminology in the lack of a better alternative as 6G is not yet standardized. Moreover, unless otherwise specified, we will typically make use of the terminology commonly adopted by O-RAN, where the following three main elements of a gNB are considered, as summarised in [10]:

➲ **RU**: this is the radio unit that handles the digital front end and the parts of the PHY layer, as well as the digital beamforming functionality.

➲ **DU**: this is the distributed unit that sits close to the RU and runs the RLC, MAC, and parts of the PHY layer. This logical node includes a subset of the gNB functions, depending on the functional split option, and its operation is controlled by the CU.

➲ **CU**: this is the centralized unit that runs the RRC and PDCP layers. The gNB consists of a CU and (at least) one DU connected to the CU via Fs-C and Fs-U interfaces for CP and UP respectively. A CU with multiple DUs will support multiple gNBs. The split architecture allows to utilize different distribution of protocol stacks between CU and DUs depending on midhaul availability and network design. It is a logical node that includes the gNB functions like transfer of user data, mobility control, RAN sharing (MORAN), positioning, session management etc., with the exception of functions that are allocated exclusively to the DU. The CU controls the operation of several DUs over the midhaul interface.

3.1 OVERVIEW OF SPLIT OPTIONS FOR 6G-NTN

This section discusses the relevance in the context of 6G-NTN of the several architectural options, which were studied and captured in [1] during the development of 5G NTN, namely:

➲ Transparent satellite as sketched in Figure 25. It shall be mentioned that this is the baseline architecture assumption for Release 17/18 NTN design. In this option, no RAN and CN functionalities are implemented in space.

In 6G-NTN the objective is that the LEO satellite payloads will be based on a regenerative architecture meaning that data can be processed and routed based on the properties of the data. **This means that for the LEO constellation, which is the focus of this chapter, no transparent (repeater like) architecture as in Figure 25 will be studied. However, for GEO and HAPs, transparent payloads as depicted in Figure 25 might still be applicable.**
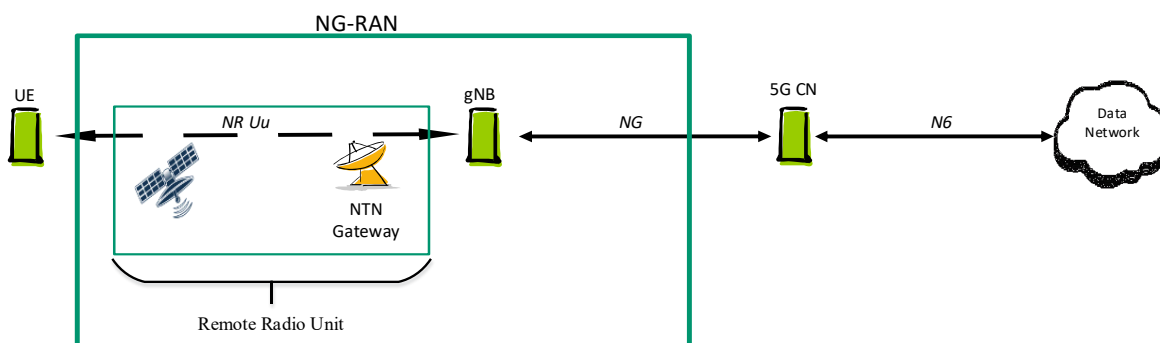

FIGURE 25: TRANSPARENT PAYLOAD [1]

➲ Regenerative satellite with full gNB on board, as sketched in Figure 26 which shall be supported by Rel-19 .

This option foresees the integration of all required protocol stacks in the gNB to be implemented on the mobile base station, which implies the complete RU, gNB-DU and gNB-CU for the user as well as the control plane.

With a full base station onboard, the complete radio protocol stack must be implemented in each satellite, this would be SDAP (Service Data Adaptation Protocol), RRC (Radio Resource Control), PDCP (Packet Data Convergence protocol), RLC (Radio Link Control), MAC (Medium Access Control) and PHY (Physical). The feeder link (or the combination of ISLs and feeder links in case the satellite has no direct visibility to a ground station) will transport traditional backhaul, which for 5G would be NG interface between core and base station to transport N1, N2 and N3 from the 5G core and also Xn. All RRC signaling between the UE and gNB would be terminated in the satellite. The required capacity of ISLs and feeder links would scale with requested user data. One important observation is that the NG interface was not specified for frequent set-up / tear down due to a moving base station. That may be required when a satellite connects to another ground station. In future standardization of 6G, base station mobility capability should also be addressed.

One additional extension of this solution foresees the need for also bringing selected CN functionalities to space. The 5G core network is defined in logically independent functions and their placement is a matter of implementation. 6G Core is likely an evolution of 5G Core where incremental additions to the 5G Core will take place based on the need of new capabilities, but the concept of logically independent functions will be preserved. Adding CN functionalities in the satellites shall be evaluated regarding cost, complexity, power consumption, and its relation to use cases. For instance, one of the functions of the core that could facilitate the use case of UE-to-UE link over one satellite without the need to route traffic through a ground station is the aforementioned UPF, which is typically for the routing of data packets in the core network.

The distributed LEO constellation architecture presented in Section 1.4.2 has been conceived with the goal to allow sufficient resource (power and mass) to be available in space in order to support this configuration. Please note however that Figure 26 does not rule out the case in which a certain split of the gNB functionalities is taking place in space as it will be detailed in Section 3.2.
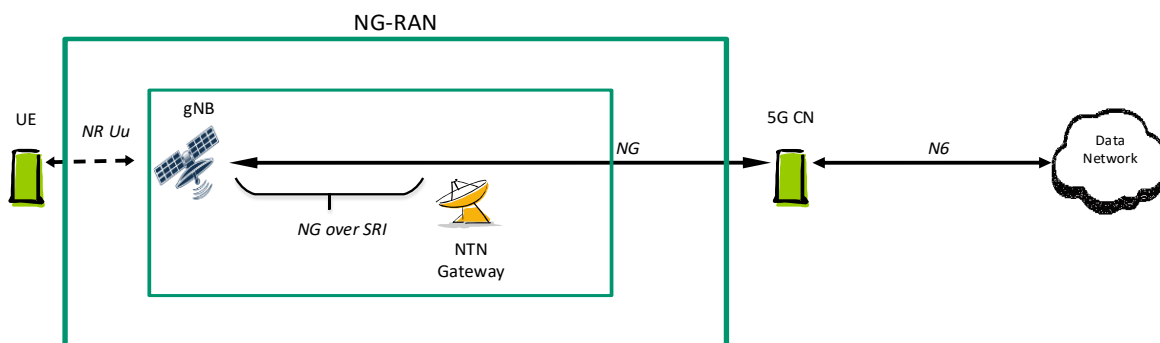

FIGURE 26: GNB PROCESSED PAYLOAD [1]

➲ Regenerative satellite with RU and gNB-DU on board and CU on ground, as sketched in Figure 27. As previously mentioned, Rel-19 has specified the full gNB, therefore, this last option was not retained for further work. We acknowledge moreover that most power consumption is occurring in the DU unit versus the CU unit consuming a fraction of that for a given processed bandwidth.

For the conventional architecture presented in Section 1.4.1, the configuration in Figure 26 might lead to a resource bottleneck in space. Depending on the results of the mass and power budgets for the LEO satellite payload, which is currently under investigation,

the split of some RAN functionalities between space and ground could become necessary for the conventional architecture. An initial analysis of the pros and cons of the different split options from the network perspective is presented in Section 3.3.1 and an analysis of the most suited split option depending on the considered use case in Section 3.3.2. **What it turns out is that different split options might be best suited for different UCs and that a "one size fits all" approach is not ideal**. Therefore, an innovative concept named "Adaptive Functional Split" (AFS) is presented in Section 3.3.4.
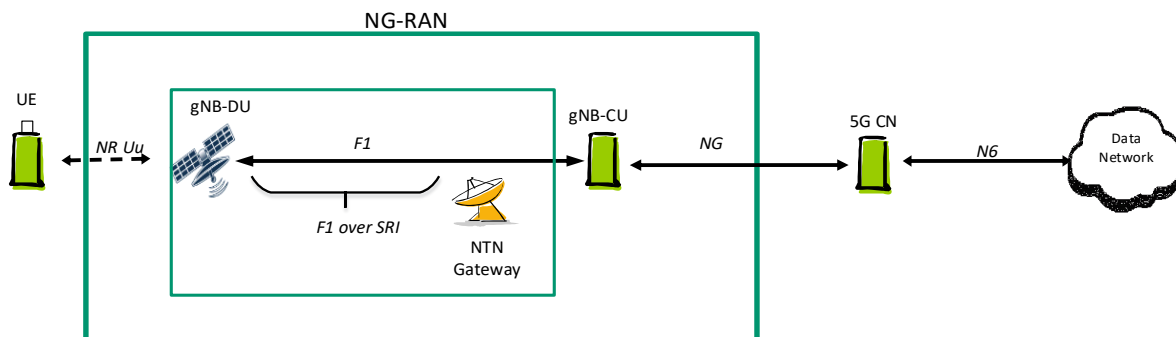
FIGURE 27: GNB-DU PROCESSED PAYLOAD [1]

In summary, the 6G-NTN architecture foresees a unified terrestrial and non-terrestrial network (i.e., 3D network) in a dynamic manner, which includes gNBs that are moving and following a satellite orbit or a flight path for HAPs. This network architecture then foresees a functional split that requires a comprehensive solution for the implementation of the RAN and core network functions in this environment of fix and mobile gNB base stations. Moreover, the satellite must have the means to route packets from one satellite to the other. Both routing within the same orbital plane as well as between orbital planes need to be supported.

Important aspects to be further analysed and consolidated in the remaining part of the projects are:

- **Interfaces:** Which interfaces are carried over the feeder link, service link or inter-satellite link.

- **UE mobility:** How UE context is managed and whether legacy solutions are enough

- **Relationships between equipment / functions:** Implication of maintaining connections between entities while satellites move (End-to-end depends on interfaces, underlying transport may also have an impact)

- **Transport through satellite network:** How to handle routing through the inter-satellite network (depends on multi-hop)

- **Capacity:** bottlenecks, traffic scalability with the number of UEs, cells or hops (depends on multi-hop), compression or bandwidth saving techniques for ISLs and feeder links traffic (depends on interfaces)

- **Satellite HW/SW impact**: payload complexity, power consumption, and memory requirements for satellites

- **Impact on standard**: estimation and strategic consideration on the standard impact / required modifications when an option is adopted

3.2 LOWER LAYER SPLIT IN SPACE FOR THE DISTRIBUTED LEO CONSTELLATION DESIGN

As already mentioned in section 1.4.2, due to constraints on the payload dimensions and power consumption, it may be advantageous to have constellations where groups of satellites providing the service link are anchored to an "aggregator" satellite via inter satellite links (ISL). Such aggregator satellite, hereafter referred to as feeder satellite for the sake of consistency with the terminology used in section 1.4.2, may be connected to the ground station via a direct feeder link as shown in Figure 28 or indirectly via a number of ISLs plus a feeder link. The feeder satellite shall contain the baseband unit (BBU) functionality, whereas the service satellites in the cluster shall carry a radio unit (RU) and provide the service link to the user terminals on the ground.
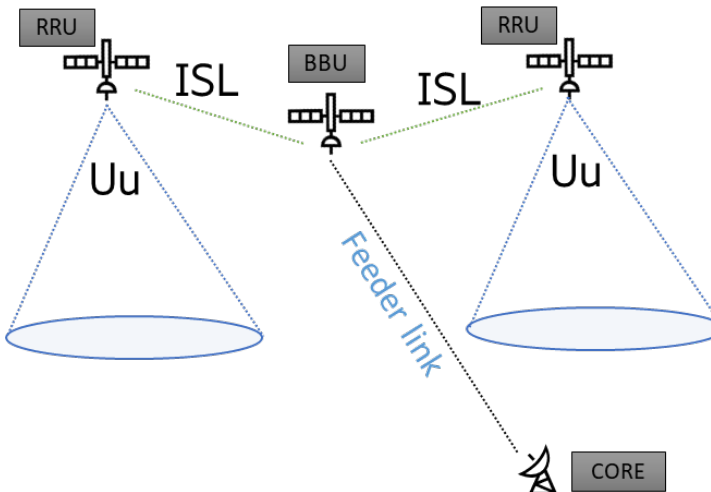
FIGURE 28: NTN SYSTEM WITH AN AGGREGATOR SATELLITE AND SERVICE SATELLITES

It should be understood that baseband includes the whole upper layers of the radio protocol stack while the lower (physical) layer processing functionalities are split between the feeder satellite and the service satellites. The connection from the feeder satellite to the service satellites in the cluster is done via optical ISLs (OISLs) supporting some variant of the fronthaul interfaces.

The split between baseband unit and radio unit is known as the lower layer split (LLS) where the O-LLS is the Open-RAN (ORAN) standardized version of such a split.

Figure 29shows how the switch/router in the BBU satellite can be used to route the backhaul from the feeder link to another feeder satellite in a neighbor cluster.

Some of the aspects that motivates this concept is that power budget and payloads can be optimized for the different roles of the satellites. The feeder satellites carrying the BBU does not have to be equipped with multiple power amplifiers for the service link, therefore more power and payload volume can be allocated for computation parts.

On the contrary, the service satellite carrying the radio unit (RU) will have less of its payload for computation, which means more volume and power for the power amplifier, antennas, and beamforming network for the service link.

One potential issue of this solution is that no centralized scheduling will be possible as each feeder satellite will have its own scheduler. The system could, on the other hand support slower radio resource management coordination, such as is done in terrestrial networks.
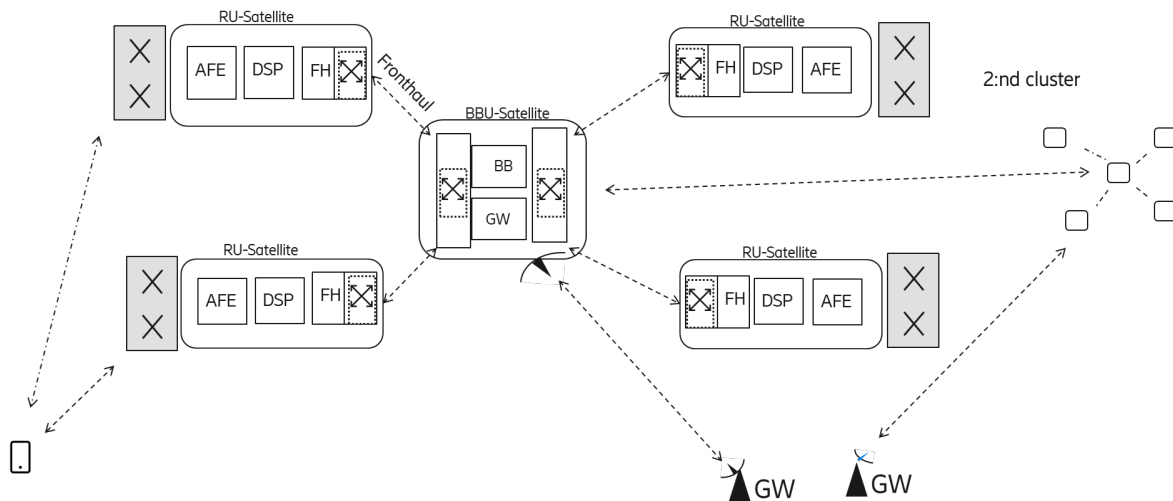
FIGURE 29: FEASIBILITY OF LLS BASED NTN ARCHITECTURE TO ALSO ENABLE ROUTING OF TRAFFIC BETWEEN BBU SATELLITES

3.2.1 Bandwidth Requirement Analysis

This section provides a quantitative analysis of Lower-Layer split architecture option, focusing on the bandwidth requirements for links (ISL, feeder link) between nodes. Please note that the analysis presented here is also relevant to the scenario in which the lower layer split is implemented for the conventional LEO constellation.

The analysis is divided in two parts. In Section 3.2.1.1 we calculate the required bandwidth for serving a fully loaded cell (all resources allocated) in uplink direction, assuming an LLS architecture. Next that section describes how many cells could be served for a given fronthaul link bandwidth.

In general, for an LLS architecture, the uplink direction is the direction driving the bandwidth requirements for the interface. For that reason, a similar analysis as the one in Section 3.2.1.1 for downlink is not included here.

In Section 3.2.1.2 we present a comparative analysis between two architectures (full base station onboard and LLS architecture) considering the bandwidth requirement to transport a full slot of data. Here the focus is not so much on how many cells can be supported, but rather to give the reader a comparative notion between the two systems.

3.2.1.1 Bandwidth Requirements Analysis for the Uplink

In uplink (UL) direction, a system built with an LLS architecture will transmit the signals received from the UEs for processing in the baseband node. Since the transmit signals have traversed the channel, they will be affected by fading, noise and other impairments.

In this section we provide a quantitative analysis of the bandwidth cost for transporting UL frequency domain samples between a radio node and a baseband node. The analysis is valid for systems where baseband is deployed on the ground or in a satellite, given that the logical functional split is the same.

The following assumptions are made:

➲ **Air interface**

- The system operates in C-band. In general, if the SINR is better, that may lead to select a block floating point scheme with more bits per block
- The channel is assumed to be line-of-sight, with at most rank 1 transmission.
- The bandwidth corresponds to 273 physical resource blocks (3276 subcarriers). The underlying assumption here is that the cell is fully loaded in UL.
- There are 14 OFDM symbols per slot.
- There are 2000 slots per second.
- Subcarrier spacing is 30 kHz.
- FDD is used.

➲ LLS implementation

- The radio node consists of analog and digital front-ends, receiver beamforming, removal of cyclic prefix, FFT transforms, optional multi-user processing and equalization (e.g. one tap frequency domain equalization for OFDM systems)
- Complex (in phase/quadrature) frequency domain samples are transmitted in UL.
- The FFTs in the OFDM demodulator are performed in the service satellite.
- Receiver beamforming coefficients are pre-calculated and stored in the satellite. This assumption and its implications shall be subject of further analysis.
- No extra overhead for transmitting beamforming coefficients is considered.

➲ IQ sample representation

- Each group of 12 contiguous IQ samples (1 physical resource block) is represented in block-floating point format, with 4 bits for the mantissa for each component (I, Q) and 8 bits for a shared exponent (valid for all 12 IQ samples). In total $((4+4) * 12) + 8 = 104$ bits per physical resource block.
- This choice of block floating point representation is adequate for a system using QPSK and does not introduce relevant SINR degradation.

➲ Fronthaul implementation

- The maximum transmit unit (MTU) in the fronthaul link is 1500 bytes.
- The traffic from radio to baseband node in the fronthaul link contains only user plane packets.
- User plane packets are not allowed to carry content for more than one OFDM symbol (in time).
- Each user plane packet contains approximately 30 bytes of overhead.

Differently from downlink, the bandwidth requirements for an uplink interface do not vary with modulation and coding scheme (MCS) choice, in case the method for representing the frequency domain IQ samples is kept constant (e.g., block floating point encoding).

Similarly to DL, on the other hand, the bandwidth utilization depends on utilization of the air interface (grows with the number of allocated UEs).

To evaluate the required bandwidth, we propose to calculate the cost of transmitting the frequency domain IQ samples of a cell at maximum load (all physical resources allocated to UEs).

Next, the cost of servicing one cell (approximately 815 Mbps) is used to estimate how many cells could be supported for a given fronthaul link capacity. For the calculations, we account for the overhead in user plane fronthaul packets.

The results are collected below in Table 37. **Note that this calculation assumes a quite harsh requirement that all cells are fully loaded simultaneously. In practice, the utilization of different cells fluctuates over time, so the actual numbers of cells that can be supported are higher than shown here. Additionally, the traffic is under control of the baseband scheduler, which can assure that no overload occurs and that there is fairness between different cells sharing the same link. It is also noted, due to satellite constraints (e.g. power limit), a satellite may not be able to support the communication to a large number of cells at the same time, which would reduce the required per-cell fronthaul capacity since a cell is only scheduled for a fraction of time.**

It is possible to observe that for fronthaul links of around 100 Gbps, the interface could possibly support more simultaneous cells (active beams) than the satellite would serve (the current working assumption from T3.3 is to have 100 simultaneous beams per satellite).

TABLE 37: NUMBER OF SUPPORTED CELLS AT PEAK LOAD, UPLINK LLS

Fronthaul Link Capacity	Supported cells at peak load
5 Gbps	6
10 Gbps	12
25 Gbps	30
50 Gbps	61
100 Gbps	122

3.2.1.2 Comparative Bandwidth Requirements Analysis for the Downlink

This section provides an illustrative comparison of the bandwidth requirements for two hypothetical systems, namely:

- Option 1 - where a full base station is placed in a satellite.
- Option 2 - where the physical layer is functionally split between a baseband node on the feeder satellite and a radio node on the service satellite.

Due to the high number of variables in a real implementation, the results should be taken as an example, rather than an exact evaluation. Unless otherwise specified below, most parameters refer to an NR system.

The following assumptions are made:

➲ **Air interface**

- The system operates in C-band. In general, if the SINR is better, the downlink average coding redundancy could be smaller, making the bandwidth requirement more favorable
- The data to be transmitted fits in one NR slot.
- The channel is assumed to be line-of-sight, with at most rank 2 transmission (due to use of left, right polarization).
- The system operates with 2 antenna ports per cell.
- The bandwidth corresponds to 273 physical resource blocks (3276 subcarriers).
- There are 14 OFDM symbols per slot.
- There are 2000 slots per second.
- Subcarrier spacing is 30 kHz.
- FDD is used.
- The system operates at relatively low SNR, i.e. between MCS 0 and MCS 10 as defined in Table 5.1.3.1-2 of [2].

- The LDPC code operates with an average code rate of 0.42. This has been obtained by averaging the code rates from MCS 0 to MCS 10. In practice the average coding rate will depend on the channel conditions for each user/deployment.
- The coded transport blocks are on average 2.34 times larger than the input data (obtained by the reciprocal of average code rate).
- The system has an overhead (PDCP, RLC, MAC, physical control channels and reference signals) of 14%, as described in Section 4.1.2 of [3].

⮕ LLS implementation

- Unmodulated data is transmitted in DL (QPSK, QAM modulation is performed in the radio node).
- The FFTs in the OFDM modulator are performed in the satellite.
- Beamforming coefficients are pre-calculated and stored in the satellite. This assumption and its implications shall be subject of further analysis.
- No extra overhead for transmitting beamforming coefficients is considered.

⮕ Fronthaul implementation

- The maximum transmit unit (MTU) in the fronthaul link is 1500 bytes.
- The traffic in the fronthaul link is assumed to contain both control and user plane packets.
- For a given slot, one control plane packet per polarization per antenna port is sent.
- Each control plane packet has approximately 50 bytes.
- User plane packets are not allowed to carry content for more than one OFDM symbol (in time).
- Each user plane packet contains approximately 30 bytes of overhead.

We propose to compare both systems by a ratio of how much data needs to be sent over a link of interest for a full NR slot. For Option 1, the link of interest is a FL/OISL carrying the NG interface, while for Option 2 it is an OISL carrying the fronthaul LLS interface.

For a full base station onboard the satellite, the traffic sent over the link corresponds (except for packet headers) to what is to be sent over to the UE.

For option 2 (LLS), the data entering the base station is augmented by headers in PDCP, RLC, MAC (e.g., control elements), channel coding (LDPC for PDSCH). Besides that, there is overhead added for the fronthaul link itself.

To obtain the comparison metrics, we follow this procedure:

1. Calculate the maximum number of bits that fit in an NR slot (given all the assumptions stated above).
2. Calculate the amount of useful data in said slot (by subtracting the air interface overhead).
   a. The result obtained in step 2 is used as the amount of data required by Option 1 (full base station onboard).
3. From the useful data, we obtain the user plane overhead in fronthaul
   a. Calculate how many user plane fronthaul packets are needed, then calculate how many overhead bits for that number of packets.
4. The fronthaul control plane overhead is calculated directly from the assumptions.

The results are presented as a bar graph in Figure 30, where the capacity requirements are normalized by the requirements of the full base station onboard system (Option 1).

Option 2 requires around 2.8 times the bandwidth used for Option 1. The main contribution comes from the bandwidth expansion added by the channel coding (LDPC for NR).
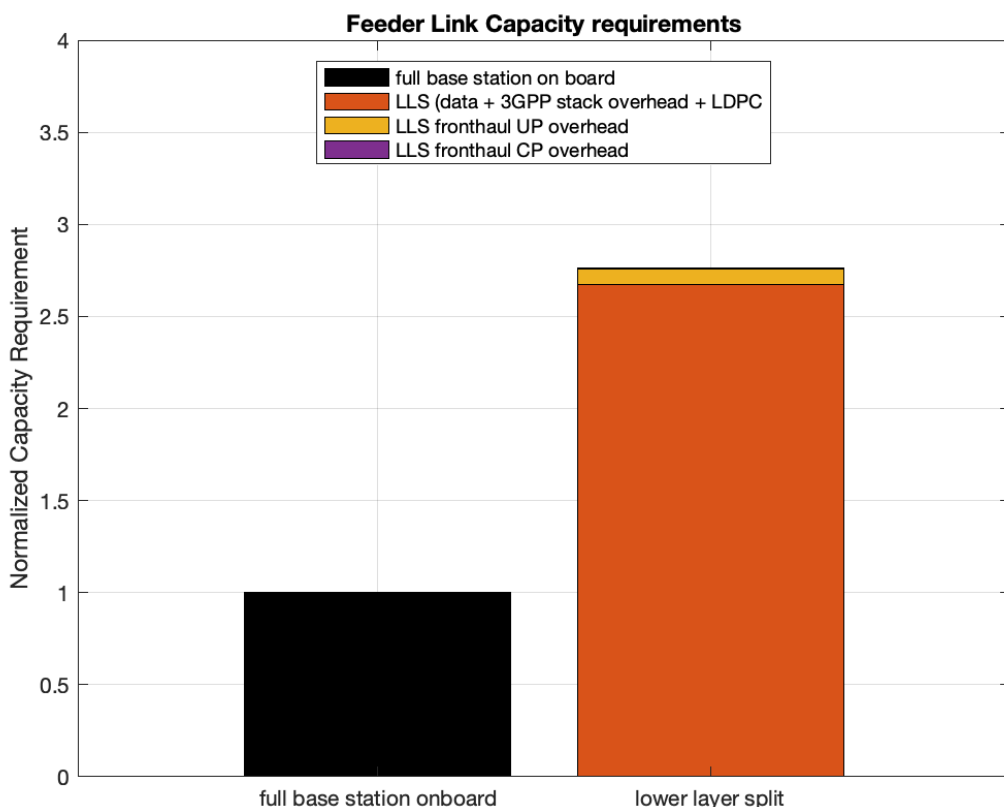

FIGURE 30: ILLUSTRATIVE COMPARISON OF SERVICE-FEEDER SATELLITE LINK CAPACITY REQUIREMENTS (NORMALIZED).

3.3 SPLIT OPTIONS FOR THE CONVENTIONAL LEO CONSTELLATION DESIGN

As already mentioned, for the conventional LEO constellation design in which each satellite implements service links, ISLs and feeder links as shown in Figure 31, potential bottlenecks are to be excepted as far as the availability of resources in space (complexity, power, and mass) is concerned. Therefore, the different split options between space and ground listed Table 38 are compared and analyzed in the next section. Please note they correspond to the split options considered for 5G TN, but in this context their pros and cons when applied to an NTN scenario are analyzed.
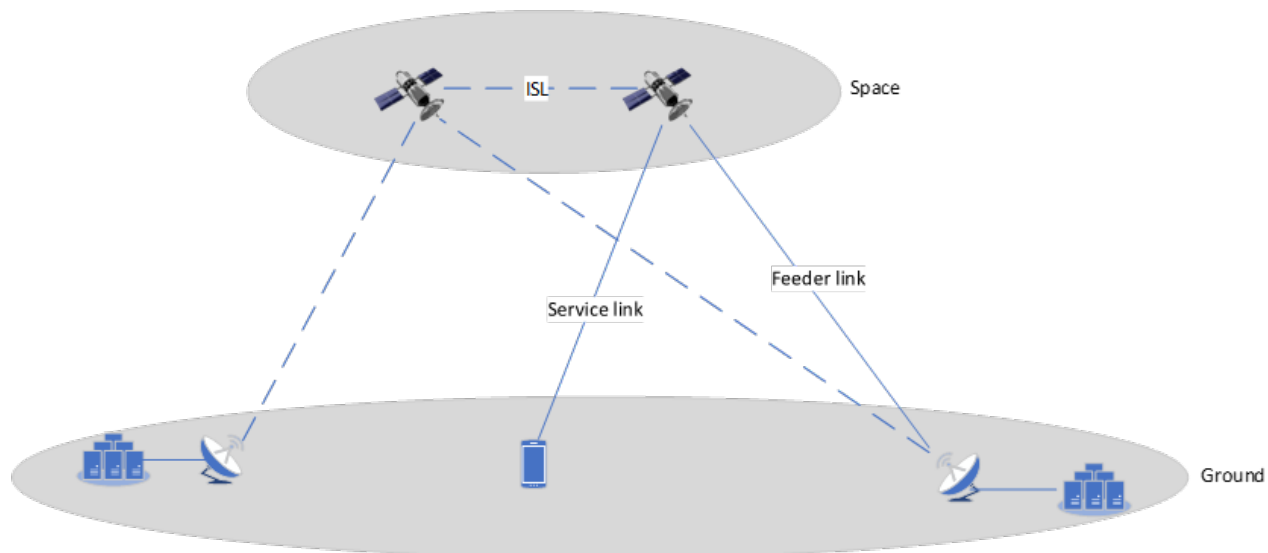
FIGURE 31: REFERENCE SCENARIO FOR THE LEO CONVENTIONAL ARCHITECTURE

TABLE 38: LIST OF SPLIT OPTIONS FOR THE LEO CONVENTIONAL CONSTELLATION

Option	Functions in space	Functions on ground
1	Complete gNB	Core network (CN) + data network (DN)
2	Complete AS layers for User Plane (UP) PDCP-and-below layers for Control plane (CP)	CN + DN for UP RRC + CN for CP
3	RLC + MAC + PHY + RU	PDCP + RRC + CN + DN
4	MAC + PHY + RU	RLC + PDCP + RRC + CN + DN
5	PHY + RU	MAC + RLC + PDCP + RRC + CN + DN
6	Lower PHY (cyclic prefix (CP) removal/addition + FFT/IFFT) + RF	Higher PHY + MAC + RLC + PDCP + RRC + CN + DN
7	RU	PHY + MAC + RLC + PDCP + RRC + CN + DN

3.3.1 Comparison of Different Split Options

➲ **Option 1**

Pros	Cons
➲ Less restriction on latency and BW requirements for the feeder link ➲ Support onboard CN function ➲ Support direct Xn interface via ISL between satellites/onboard gNBs (e.g.	➲ Fast moving gNB from CN perspective ➲ Frequent NG interface modification/reestablishment (e.g. gateway switch for satellite)

	for latency reduction, feeder link traffic offload)	⮊ (Frequent) satellite switch implies a (frequent) L3 mobility
⮊	Lower latency for RRC configuration	⮊ Highest complexity and power consumption onboard the satellite
⮊	Available NG interface design with implementation over feeder link	
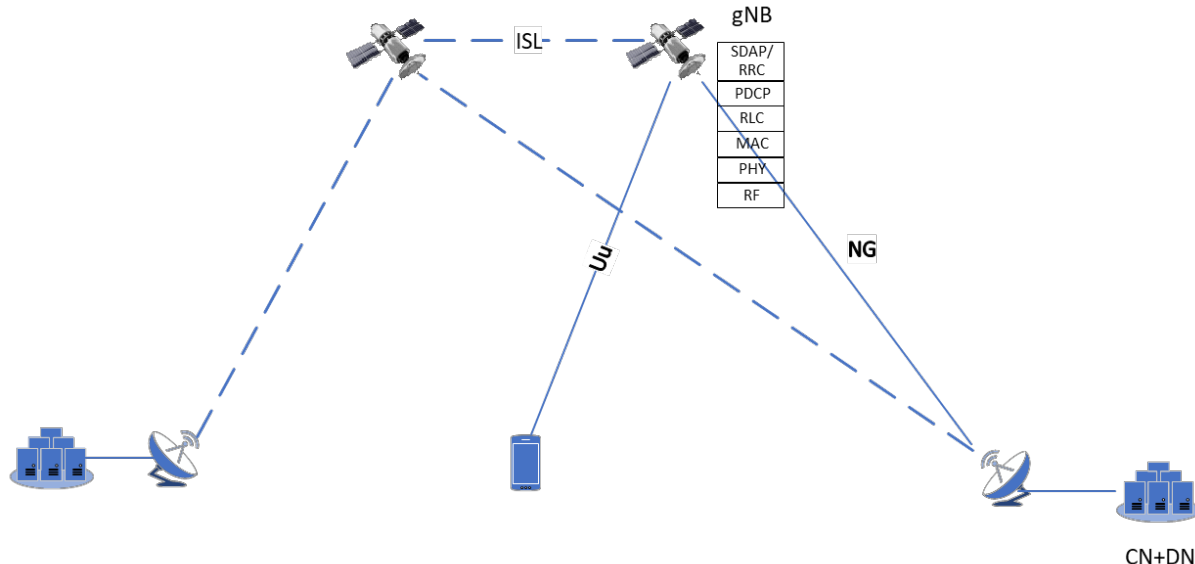
FIGURE 32: SPLIT OPTION #1 APPLIED TO THE CONVENTIONAL LEO CONSTELLATION

⮊ **Option 2**

Pros	Cons
⮊ Less restriction on feeder link latency and BW requirements	⮊ Frequent N3 interface modification/reestablishment
⮊ Support onboard user-plane (UP) CN function, e.g. UPF and MEC	⮊ If CN CP network functions (NFs) are deployed in space, additional RRC entity may be needed in space as well
⮊ Static N2 interface during satellite switch	⮊ No baseline implementation for feeder link to support this split option
⮊ Separation between CU-CP and CU-UP	
⮊ Support L2 mobility for UE during satellite switch	
⮊ ISL for supporting UP during satellite switch(Xn UP), e.g. data forwarding, UE PDCP/RLC context transfer	
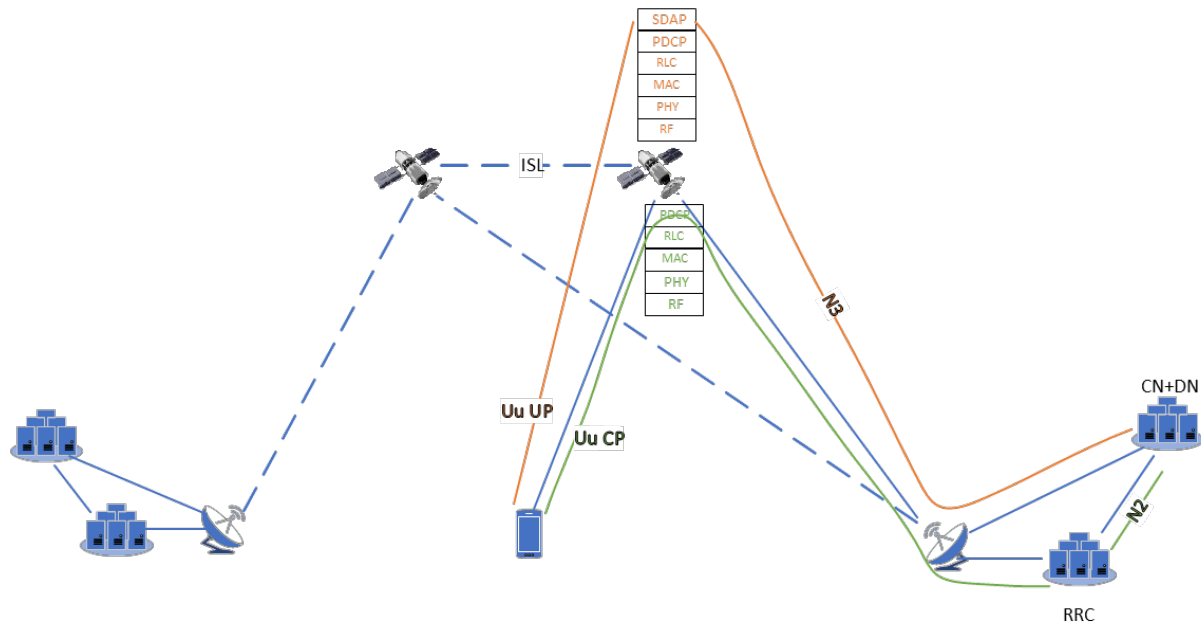
FIGURE 33: SPLIT OPTION #2 APPLIED TO THE CONVENTIONAL LEO CONSTELLATION

➲ **Option 3 (Onboard IAB could be a sub-option)**

Pros	Cons
➲ Less restriction on feeder link latency and BW requirements	➲ Dynamic F1 reestablishment and DU context transfer due to NTN mobility
➲ Legacy F1 can be reused as a baseline for the feeder link	
➲ Static NG interface during satellite switch	
➲ L2 mobility during satellite switch	
➲ Centralized PDCP during satellite switch	
➲ ISL may be used for transferring the UE RLC context during satellite switch (e.g. UE's RLC remains during mobility)	
➲ Fast RLC re-Tx	
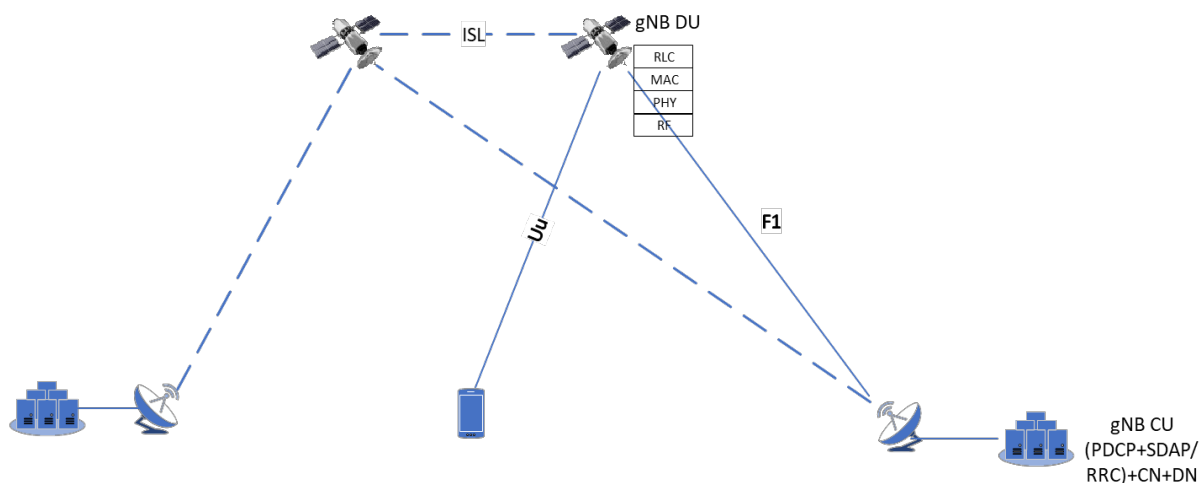
FIGURE 34: SPLIT OPTION #3 APPLIED TO THE CONVENTIONAL LEO CONSTELLATION

⮞ Option 4

Pros	Cons
⮞ Increased but moderate BW requirement on feeder link	⮞ Low latency requirement on feeder link to support interaction between MAC and RLC
⮞ L2 mobility with centralized RLC and PDCP for UE context (e.g. RLC and PDCP at the UE may remain during satellite switch)	⮞ High RLC re-TX latency
⮞ Feeder link error can be handled by RLC re-TX	⮞ No baseline implementation for feeder link to support this split option
⮞ Smaller buffer is needed onboard the satellite	
⮞ Flow control	

FIGURE 35: SPLIT OPTION #4 APPLIED TO THE CONVENTIONAL LEO CONSTELLATION

➲ **Option 5**

Pros	Cons
➲ Increased but moderate BW requirement on feeder link ➲ High feeder link latency between PHY and MAC can be handled by timer/window extension as in NR NTN ➲ Centralized scheduling for performance improvement ➲ L2/L1 mobility during satellite switch ➲ Feeder link error can be handled by HARQ re-Tx	➲ High HARQ re-Tx latency ➲ High RACH latency ➲ High CSI latency ➲ No baseline implementation for feeder link to support this split option
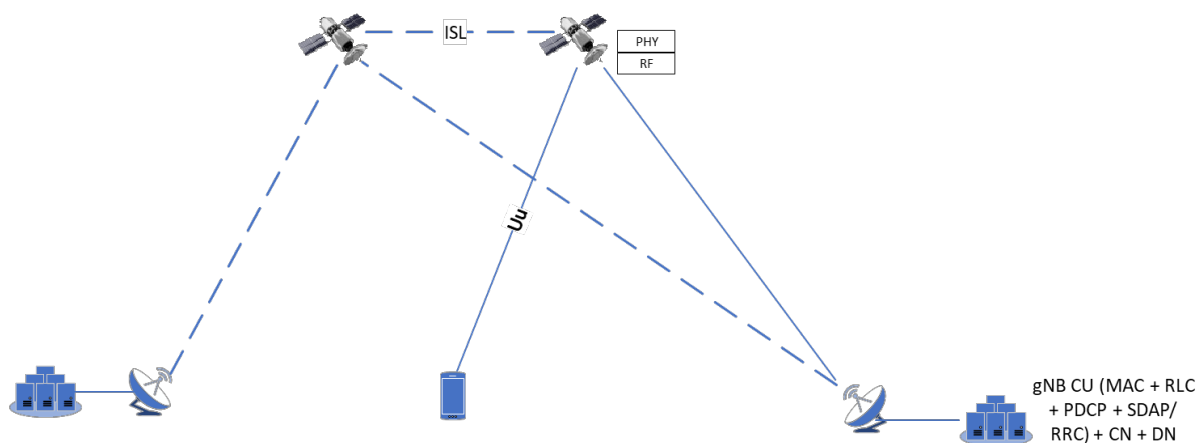
FIGURE 36: SPLIT OPTION #5 APPLIED TO THE CONVENTIONAL LEO CONSTELLATION

➲ **Option 6 (Low Layer Split)**

Please note that this split option is conceptually the same proposed in Section 3.2 for the distributed LEO constellation, however in this case only the RU is placed in space and the rest of the gNB and CN functionalities on ground. Therefore, the same analysis regarding the bandwidth requirements carried out in Section 3.2.1 is still valid in this case, but it will affect the link between the satellite and the ground, which depending on the satellite position could be a simple feeder link or the combination of a certain number of OISL(s) with one feeder link. In the latter scenario, data might aggregate during each hop in space, leading to potentially very demanding bandwidth requirements especially for the feeder link.

Pros	Cons
➲ O-RAN 7-2x interface can be considered as a baseline ➲ Centralized scheduling ➲ High feeder link latency can be handled by timer/window extension as in NR NTN ➲ L2/L1 mobility during satellite switch	➲ High HARQ re-Tx latency ➲ High RACH latency ➲ High CSI latency ➲ High BW requirement on ISL and feeder link

➲ Digital beamforming and waveform generation can be done onboard the satellite	
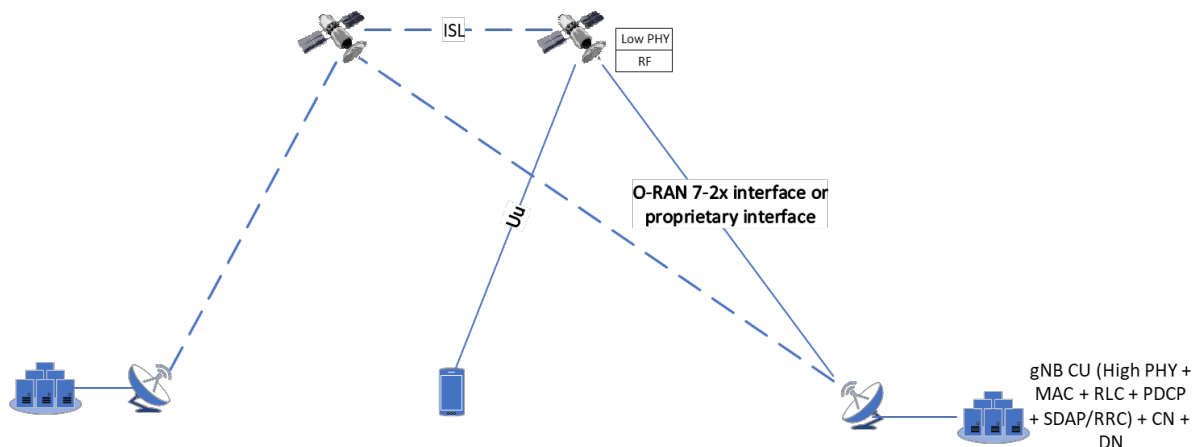
FIGURE 37: SPLIT OPTION #6 APPLIED TO THE CONVENTIONAL LEO CONSTELLATION

➲ **Option 7**

Pros	Cons
➲ Centralized pooling for the entire set of RAN protocol stacks ➲ High feeder link latency can be handled in NR NTN already ➲ L2/L1 mobility during satellite switch ➲ Low complexity and power consumption onboard the satellite	➲ High radio layer E2E latency ➲ High BW requirement on feeder link if digital-to-analog conversion (DAC) is performed in RF
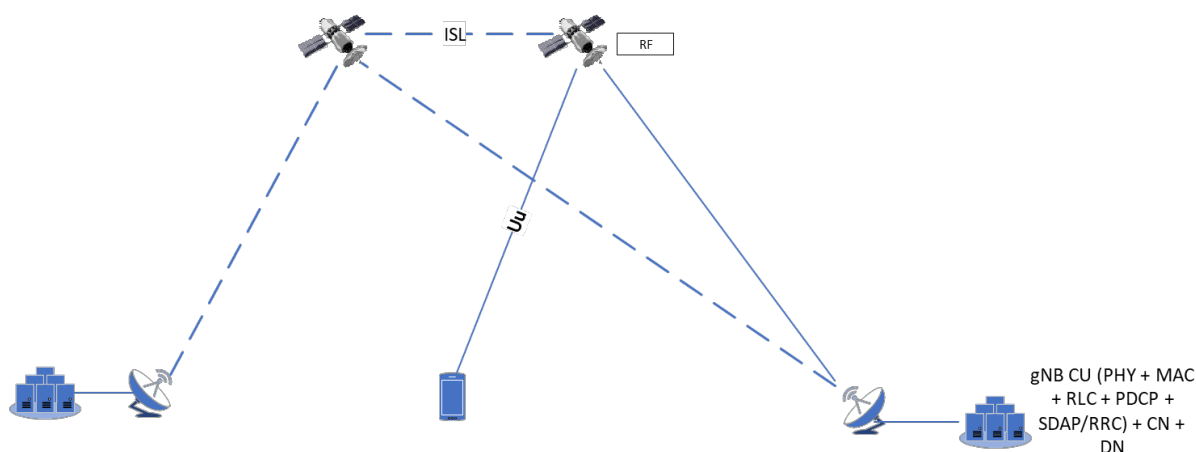
FIGURE 38: SPLIT OPTION #7 APPLIED TO THE CONVENTIONAL LEO CONSTELLATION

To complete this analysis, a summary table is reported below in Table 39, showing that different split options might have different advantages, where different colours are used to indicate if the considered split option shown in the row is desirable by considering the

characteristic/feature shown in the corresponding column. In particular, the following comments are in order:

- Payload complexity decreases when moving from split option 1 to 7.
- Onboard edge computing requires typically CN functionalities, so it's feasible only with split options 1 and 2
- Latency critical services might be especially problematic with split options 5 to 7.
- Dynamic resource sharing might be more difficult to support with split options 1 to 4.
- Centralized RRM may require either a central RRC entity or two very-tightly coordinated RRC entities serving neighbor/overlapping areas with ideal connection between them, in order to optimize the system level management and the system performance, e.g. to improve mobility support by collecting and considering more global information. Thus, such centralized RRM may not be easily supported with split option 1, since different neighbor/overlapping areas served by different NTN-NTN gNBs and/or different NTN-TN gNBs have different RRC entities that are located far away from each other.

It shall be noted once more that the split options are those currently defined in 5G. Up to which point and how these shortcomings could be mitigated or completely solved in 6G will be subject of further investigation in the rest of the project.

TABLE 39: ANALYSIS SUMMARY OF THE DIFFERENT SPLIT OPTIONS FOR THE LEO CONVENTIONAL CONSTELLATION

Split Option	Required feeder link and ISL data rate	Allowed feeder link latency	Required onboard CN	Existing design / baseline implementation for feeder link	Usage of ISL	Applicable mobility scheme	Latency for RRC, RLC re-TX, HARQ and RACH, CSI	Separation between CU-CP and CU-UP	Centralized scheduling	Centralized RRM
1	Low	High	Yes for CP/UP	NG	Xn	L3	Low for all	No	No	No
2	Low	High	Yes for UP	No	Xn-U	L2	Low for all except RRC	Yes	No	Yes
3	Low	High	No	F1/IAB	RLC context transfer	L2	Low for all except RRC	No	No	Yes
4	Medium	Low	No	No	Gateway coverage extension	L2	Low for HARQ and RACH, CSI	No	No	Yes

5	Medium	High	No	No	Gateway coverage extension	L2/L1	High for all	No	Yes	Yes
6	High	High	No	O-RAN 7-2x	Gateway coverage extension	L2/L1	High for all	No	Yes	Yes
7	High	High	No	No for onboard analog conversion; Yes for pure RF repeater	Gateway coverage extension	L2/L1	High for all	No	Yes	Yes

3.3.2 Mapping of Functional Split Options vs. 6G-NTN Use Cases

Since the analysis of the different split options in the previous section based on network considerations resulted in a scenario where no clear "winner" could be identified, a further comparative analysis is carried out in this section from a different angle, namely which split option could better support the 6G-NTN use cases defined in D2.1 [4].

Table 40 provides such initial analysis with respect to the different UCs. In this table, as an example, "+++" implies a preferred option than an option with "++", which is further preferred than an option with "+". It is to be noticed that this analysis reuses the current 5G protocol stack layers and terminologies, as it is unknown how 6G will change and evolve comparing to the 5G at this moment. For example, a radio unit (RU) mainly contains the RF elements, a gNB L1-low contains the lower part of physical layer functions, (e.g., IFFT/FFT, and CP insertion/removal) of a 5G gNB, a gNB DU contains the radio layers below the PDCP layer, such as higher part of the physical layer functions together with MAC and RLC layers, while CU contains the PDCP+SDAP/RRC layers. In addition, the option of "RU+DU+CU+routing fun+AF" indicates to equip a routing function for the E2E link traffic at the space, e.g., on a satellite as illustrated in Section 3.3.3. Please note, this initial analysis is subject to further changes in the rest of the project duration, e.g., based on the progress and the technical solution developments on the relevant topics.

TABLE 40: INITIAL ANALYSIS ON FUNCTIONAL SPLIT OPTIONS VS. 6G-NTN USE CASES

Functional split Space - Ground		UC1	UC2	UC3
Space	Ground	Maritime Coverage for search and rescue coast guard intervention	Autonomous Power Line Inspection Using Drones	Urban Air Mobility
RU	DU+CU+Core	Can be discarded if no connection between Sat and ground segment	+++	+++
RU+L1-LOW	DU (w/o L1-Low)+CU+Core	Can be discarded if no connection between Sat and ground segment	+++	+++
gNB-DU processed payload: RU+DU	CU+Core	+	Can be discarded	Can be discarded
gNB processed payload: RU+DU+CU	Core	+	Can be discarded	Can be discarded
RU+DU+CU+routing fun+AF	Core	+++ (Routing function)	+++(UPF+AF: NTN edge computing enabler)	+++(UPF+AF: NTN edge computing enabler)
Requirements and scenarios to be supported		• Coast Guard Intervention with Seamless Handover to Different Feeder Links for NTN Network Connection • Coast Guard Intervention without Terrestrial Coverage and with only NTN coverage	Drones are intended to gather pictures and videos for Routine inspection.	Requires NTN edge computing.

Functional split Space - Ground		UC4	UC5	UC6	UC7
Space	Ground	Adaptation to PPDR or Temporary Events	Consumer Handheld Connectivity and Positioning Areas	Continuous Bidirectional Data Stream in High Mobility	Direct Communication over Satellites
RU	DU+CU+Core	+++	Less correlated w/ split opt	+	Can be discarded
RU+L1-LOW	DU (w/o L1-Low)+CU+Core	+++	Less correlated w/ split opt	+	Can be discarded
gNB-DU processed payload: RU+DU	CU+Core	Can be discarded	Less correlated w/ split opt	+++	Can be discarded
gNB processed payload: RU+DU+CU	Core	Can be discarded	Less correlated w/ split opt	++ (TN-NTN HO) +++ (NTN –NTN HO)	Can be discarded
RU+DU+CU+routing fun+AF	Core	Can be discarded	Less correlated w/ split opt	Can be discarded	+++(no need for AF)
Requirements and scenarios to be supported		6G TN and 6G NTN coexistence	Light indoor coverage	Requires performance increase (especially RTT)	Resiliency of 6G NTN communication, w/o a tight dependency on the feeder link availability. Latency reduction. Offloading the load on the feeder link.

In certain scenarios of UC1 for maritime communication, it is important to support communication when the satellite cannot be directly connected to the on-ground gateway, e.g., when the satellite moves to a remote area or when the satellite is in the middle of an ocean. In this case, one option is to use ISLs to connect the satellite to the gateway, where the additional traffic load posed by the remote satellite on the ISLs and the feeder links of the satellite in visibility of the ground station needs to be accounted. In order to reduce these traffic burdens on the ISLs link and the feeder links, it may be preferred to use a higher layer split option, e.g., to equip the satellite with RU+DU, or even RU+DU+CU, which have the advantage of consuming less bandwidth of the backhaul link comparing to a lower layer split option. Another architectural option is to enable the direct NTN communication by implementing a routing function in the satellite(s), e.g., as illustrated in Section 3.3.3. With the direct NTN communication, the traffic can be routed directly from one UE to another, which can further avoid routing all traffic through the feeder links.

For UC2 and UC3, where drones are used for inspecting the power line or transporting goods and passengers, it may be preferred to have a lower layer split option to reduce the required computational capabilities in the satellite payload, since direct communications between drones are not relevant for these UCs. However, there are some considerations in UC2 and UC3 to enable edge computing technology such that certain processing can be performed at the satellite. In that case, in order to support edge computing, at least the User-plane (U-plane) core network function needs to be implemented in the satellites together with the application function to support edge computing, i.e., UPF+AF need to be carried by the satellites for directing the data of a considered Protocol data Unit (PDU) session to the proper edge entity, wherein the PDU session needs to be transported over the Access Stratum (AS) radio layers.

UC4 considers the coexistence between TN and NTN. In such a scenario, it may be preferred to have a centralized scheduler, e.g., for dynamic resource sharing and/or interference reduction/avoidance. Thus, a centralized MAC entity may be deployed on the ground to schedule both the coexisting TN and NTN cells, while the remaining lower layer functions can be moved to the space segment. The scenario where only RU and L1-low is implemented in the space and the rest of RAN functionalities as well as all CN functionalities are left on ground is analysed in detail in Section 3.3.4.

UC5 targets at improving the NTN coverage in 6G, while its impact from/on the desired functional split option is not clear at this moment.

The high mobility scenario investigated in UC6 requires an improved mobility support between TN and NTN, as well as between NTN and NTN. In addition, it also requires a low latency for supporting certain latency critical services such as gaming and even Virtual Reality (VR). In this case, to reduce the latency, it may be preferred to have an onboard MAC layer and an RLC layer at the satellite, such that the Hybrid Automatic Repeat Request (HARQ) process and ARQ process can be carried out between the UE and the satellite directly, which can avoid the impact of feeder link propagation delay on retransmission latency. Furthermore, to improve the mobility performance between TN and NTN, it may be preferred to have a centralized RRC layer on the ground, e.g., to achieve a centralized RRM. Regarding the NTN-NTN mobility, if ISL can be used to implement the Xn interface between two neighbor satellites, it may be preferred to have onboard RRC layers at the different satellites. In this manner, the feeder link propagation delay is not involved in some Handover (HO) steps and the corresponding signalling transmissions, such that the latency for HO can be reduced, which in turn reduces the service interruption time.

UC7 aims at reducing the dependency of the operability of NTN network on feeder link and in general ground segment availability, such that an E2E communication can be set up and supported even when a feeder link is unavailable. In this case, it is preferred to have onboard routing function equipped at the satellite. This scenario is analysed in detailed in Section 3.3.3.

What it turns out of this preliminary analysis is that different split options might be best suited for different UCs and that a "one size fits all" approach is not ideal. Therefore Section 3.3.4 analyses a novel concept named Adaptive Functional Split (AFS). Up to which point this flexibility could be implemented, will be subject of further analysis.

3.3.3 Architectural Options for Direct NTN Communications

As can be seen from Figure 25, Figure 26, and Figure 27, the legacy architectures require a connection between the NTN payload and the on-ground network, e.g., CN and DN.

It is noted that it might be not always possible and/or desirable to connect an NTN node (e.g., a satellite or HAP) with the ground network. For instance, when the UE needs to set up a communication with the peer UE, the gateway may become unavailable for the UE's serving satellite, e.g., during a natural disaster, which may destroy the gateway or causes power outage at the ground network. In such cases where the connection to the ground network becomes unavailable, a communication between two UEs via the ground network cannot be supported based on the legacy NTN architectures.

However, an NTN platform may serve a coverage area much larger than that of a legacy TN access point, e.g., a TN gNB. For example, the area covered by a LEO satellite may have a size of up to one thousand kilometres. Therefore, in many scenarios, a satellite may cover two communicating UEs with a high probability. In this case, a direct communication between two UEs can take place over the satellite without the need for the data to go through the ground network, e.g., as shown in Figure 39. In addition, ISLs can be used to further enlarge the

coverage area of the direct NTN communication, e.g., as shown in Figure 40. More detailed information and use cases of the direct NTN communication can be found in [4].
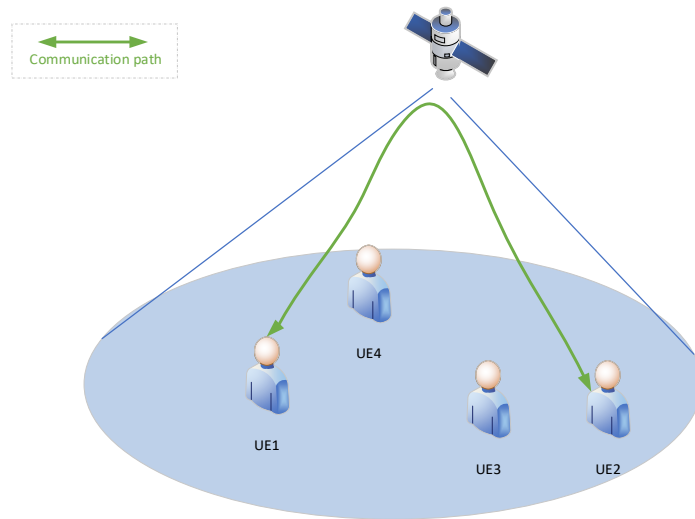

*FIGURE 39: DIRECT NTN COMMUNICATION OVER A SINGLE SATELLITE.*
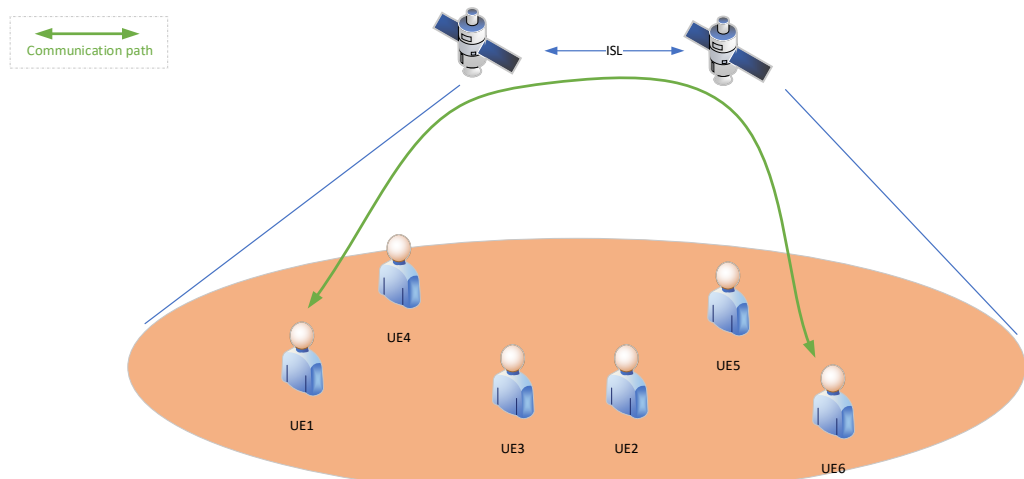
FIGURE 40: DIRECT NTN COMMUNICATION OVER TWO SATELLITES CONNECTED OVER ISL.

Based on the above description, the potential benefits of the direct NTN communications include:

- Latency reduction
- Feeder links and ISLs load reduction
- Support communication in case of ground network unavailability (natural or man-made disasters but also cyber-attacks)
- Enable future NTN NW to be decoupled from the ground network deployment

Therefore, in this section we analyse the different system architecture options where the feeder link to ground NW is not used for direct NTN communication, e.g., when the connection to the ground network is/becomes unavailable.

Please note, since 6G architecture has not been defined at the time of this report, the 5G system architecture and the terminologies for the corresponding functions are reused in this subsection as a baseline to describe the different options.

3.3.3.1 Option 1: NTN Node Equipped with gNB, CN Functions and even DN/AF/Server

In this option, the NTN nodes can be equipped with a RAN function/node, e.g., a gNB, together with one or multiple CN functions, e.g., UPF, AMF, SMF, AUSF, PCF, UDM, etc. If needed, even DN/AF/server can be deployed onboard the NTN platform to enable onboard data processing. To some extent, this option is similar to moving the complete TN network and the corresponding functions to the space, which allows the future NTN network to be independent from the legacy TN. With this option, the considered direct NTN communication can take place by using the available TN solutions, since all the needed functionalities would be available in the space.

An illustration of the control plane protocol architecture for this option is shown in Figure 41. As it can be seen, both the RRC layer used for AS layer control and the NAS layer are terminated at the UE and the satellite(s). For the sake of simplicity, Figure 41 shows that both RRC and NAS are terminated at the same satellite, e.g., a satellite is equipped with both RAN for RRC and CN functions for NAS. However, in a multi-layer 3D NTN architecture with distributed NFs, the gNB and the CN functions, e.g., AMF and SMF, can be distributed in different NTN nodes, e.g., on different satellites that are connected via ISLs. In that case, the RRC layer and the NAS layer of the UE can be terminated at different satellites.

Figure 42 shows the user plane protocol architecture for Option 1. As can be seen, the E2E data can be transmitted over the PDU sessions of the two UEs. Besides, the PDU session of a UE is supported and controlled by the CN functions deployed in the space segment, e.g., in satellite(s). With this architecture, the routing of the user traffic from one UE to another UE can be performed by the CN function, e.g., a UPF, which is controlled by another SMF onboard the same satellite or another satellite but with ISL connection to the satellite carrying the UPF. As another alternative, it is also possible to rely on an onboard AF to route the traffic, if the AF can be deployed on the satellite(s).

With this option, the UE may need less modifications at the AS layer, and the legacy TN solutions can be reused as the baseline. However, this solution may also face some technical challenges, such as:

➲ Increased complexity and power consumption at satellite, e.g., due to the deployment of various CN functions at a satellite, which can be a potential bottleneck impacting the success of 6G NTN.

➲ Potentially a large impact on CN due to moving CN nodes. In legacy network deployment, a CN node is normally static and deployed on the ground. However, if a CN node is deployed in the satellite, e.g. in a LEO satellite, the CN node can have high mobility, which can cause a dynamic CN topology change as well as frequent CN node change for a serving UE. Thus, to support this option, the design of CN and system architecture in 6G would need to take account of the impacts caused by the moving CN nodes.
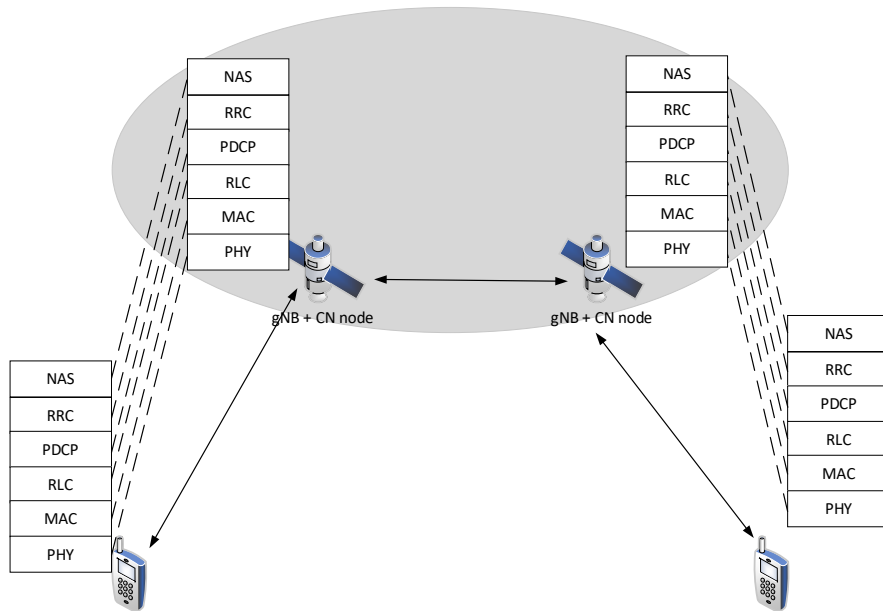
*FIGURE 41: ILLUSTRATION OF CONTROL PLANE FOR OPTION 1.*
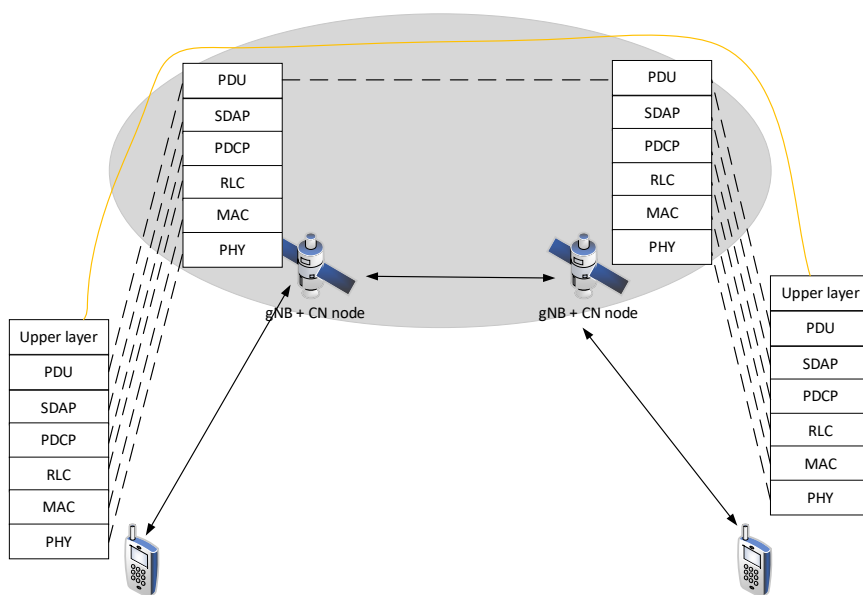
FIGURE 42: ILLUSTRATION OF USER PLANE FOR OPTION 1.-

3.3.3.2 Option 2: NTN Node Equipped with an Onboard Relay-Like gNB

In this option, a RAN node, e.g., a gNB, is available at the NTN node. In order for this option to support an E2E link between two UEs without connectivity to the ground network, modifications may be needed at the onboard RAN node, comparing to the legacy RAN node. For example, since the legacy gNB does not support a direct routing between two UEs, the onboard RAN node needs an additional routing function to route the E2E traffic from one UE to another UE via one or multiple satellite(s).

Figure 43 and Figure 44 illustrate the control plane protocol architecture and the user plane protocol architecture for Option 2, respectively. As can be seen, the Uu air interface designed

for NTN (e.g., the Uu interface designed in the legacy 5G NTN) can be used as the baseline for the direct NTN communication. It is noted the onboard NTN payload in Option 2 only terminates the RAN protocol stacks for a UE, which is different from Option 1, since the NTN node(s) in Option 1 carries the CN functions as well. In addition, the control plane in Option 2 can leverage the RRC layer to control the UE and, thus, it can handle the NTN mobility caused by the high mobility of the NTN node(s), e.g., with the help of Xn interface carried over the ISL.
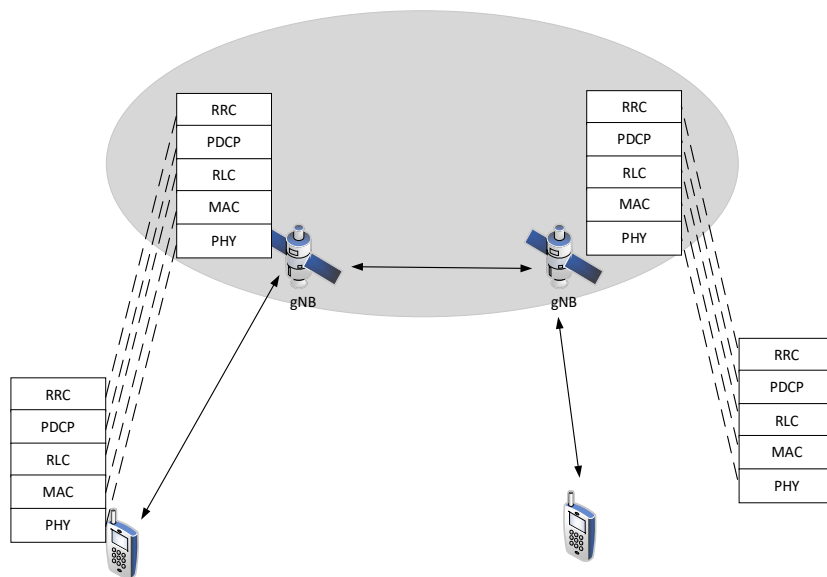
FIGURE 43: ILLUSTRATION OF CONTROL PLANE FOR OPTION 2.
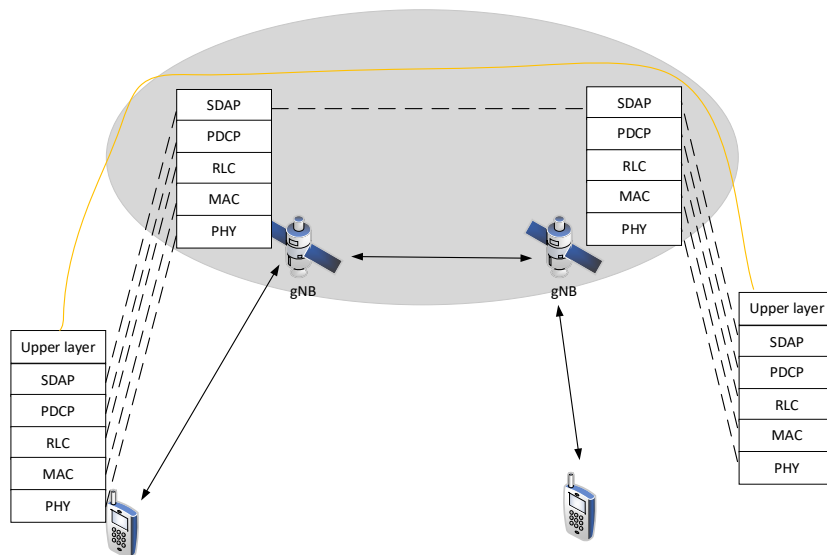
FIGURE 44: ILLUSTRATION OF USER PLANE FOR OPTION 2.

In addition to the mentioned routing function, modifications may be needed for supporting additional upper layer protocols and procedures in Option 2. For instance, authorization, policy/parameter provision, and security/privacy protection may be desired for direct NTN communication. In order to do that, the similarity of direct NTN communication with sidelink (SL) UE-to-UE (U2U) relay is noted. For SL U2U relay, a UE can act as a relay UE to route the traffic between two remote UEs, even when the relay UE is out of the network coverage. Thus, as an example, the technical solutions in SL U2U relay can be considered as a baseline for

authorization, policy/parameter provision, and security/privacy protection in direct NTN communication. It is further noted that, differently from the SL U2U relay that applies the PC5 interface to facilitate the proximity communication between the remote UE and the relay UE, the satellite in the considered direct NTN communication leverages the NTN Uu interface at AS layer to transport the upper layer data (e.g., application or service data) between the two end UEs. Moreover, if charging is required for direct NTN communication, offline charging may be applied, where the satellite and its payload may generate and keep a record of the amount of data consumed by a UE with the direct NTN communication.

Furthermore, in order to support the onboard routing function for the E2E link, an additional layer/function may be added on top of the user plane architecture shown in Figure 44. The additional function/layer is not shown in Figure 44, since it may have different design options. For example, Figure 45 shows an example of using layer-3 (L3)-based routing function, where the additional routing function/layer for the E2E link may be added on top of the SDAP layer. In another example, Figure 46 gives an example of using layer-2 (L2)-based routing function, where the additional routing function/layer for the E2E link may be added on top of the RLC layer.

For the L3-based solution shown in Figure 45 the onboard gNB manages/updates the routing by using an additional layer/function above the AS layer, e.g. based on IP, QoS flow, radio bearer, RNTI, peer UE's location, and/or a header at an additional layer/function. In case a UE in the considered direct NTN communication is restricted with only one peer UE, i.e., a 1-to-1 mapping between the TX UE and the RX UE, routing can be performed based on the TX UE identity. Moreover, additional layer/function may be optionally needed at the UE, e.g., depending on if one UE is restricted to communicate with only one peer UE. In addition, two UEs of an E2E link may set up an E2E control layer, e.g., an E2E RRC/NAS layer as shown in Figure 47, where the E2E RRC/NAS layer is transported over NTN node(s) and Uu PDCP-and-below layers. The E2E RRC/NAS layer can be used for optimizing E2E and joint link control. In one example, the E2E RRC/NAS layer at the UE can be used to initiate the setup/release of the E2E link and/or store the status information of the E2E link.
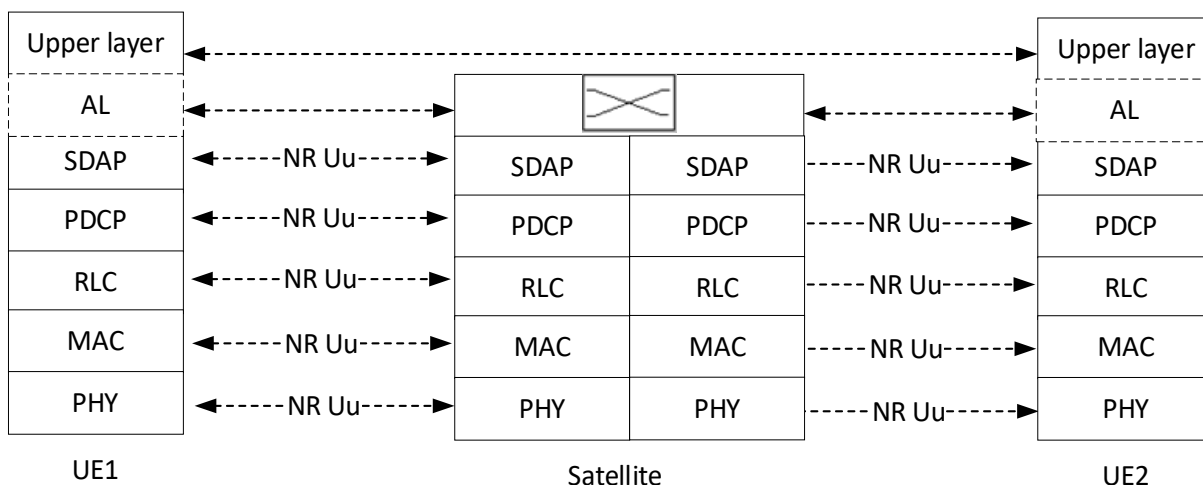

*FIGURE 45: ILLUSTRATION OF LAYER-3-BASED ROUTING ON USER PLANE WITH A SINGLE SATELLITE.*
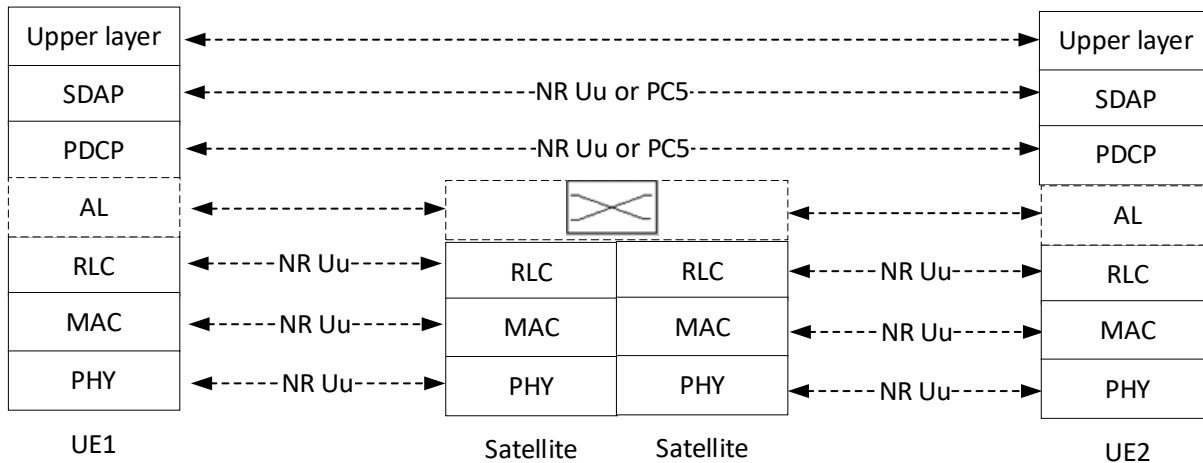
*FIGURE 46: ILLUSTRATION OF LAYER-2-BASED ROUTING ON USER PLANE WITH A SINGLE SATELLITE.*
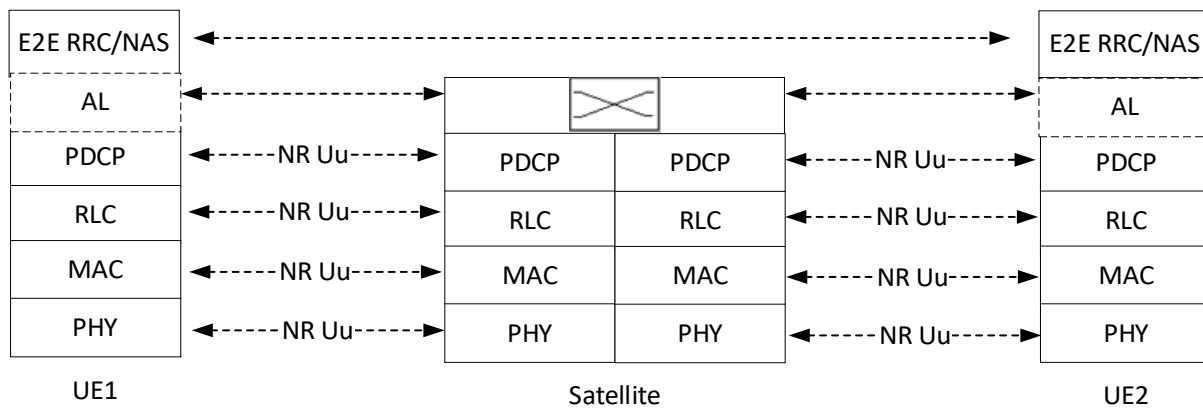
FIGURE 47: E2E LINK CONTROL-PLANE FOR L3-BASED SOLUTION.

As shown in Figure 46, for the L2-based solution, onboard gNB implements an additional layer (AL)/function above the RLC layer to route data packets, wherein layers below PDCP terminate at each UE and the satellite but the PDCP-and-above layers terminate at two end UEs. It is noted, though both Uu and PC5 may be considered for the PDCP-and-above layers, the PDCP and SDAP layers of PC5 may need to be modified, e.g., to handle the large propagation delay in NTN. In this solution, comparing to the L3-based solution, the satellite is not involved in E2E UP security since the PDCP layer is terminated at both UEs. Similar asto the L3-based solution, an optional E2E control layer, e.g., an E2E RRC/NAS layer, can be transported over NTN node(s) and leveraged for the E2E link control, as shown in Figure 48.

As described above, since Option 2 does not require CN deployment on the NTN platform(s), the amount of satellite complexity and power consumption can be expected to be lower than that in Option 1. However, Option 2 would have impact on the RAN specifications, e.g., to implement the required modifications.

It is noted that the additional complexity and specification effort for Option 2 may depend on the considered use case. For instance, some use cases may not require a mobility support, e.g., when the direct communication is used for a one-time short message transmission. While in some other use cases, the direct communication may be used to relay a broadcasted message from one transmitter UE to other users in the proximity of the transmitter UE, which may impact the routing function design at the onboard gNB.
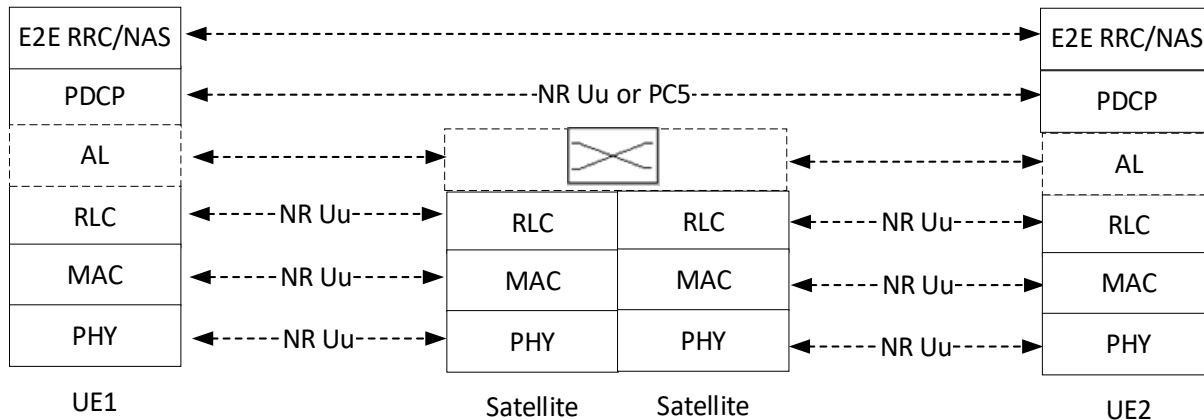
FIGURE 48: E2E LINK CONTROL-PLANE FOR L2-BASED SOLUTION.

3.3.3.3 Option 3: NTN Node Acting as a Sidelink Relay

It is noted, that the considered direct NTN communication may leverage the SL U2U relay design, whose design is currently ongoing in 3GPP Rel-18. The SL U2U relay technology is able to use a UE as a relay UE between two remote UEs and, thus, the E2E traffic between the two remote UEs can be relayed over the relay UE. The communication between a remote UE and the relay UE takes place over the PC5 interface, and the SL U2U relay can work even when all the involved UEs (i.e. including the relay UE and the remote UEs) are out of ground network coverage. Similarly, in Option 3, an NTN node (e.g., a satellite) may act as a SL relay to forward the traffic between two end UEs, as shown in Figure 49.
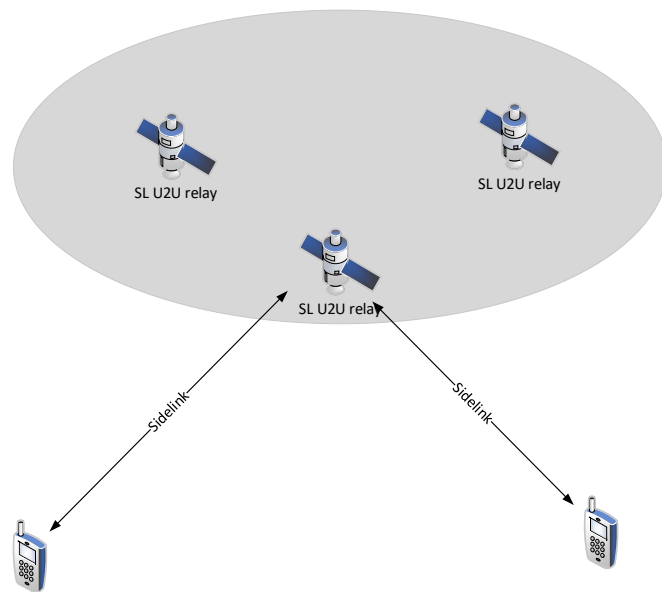
FIGURE 49: NTN PLATFORM ACTS AS A SL U2U RELAY.

In this option, the architecture design of SL U2U relay can be largely reused to support the considered use case. However, more modifications may be needed on the SL air interface design (e.g., PC5 PHY/MAC) to handle the NTN-specific characteristics, since SL was not designed for supporting the long-distance communication between a UE and a satellite. Thus, it means that a UE supporting TN SL operation, e.g., a vehicle, may need to implement an additional capability for supporting SL operation in the considered SL U2U relay over a satellite. In addition, both the UE and the NTN payload may need to use different air interfaces for:

● regular NTN communications by going through the ground network, e.g., via Uu air interface, and

● direct NTN communication without going through the ground NW, e.g., via PC5 air interface.

Thus, this option may increase the complexity at both the UE and the satellite. In addition, since the current SL U2E U2U relay is designed for being equipped at a UE, it has less capability than a gNB. Thus, it may provide less efficiency and robustness than Option 2, e.g., for handling satellite switch due to NTN mobility.

Based on the above analysis, Table 41 summarizes the differences among the three options in supporting the considered direct NTN communication.

TABLE 41: COMPARISON AMONG DIFFERENT OPTIONS FOR DIRECT NTN COMMUNICATIONS

	Option 1: Satellite equipped with RAN and CN	Option 2: Satellite equipped with RAN	Option 3: Satellite equipped with Sidelink Relay
Routing the E2E traffic	Supported by CN	Need to add new function/layer at RAN	Yes (TBC)
Impact on the onboard CN nodes	Yes (To handle mobile CN nodes)	No	No
Added satellite complexity and power consumption	High	Medium	Medium
PHY/MAC support	Yes (R-17/18 or 6G NTN solutions)	Yes (R-17/18 solutions)	No (Need additional RAN1/RAN2 work)
Mobility and service continuity support	Less efficient (CN node switch)	Good (RAN node switch by reusing Uu RRC)	Middle (RAN node switch by SL signaling)
RAN impact	No/Minimum	Yes	Yes
Added UE complexity	Small	Medium	High
Architecture impact	Yes (Mostly on CN)	Yes (Mostly on RAN)	Little (Reuse SL U2U architecture)

3.3.4 Adaptive Functional Split

As discussed in Section 3.3.1, different use cases (UCs) are associated to different requirements and, thus, a "one size fits all" approach is not ideal. For example:

● Higher layer split is preferred for:

  ➢ Traffic load reduction over ISL and the feeder link (UC1)

  ➢ Equipping onboard MEC (UC2 and UC3)

  ➢ Achieving lower latency (UC6)

  ➢ Supporting direct NTN communication without feeder link (UC7)

● Lower layer split is preferred for:

  ➢ Onboard complexity/power reduction (e.g. in drones in UC2 and UC3)

  ➢ Central scheduling for dynamic resource sharing (UC4)

  ➢ Enabling lower layer mobility (UC6)

It is noted, that different from a TN platform in the legacy design, an NTN platform (e.g. a satellite) may have to support different scenarios/use cases at different times and/or different areas, due to the special characteristics in NTN, such as:

- High mobility of a satellite, which is much higher than that of a TN platform, which implies that the satellite may move from one area to another area, e.g. from one country/continent to another country/continent, where conditions in the different areas may be much different, which poses the need for satellite to support different use cases at different times

- Large coverage area of a satellite, which is much larger than that of a TN platform, may imply a high possibility for the satellite to cover different areas with different scenarios and different technical requirements at a considered time instance

Therefore, in order to better support the different use cases in future 6G NTN, it is proposed to consider an adaptive functional split (AFS) technology, which enables the satellite to adapt the functional split in time and/or space domain.

In this section, four options for AFS are provided for their initial analysis in this deliverable. Please note, more detailed analysis, such as impact on technical specifications and/or implementation options, may be provided in the future deliverables.:

- Cell/area-specific AFS: Different functional split options for different cells/areas

- Scenario-specific AFS: Different functional split options in different scenarios

- UE-specific AFS: Different functional split options for different UEs

- Service-specific AFS: Different functional split options for different services

Please note, to illustrate the different AFS options in the rest of this section, a lower layer functional split option, which splits the PHY layer to a lower PHY sub-layer and a higher higher-PHY sub-layer, is used as an example, while a higher layer functional split option, which contains the entire gNB protocol layers, is used as another example. However, these options are only used for illustration purposes, and they should not be interpreted as the only options for supporting the proposed AFS.

3.3.4.1 Cell/Area-Specific AFS
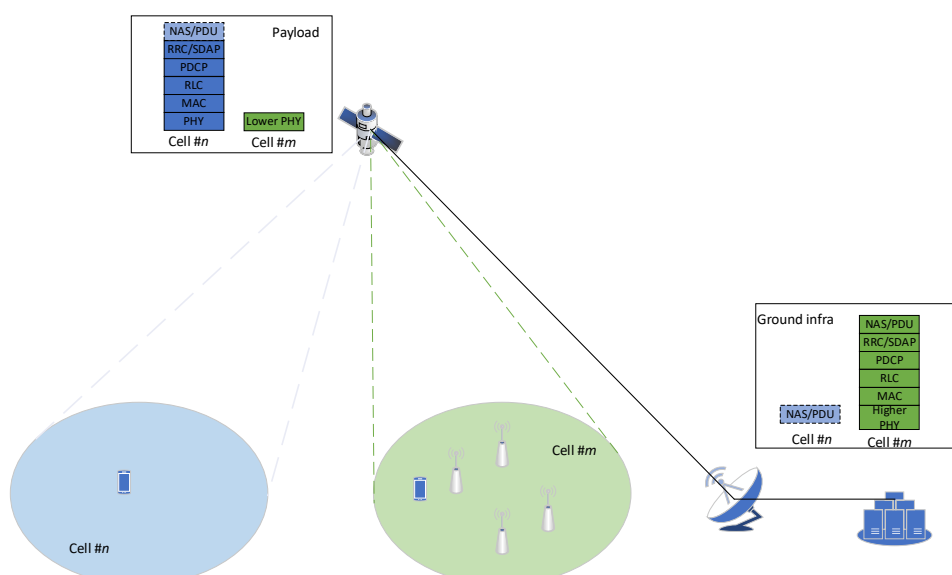
FIGURE 50: ILLUSTRATION FOR THE CELL/AREA-SPECIFIC AFS

Figure 50 shows an example for the cell/area-specific AFS scheme. In this scheme, a satellite may serve different cells or different areas by using different functional split options at the same time. For example, TN and NTN NW may coexist in the area covered by cell #m, e.g. along a seashore, which may prefer to deploy a lower layer function split such that more AS protocol layers can be centrally located on the ground, which enables to apply a central scheduling for handling TN-NTN coexistence and lower layer mobility solutions for TN-NTN mobility. In contrast, cell #n may cover an area without TN coverage, e.g. in the deep sea. In this case, cell #n may benefit from using a higher layer function split, which can help to achieve a lower latency in the AS layer and support onboard MEC in 6G NTN.

Please note, cell #n and cell #m may use the same physical lower PHY entity onboard the satellite, and they are logically separated in Figure 50 for illustration purpose only. Please also note, the same note applies for the rest of the figures in this section.

3.3.4.2 Scenario-Specific AFS
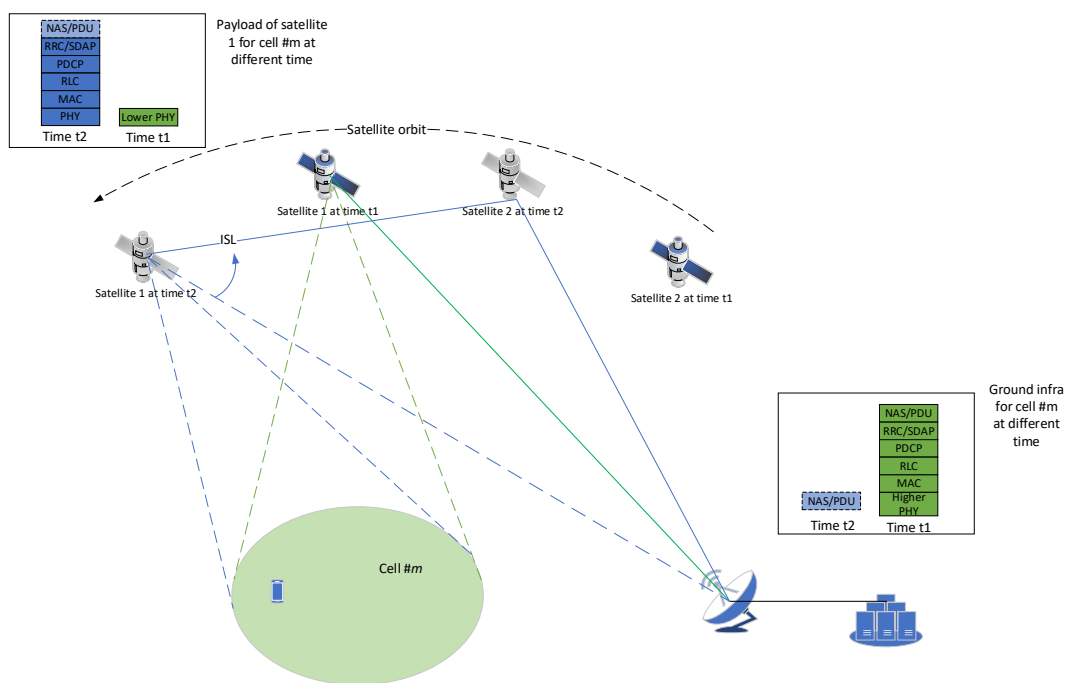
FIGURE 51: ILLUSTRATION FOR THE SCENARIO-SPECIFIC AFS

Figure 51 illustrates an example for the scenario-specific AFS, where the satellite may determine to adapt its functional split based on the real time scenario, e.g. if an ISL is needed. As shown in this figure, satellite 1 at time t1 may have a direct feeder link connection to the gateway and ground network, and it may apply a lower layer split function. However, afterwards, satellite 1 may move away from the gateway. And at time t2, satellite 1 has to establish an ISL towards another intermediate satellite (e.g. satellite 2) for its connection towards the ground network, since satellite 1 has moved out of the gateway's reachability. In this case, in order to reduce the load posed by the data of satellite 1 on the ISL and/or the feeder link of satellite 2, it may be preferred for satellite 1 to switch from lower layer split to higher layer split.

3.3.4.3 UE-Specific AFS
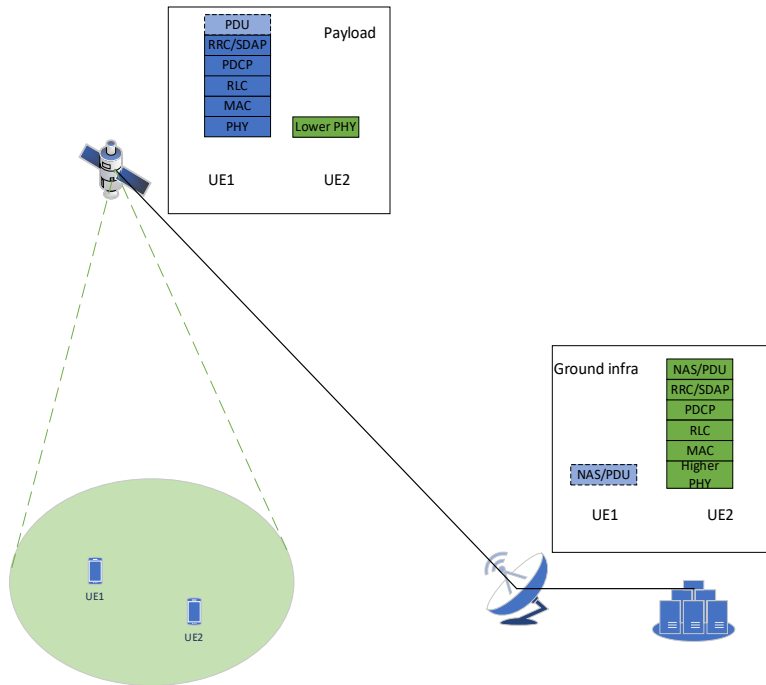
FIGURE 52: ILLUSTRATION FOR THE UE-SPECIFIC AFS

Due to the complexity/resource/power constraint at satellite, a satellite may only be able to support some of the UEs with additional onboard protocol layers and computing resource, but the other UEs may only be supported with lower protocol layers onboard the satellite. Thus, in Figure 52, a UE-specific AFS scheme is shown, where different function split options may be applied for serving different UEs. For example, UE1 may be consuming a low latency service, but not UE2. Thus, in this example, the satellite may apply a higher layer split for UE1 but not UE2, which allows to use the precious onboard resource in a smart manner by taking account of each UE's specific requirement.

3.3.4.4 Service-Specific AFS
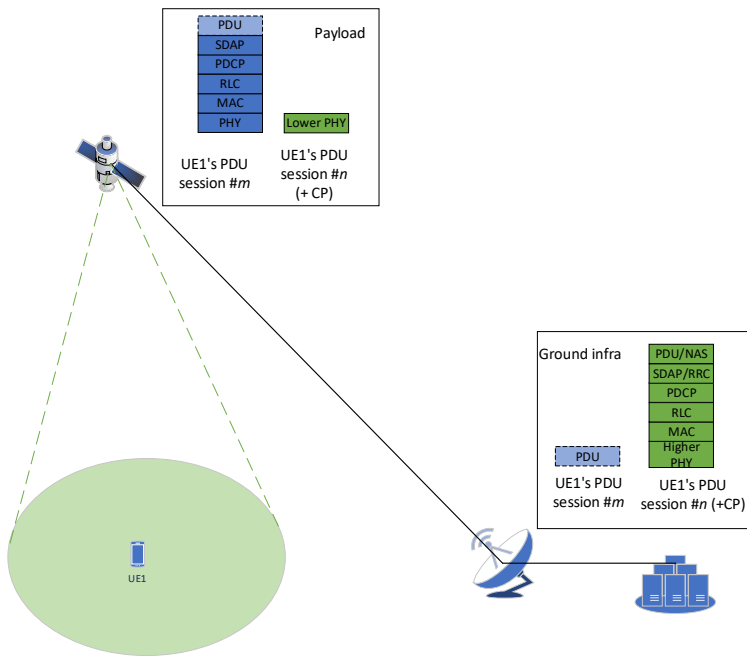
FIGURE 53: ILLUSTRATION FOR THE SERVICE-SPECIFIC AFS

In Figure 53, an example for supporting the service-based AFS is illustrated. In this example, the different services or PDU sessions of the considered UE may be served by using different split options. For example, the UE's session requiring an onboard MEC or low latency (e.g. UE1's PDU session #m) may be served by a high layer split, but lower layer split may be preferred for serving another session (e.g. UE1's PDU session #n) and the control plane of the UE to save the precious onboard resources. This scheme provides a finest granularity level for NTN NW to adapt its functional split function, based on the UE's service-specific requirements.

Please note, the condition(s) used for describing the proposed adaptive function split is only for illustration purpose in Sections 3.3.4.1 - 3.3.4.4, and they should not be considered as an exclusive set of triggers in real implementation. As one example, in the next section, AFS may be triggered and applied by NTN to enable satellite-sharing.

3.3.4.5 Native Support for Satellite Sharing by AFS

The mobility of an NTN node (e.g. LEO/MEO satellite) that causes the NTN node to move across continent and ocean makes NTN much different from TN, since it is possible for the coverage area of one satellite to move from one operator's network to another operator's network, e.g. from one country to another. In this case, an important design target for 6G NTN is to enable satellite sharing among different network operators. In one example, a moving satellite provided and controlled by one satellite network operator (SNO) may be shared by two or multiple different mobile network operators (MNOs) to provide communication coverage to their subscribers.

However, different MNOs may face different conditions, which make them:

➲ Prefer different functional split options

➲ Sign different agreements with one satellite network operator (SNO) w.r.t. the applied functional split option

➲ Face different local regulation requirements

Thus, a critical issue is how to natively support satellite sharing and meet the requirements of the different operators. Based on the initial analysis, the AFS scheme discussed before can support satellite-sharing for multi-operators natively, e.g. by leverageing the cell/area-specific AFS and the scenario-specific AFS.
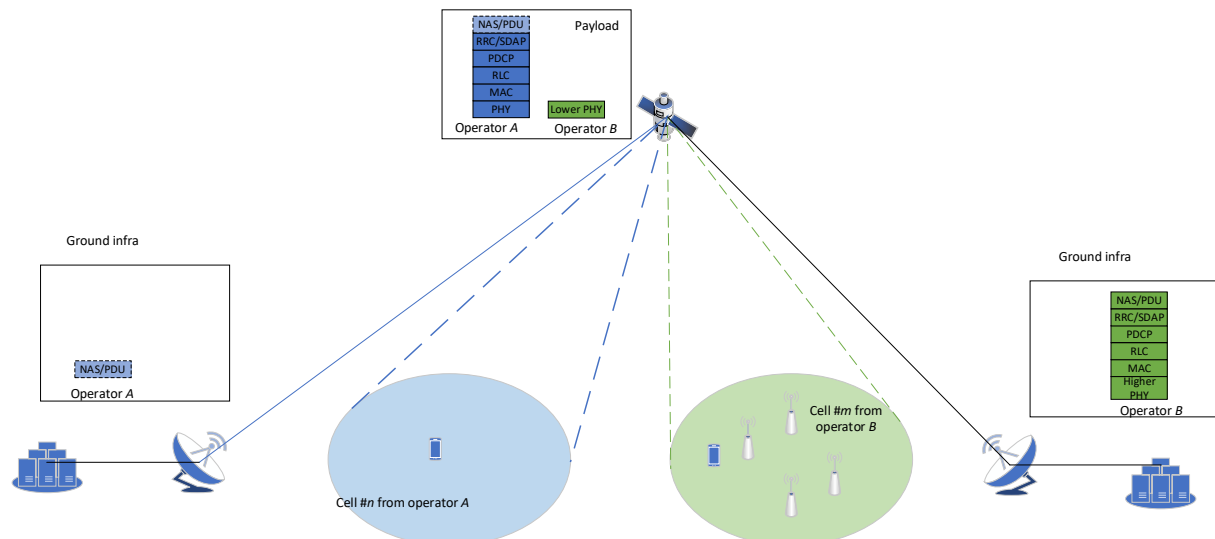

FIGURE 54: ILLUSTRATION ON THE NATIVE SUPPORT FOR SATELLITE-SHARING BY CELL/AREA-SPECIFIC AFS

In Figure 54, the cell/area-specific AFS described in section 3.3.4.1 is used to support satellite sharing with different functional split options for different operators at the same time. As it shows, when the satellite moves to a position and covers the areas of the two different network operators, e.g. Operator A and Operator B, the satellite may use different functional splits for serving the coverage areas of the different operators, e.g. based on the agreements/configurations between the SNO and each individual MNO, correspondingly.
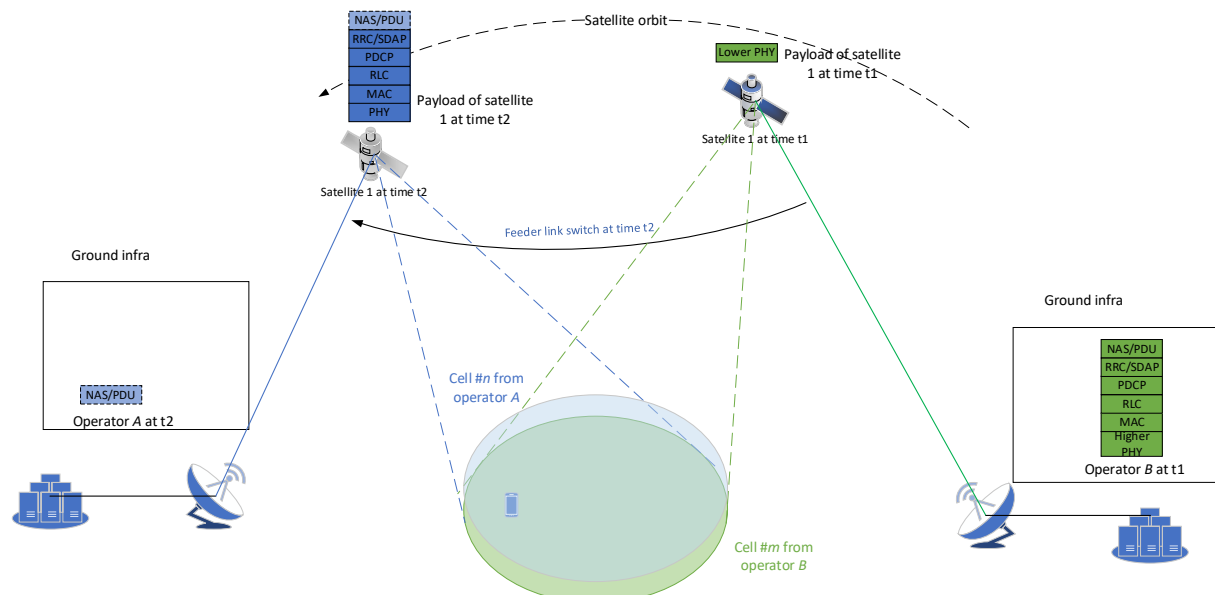

FIGURE 55: ILLUSTRATION ON THE NATIVE SUPPORT FOR SATELLITE-SHARING BY SCENARIO-SPECIFIC AFS

Figure 55 shows how to enable the satellite to switch its functional split options for connecting to different operators' networks. For example, at time t1, satellite 1 may apply a lower layer function split to connect to Operator B's ground infrastructures, based on the agreement/configuration between SNO and Operator B. Later on, at time t2, satellite 1 may move closed to Operator A and, thus, it switches its feeder link and connects to the Operator A's ground infrastructures by adapting to a higher layer split option, based on the agreement/configuration between SNO and Operator A.

4   CONCLUSIONS

The main outcomes of this deliverables are already summarized in the executing summary. Hence, this concluding chapter is focussing on the next steps and main lines of innovation.

4.1.1   Next Steps (towards Deliverable D3.6)

➲ Consolidate service and feeder link budgets and throughput analysis considering the progress in Task 3.2 and 3.3.

➲ Perform a detailed performance assessment of the LEO constellations including not only throughput but also delay performance. Results will be also mapped on the corresponding performance requirements defined in WP2.

➲ Perform mass and power budgets to ensure all required RAN, CN and eventually edge computing functionalities can be implemented in space. This will allow consolidating the functional split analysis.

➲ Carry out a cost assessment of the two proposed LEO constellation architectures.

➲ Provide further insights on the role, capabilities, functionalities and payload architecture of GEOs and HAPs

➲ Address sustainability aspects

➲ Address security aspects in coordination with WP5.

4.1.2   Main Potential Innovations

➲ Q/V band antenna for UEs (carried out in Task 3.2) and for NTN nodes (carried out in Task 3.3)

➲ Distributed architecture for the LEO constellation separating service link payloads from transport network (ISLs and feeder links) with enhanced processing capabilities in space (joint activity with Task 3.4)

➲ Support for full gNB and CN functions within the aforementioned distributed architecture in space

➲ Adaptation of Xn interfaces to work over concatenation of error prone links with high delay

➲ Design of the adaptive (use-case-based or service-based) function split to efficiently distribute network functions

➲ Support for direct NTN communication without the need for an available feeder link

REFERENCES

[1] 3GPP TR 38.821: Solutions for NR to support non-terrestrial networks (NTN) V16.2.0 (Release 16). 2023-03.

[2] 3GPP TR 38.214: Physical layer procedures for data V18.1.0 (Release 18). 2023-12.

[3] 3GPP TS 38.306: User Equipment (UE) radio access capabilities V18.0.0 (Release 18), 2023-12.

[4] 6G-NTN Deliverable 2.1, "Use Case Definition", v1.0.

[5] 6G-NTN Deliverable 2.2, "User Requirements" , v1.0.

[6] 6G-NTN Deliverable 2.3, "Report on System Requirements" , v1.0.

[7] https://www.tesat.de/images/tesat/products/240306_DataSheet_SCOT80_A4_Druck.pdf

[8] Paul Berceau, Stéphane Angibault, Adrien Barbet, Jean Claude Barthes, Damien Blattes, Nicolas de Guembecker, Raphael Fidanza, Emilie Gary, Vincent Lefftz, Thibault Marduel, Florent Tajan, Ludovic Zurawski, "Space optical instrument for GEO-Ground laser communications", Proceedings Volume 12777, International Conference on Space Optics – ICSO 2022; doi: 10.1117/12.2690326

[9] https://www.nasa.gov/smallsat-institute/sst-soa/

[10] https://www.rcrwireless.com/20200708/fundamentals/open-ran-101-ru-du-cu-reader-forum

[11] L. M. P. Larsen, A. Checko and H. L. Christiansen, "A Survey of the Functional Splits Proposed for 5G Mobile Crosshaul Networks," in IEEE Communications Surveys & Tutorials, vol. 21, no. 1, pp. 146-172, Firstquarter 2019, doi: 10.1109/COMST.2018.2868805.

[12] Y. Huang, C. Lu, M. Berg and P. Ödling, "Functional Split of Zero-Forcing Based Massive MIMO for Fronthaul Load Reduction," in IEEE Access, vol. 6, pp. 6350-6359, 2018, doi: 10.1109/ACCESS.2017.2788451.

[13] Y. Huang, W. Lei, C. Lu and M. Berg, "Fronthaul Functional Split of IRC-Based Beamforming for Massive MIMO Systems," 2019 IEEE 90th Vehicular Technology Conference (VTC2019-Fall), Honolulu, HI, USA, 2019, pp. 1-5, doi: 10.1109/VTCFall.2019.8891191.

[14] Volume of data/information created, captured, copied, and consumed worldwide from 2010 to 2020, with forecasts from 2021 to 2025 – Source: Statista Research Department; Sep 8, 2022.

[15] Global mobile network data traffic (EB per month) Ericsson Mobility report – November 2022 . Available : https://www.ericsson.com/en/reports-and-papers/mobility-report.

[16] EU COST ACTION on Future Generation Optical Wireless Communication Technologies - NEWFOCUS CA19111 White Paper on Optical Wireless Communications, 2021.

[17] J. Poliak & all, "Demonstration of 1.72 Tbit/s Optical Data Transmission Under Worst-Case Turbulence Conditions for Ground-to-Geostationary Satellite Communications", IEEE Communications Letters (Volume: 22, Issue: 9, Sept. 2018), DOI: 10.1109/LCOMM.2018.2847628.

[18] M. J. Jang, WPAN 15.7 Amendment—Optical Camera Communications Study Group (SG 7a), IEEE Standard IEEE 802.15. Accessed: Feb. 9, 2021.

[19]   M. Zaman Chowdhury & all, "The Role of Optical Wireless Communication Technologies in 5G/6G and IoT Solutions: Prospects, Directions, and Challenges", Appl. Sci. 2019, 9(20), 4367; https://doi.org/10.3390/app9204367

[20]   Ravinder Singh & al, "Design and Characterisation of Terabit/s Capable Compact Localisation and Beam-Steering Terminals for Fiber-Wireless-Fiber Links", Journal of lightwave technology, Vol. 38, N° 24, December 15, 2020, https://ieeexplore.ieee.org/document/9187939

[21]   ICT WORTECS (2017 – 2020) explores Terabit/s capability of above 90GHz spectrum, combining radio and optical wireless technologies, https://wortecs.eurestools.eu/

[22]   A. A. Jorgensen and all, "Petabit-per-second data transmission using a chip-scale microcomb ring resonator source", Nature Photonics, 20 October 2022, https://www.nature.com/articles/s41566-022-01082-z

[23]   Francesco Alessio Dicandia & al., "Space-Air-Ground Integrated 6G Wireless Communication Networks: A Review of Antenna Technologies and Application Scenarios", Sensors 2022, 22, 3136. https://doi.org/10.3390/s22093136

[24]   Cvijetic, M., & Djordjevic, I. (2013). Advanced optical communication systems and networks.

[25]   2. Tan, L., Ma, J., Huang, B. (1999). Intersatellite Optical Communication System and Its Development. Telecommunications Science (01).

[26]   [Online] Available: https://www.nasa.gov/smallsat-institute/sst-soa/communications#_Toc120879853 (pdf version : https://www.nasa.gov/sites/default/files/atoms/files/9._soa_comm_2022.pdf)

[27]   Xiao, J. & Wang, P. (2009). Optical Satellite Communication Technology. Digital Communication World (06),73-74.

[28]   Liu, S. & Liu, H. (2014). Constellation Design and Performance Simulation of LEO Satellite Communication System. GNSS World of China, 39(3).

[29]   Wenyi Fu, "Analysis of Optical Satellite Communication Technology and Its Development Trend", STEHF 2022, SHS Web of Conferences 144, (2022) https://doi.org/10.1051/shsconf/202214402013

[30]   M. Toyoshima, "Recent Trends in Space Laser Communications for Small Satellites and Constellations," JLT 39, 3, 693–699 (2021).

[31]   G.C. Baister and P.V. Gatenby, "Why optical communication links are needed for future satellite constellations", IEEE 1996

[32]   M. Toyoshima, "Applicability of Space Laser Communications for Low Earth Orbit Satellite Constellations," OFC 2022 © Optica Publishing Group (2022).

[33]   Cui, X. (2021). Analysis of key technologies and development trend of satellite optical communication [J]. Information and Communications Technology and Policy, 2021(11):65-72.

[34]   Viswanath, A., Kaushal, H., Jain, V. K., et al., "Evaluation of performance of ground to satellite free space optical link under turbulence conditions for different intensity modulation schemes". Free-Space Laser Communication and Atmospheric Propagation XXVI. International Society for Optics and Photonics, 2014, 8971: 897106.

[35]   Kaymak, Y., Rojas-Cessa, R., Feng, J., et al., "A Survey on Acquisition, Tracking, and Pointing Mechanisms for Mobile Free-Space Optical Communications", IEEE Communications Surveys & Tutorials, vol. 20, no. 2, pp. 1104-1123, 2018, doi: 10.1109/COMST.2018.2804323.

[36]   Yagiz Kaymak & al, "A Survey on Acquisition, Tracking, and Pointing Mechanisms for Mobile Free-Space Optical Communications", Electrical and Computer Engineering, Published - Apr 1 2018.

[37]   E. Leitgeb & al, "Chapter "Clear Sky Optics" of the e-Book "Influence of the variability of the propagation channel on mobile, fixed multimedia and optical satellite communications", Satellite Communications Network of Excellence IST Network of Excellence No 507052, 2006.

[38]   Yi-Jun Cai & al, "10 Gbps Laser Communication for Low Earth Orbit Satellites with Volterra and Machine Learning Nonlinear Compensation Providing Link Budget up to 74 dB", OFC 2022 © Optica Publishing Group 2022.

[39]   Available: https://www.nict.go.jp/en/data/report/NICTREPORT2023.pdf

[40]   Available : https://journals.aps.org/rmp/abstract/10.1103/revmodphys.94.035001

[41]   P. Villoresi, T. Jennewein, F. Tamburini, M. Aspelmeyer, C. Bonato, R. Ursin, C. Pernechele, V. Luceri, G. Bianco, A. Zeilinger and C. Barbieri, "Experimental verification of the feasibility of a quantum channel between space and Earth," New J. Phys. 10, 2008.

[42]   S. Nauerth, F. Moll, M. Rau, C. Fuchs, J. Horwath, S. Frick and H. Weinfurter, "Air-to-ground quantum communication," Nature Photonics, vol 7, pp. 382–386, 2013

[43]   A. Carrasco-Casado, H. Kunimori, H. Takenaka, T. Kubo-Oka, M. Akioka, T. Fuse, Y. Koyama, D. Kolev, Y. Munemasa, and M. Toyoshima, "LEO-to-ground polarization measurements aiming for space QKD using Small Optical TrAnsponder (SOTA)," Optics Express, vol. 24, pp. 12254-12266, 2016.

[44]   Y. Juan, Y-H. Li, S-K. Liao, M. Yang, Y. Cao, L. Zhang, J-G. Ren, et al., "Entanglement-based secure quantum cryptography over 1120 kilometres," Nature, vol. 582, pp. 501-505, 2020.

[45]   J. S. Sidhu, S. K. Joshi, M. Gündoğan, T. Brougham, D. Lowndes, L. Mazzarella, et al., "Advances in space quantum communications," IET Quantum Communication, vol. 2(a), pp. 182-217, 2021.

[46]   Available: HTTPS://ARXIV.ORG/ABS/2303.17224

[47]   Available : https://opg.optica.org/optica/fulltext.cfm?uri=optica-9-8-933&id=492969

[48]   Available : https://www.esa.int/Applications/Connectivity_and_Secure_Communications/How_security_in_space_helps_Europe_to_cope_with_crises_on_Earth

[49]   Safety of Laser Products - Part 1: Equipment Classification, Requirements and User's Guide, International Electrotechnical Commission (IEC) 60825-1:2014 Std., Aug. 2014.

[50]   Toyoshima, M. (2005). "Trends in satellite communications and the role of optical free-space communications". Journal of Optical Networking, vol. 4, Issue 6, p.300

[51]   [Online] Available: https://www.space.com/spacex-starlink-satellites-phone-home-dimming.html

[52]   [Online] Available: https://aws.amazon.com/jp/ground-station/

[53]   [Online] Available: http://www.laserlightcomms.com/

[54]   [Online] Available: https://www.analyticalspace.com/

[55]   [Online] Available: http://www.bridgecomminc.com/

[56]   [Online] Available: https://kleo-connect.com/

[57]   W. Tong, "A Perspective of Wireless Innovations in the Next Decade," presented at

IEEE Globecom 2018, Keynote Session, Abu Dhabi, UAE, December 9-13, 2018.

[58]   [Online] Available: https://transcelestial.com/

[59]   [Online] Available: https://www.golbriak.space/

[60]   Toyoshima, M. (2005). "Trends in satellite communications and the role of optical free-space communications". Journal of Optical Networking, vol. 4, Issue 6, p.300

[61]   Alberto Carrasco-Casado & al, "Free-space optical links for space communication networks", Chapter from the book "Springer Handbook of Optical Networks" (pp. 1057-1103) https://doi.org/10.1007/978-3-030-16250-4.

[62]   F. Long, Satellite Network Robust QoS-aware Routing, 2014.

[63]   Available: https://standards.ieee.org/ieee/1905.1/4995/

[64]   Alimi, I.A. et al., 2019. « Effects of Correlated Multivariate FSO Channel on Outage Performance of Space-Air-Ground Integrated Network (SAGIN). Wireless Pers.Commun. 106, 7–25.

[65]   Zhou et al., ''Delay-Aware IoT Task Scheduling in Space-Air-Ground Integrated Network,'' 2019 IEEE Global Communications Conference (GLOBECOM), Waikoloa, HI, USA, 2019, pp. 1-6, 10.1109/GLOBECOM38437.2019.9013393.

[66]   Liu, J., Shi, Y., Fadlullah, Z. M. and Kato, N. (2018), "Space-Air-Ground Integrated Network: A Survey", IEEE Communications Surveys & Tutorials, vol. 20, no. 4, pp. 2714-2741, Fourthquarter 2018, doi: 10.1109/COMST.2018.2841996.

[67]   R. Bedington, J.M. Arrazola, and A. Ling. "Progress in satellite quantum key distribution." Npj Quantum Information Vol. 3, 30, 2017.

[68]   P. Serra, O. Čierny, W. Kammerer, E.S. Douglas, D.W. Kim, J.N. Ashcraft, G. Smith, C. Guthery, T. Vergoossen, A. Lohrmann, R. Bedington, C. Perumangatt, A. Ling, K. Cahoy. "Optical front-end for a quantum key distribution cubesat." Proc. SPIE 11852, International Conference on Space Optics, 118523C, June 11, 2021.

[69]   D. Jacobs, J. Bowman, M. Patterson, M. Horn, C. McCormick and M. Adkins. "Plan for On-Orbit Demonstration of the Deployable Optical Receiver Array." IEEE Aerospace Conference (AERO), pp. 1-8, 2022.

[70]   J.E. Velazco and J.S. de la Vega. "Q4 – A CubeSat Mission to Demonstrate Omnidirectional Optical Communications." IEEE Aerospace Conference, pp. 1-6, 2020.

[71]   A. Carrasco-Casado et al., ""Intersatellite-Link Demonstration Mission between CubeSOTA (LEO CubeSat) and ETS9-HICALI (GEO Satellite)." IEEE International Conference on Space Optical Systems and Applications (ICSOS), pp. 1-5, 2019.

[72]   W. Kammerer, P. Grenfell, L. Hyest, P. Serra, H. Tomio, N. Belsten, C. Lindsay, O. Čierny, K. Cahoy, M. Clark, D. Coogan, J. Conklin, D. Mayer, J. Stupl, J. Hanson. "CLICK Mission Flight Terminal Optomechanical Integration and Testing." International Conference on Space Optics — ICSO, 2022.

[73]   Tesat. " SMALLEST LASER COMMUNICATION TRANSMITTER WORLDWIDE." Technical Datasheet. [Online] 2022. Available at: https://www.tesat.de/images/tesat/products/220607_DataSheet_CubeLCT100M_A4.pdf

[74]   [Online] Available: https://www.sda.mil/wp-content/uploads/2022/04/SDA-OCT-Standard-v3.0.pdf

[75]   [Online] Available: https://www.dlr.de/kn/en/desktopdefault.aspx/tabid-17409/#gallery/36183

5   APPENDIX B: LLS IN TERRESTRIAL NETWORKS

In terrestrial networks it is common to separate RAN functionality in different nodes that implement a subset of the physical layer functionality. Historically, base stations were monolithic, containing both Digital Signal Processing (DSP) equipment and RF in the same node. Antenna panels (and power amplifier) were mounted on masts and connected to the base station via coaxial cables.

Over time, the building practices shifted to separating DSP and RF equipment in two nodes (baseband and radio) and mounting the radio node closer to the antennas. This reduces the thick coax cable runs used to connect radio to antenna panels, which were then substituted by fiber. The main enabler for this type of construction was the Common Public Radio Interface (CPRI). CPRI is a digital TDM interface that allows the transmission of time-domain samples between baseband and radio, besides control information and timing reference signals. It allowed the link between baseband node and radio node to become longer, in the range of a few tens of kilometers. This range extension also allowed operators to start installing baseband processing nodes in centralized locations, in more controlled environments, not necessarily close to the sites or exposed to the elements.

Another outcome of this architectural change was that split base stations have the advantage of decoupling the life cycles of the units. It is possible and common to upgrade baseband features and capacity and while reusing the radio, which is already deployed in the field.

With the introduction of 5G-NR, the number of antennas managed by each base station grew substantially, due to the Radio Access Technology (RAT) taking advantage of beamforming and multi-user massive Multiple Input Multiple Output (MIMO). The increase in number of antennas made a fronthaul interface carrying time-domain samples, such as CPRI, less advantageous. The bandwidth requirements for such a fronthaul link were too demanding, in the tens or hundreds of gigabits per second.

The industry and academia started considering alternative physical layer splits, by moving more functionality from baseband node to radio node. In an Orthogonal Frequency Division Multiplexing (OFDM) based RATs, a relevant change is to move the Fast Fourier Transform (FFT) to the radio node. That provides a reduction in overall required bandwidth, while also enabling the traffic on the fronthaul interface to be proportional to the user traffic instead of the bandwidth of the cell.

The variable traffic in the fronthaul interface allows for statistical multiplexing in the fronthaul infra-structure. That in turn, led to the adoption of high-volume Ethernet transceivers to implement packet based intra-PHY split base stations.

Connecting the baseband and radio nodes over a packet-switched fronthaul network allows the operators to leverage statistical multiplexing in their transport infra-structure but also enables simplified deployment and maintenance due to remote connectivity and configuration of the interconnects between the nodes.

A survey of functional-split related research for 5G is presented in [7]. A subset of the paper covers the intra-PHY split options. [12] and [13] propose adaptations for uplink receiver algorithms in a PHY-split base station. The authors develop specific formulations for zero forcing and interference rejection combining taking into consideration what operations shall be executed in each node. They develop the adaptations with the intent of minimizing traffic demands on the fronthaul interface while taking into consideration restrictions in the compute resources in the radio node.

6 APPENDIX C: OPTICAL SATELLITE COMMUNICATION (OSC)

6.1 INTRODUCTION

Inter-satellite links between LEOs and between GEOs are supposed to be based on optical communications. This technology, which has proven its full technological maturity in the Earth Observation domain with the European Data Relay System (EDRS), is still at prototyping / pre-operational stage for telecom applications. Therefore, a thorough review is provided in this Appendix for interested readers.

6.1.1 Data Communication

The expected evolution of data traffic volumes (Figure 56 A) has a potential large impact on the energy consumption of ICT infrastructure, including Non-Terrestrial-Network segment. This forces the scientific community to propose a new vision for the network of tomorrow. Roughly every 10 years, the mobile communication ecosystem engages in designing a system using the most up-to-date techniques to answer to increased traffic (Figure 56 B). This periodicity stems from the time needed for research, standardization, international spectrum harmonization, and industrialization.


(A) *(B)*
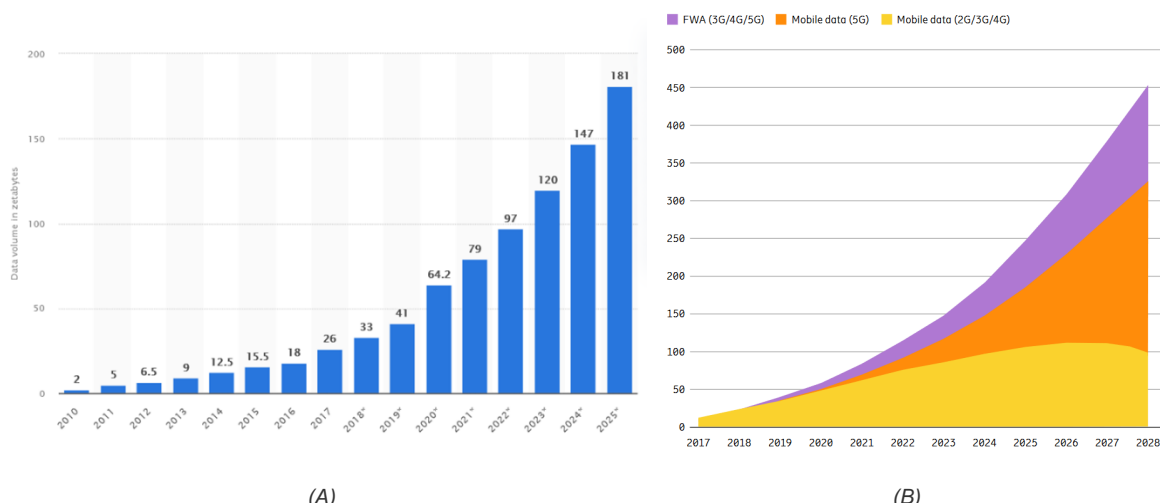
FIGURE 56: TRAFFIC EVOLUTION: (A) GLOBAL DATA VOLUME [6], (B) MOBILE NETWORK DATA TRAFFIC EVOLUTION [7]

The percentage of energy required for operating the global ICT infrastructure could be between 20% and 30% by 2030 (depending on certain assumptions concerning electricity production by 2030). ICT actors need to react on the access and enterprise segments as they account for most of the energy usage. It is hence urgent to propose innovations in these parts of the network (access and enterprise or in-building).

"6G" is the next generation of mobile communication technology with anticipated commercial deployments from 2030 onward. This is the reason why 6G technologies are already subject to intense research efforts with new usages and emerging candidate techniques. These techniques include sub-terahertz (sub-THz) and Terahertz (THz) spectrum band investigation, Reconfigurable Intelligent Surfaces (RIS) solution, NTN with satellite and High-Altitude Platforms (HAPs), and still its infancy, Optical Wireless Communication (OWC).

6.1.2 Optical Wireless Communication (OWC)

OWC use light to connect across free space without the confinement to a waveguide (Figure 57) [16]. Both LEDs and Lasers can be modulated to provide data communications, for instance, outdoor point-to-point (known as Free-Space-Optics or FSO) with capacity as high as 1.72 Tb/s [17]). Similar systems have also been demonstrated for indoor point-to-multipoint solutions (Light Fidelity or LiFi) with data rate up to several Gb/s or between devices (Optical Camera Communication – OCC) with few kb/s [18] and [19]. A new approach to OWC known as Fiber Wireless (FiWi) offers a direct connection between two optical fibers [20]. Under this concept, light emitted by an optical fiber is collimated and then steered to a receiver. At the receiver, the incoming light is coupled again into an optical fiber. This FiWi operates bidirectionally, and speeds greater than 1Tb/s have been attained (WORTECS project - wireless world record [21]) with a theoretical capacity up to 1.84 Pb/s [22].

OWC has an available spectrum 2600 times greater the radio spectrum (considering the band from 400 to 1900 nm) and can be used to add new capacity to existing radio systems rather than replacing them. Additionally, OWC beam is usually collimated, thereby providing a first physical layer of security and the ability to reuse the same wavelengths in adjacent link, thus radically increasing the total system data throughput capacity.
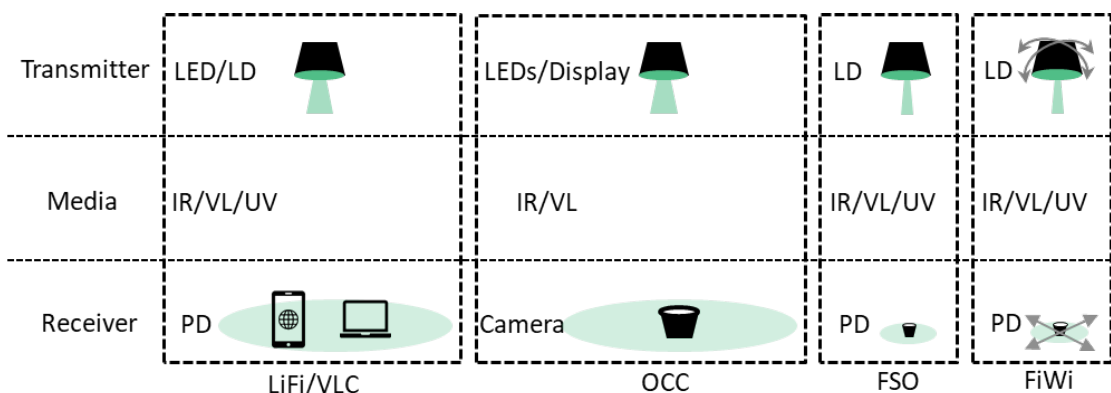

FIGURE 57: OWC WITH PHOTODIODE (PD), LASER DIODE (LD), INFRARED (IR), ULTRAVIOLET (UV) AND VISIBLE LIGHT (VL)

The main OWC applications can be define into five categories with respect to the transmission range:

- Ultra-short range: chip-to-chip communications in cable replacement.
- Short Range: define by Wireless Body Area Network (WBAN) or Wireless Personal Area Network (WPAN) applications and linked to IEEE 802.15.7 standard with for instance OCC or VLC.
- Mid-Range: Indoor multi user application for Wireless LANs (WLAN) define as Light Fidelity (LiFi) or Fiber Wireless (FiWi) and vehicular communications.
- Long range: Outdoor point to point Free Space Optical communications (FSO) and underwater communications.
- Ultra-long range: Optical Satellite Communication (OSC) for Inter-Satellite Links (ISL), Telescope Optical Ground Station (OGS) to satellite communication and Non terrestrial Network (NTN) satellite constellations.

6.1.3 Optical Satellite Communication (OSC)

Due to the wide range coverage and highly accurate communication aspects, satellite communication offers positives aspects. Basically, several types of satellites exist as defined

on Figure 58 but mainly there is: (i) LEO, (ii) MEO and (iii) GEO. LEO satellites orbit the Earth between 160 and 2000 km. MEO satellites are between 2000 and 36000 km above the Earth. GEO satellites have a stationary orbit of 22236 km. The latter are mainly used to provide network access medium, for instance: Radio spectrum Ku band – 12 to 18 GHz with data transmission rate around 500 Mbps and 100-6000 km coverage.

Orbit	Altitude	Onboard Angular Range	Visibility Time	Latency
VLEO	<500 km	Beyond ± 60°	<20 min.	<20 ms
LEO	~1000 km	±60°	20 min.	~20 ms
MEO	~10,000 km	±20°	45 min.	~100 ms
GEO	35,786 km	±8.7°	Permanent	~250 ms
HEO	Up to 40,000 km at apogee	±10°	A few hours	~250 ms

FIGURE 58: KEY PARAMETERS OF TYPICAL SATELLITE EARTH ORBITS [15]

Optical Satellite Communication is communication by light which carries information between satellites or between satellites and the ground [24]. The optical system consists of the light source, transmission, and reception subsystems [25].

On average, a data rate of 1 Gbps is achieved (minimum of 0.15 Gbps and maximum currently 10 Gbps). Basically, communication signals are processed in baseband, potentially encrypted, and modulated via the optical antenna and received by one or more optical receiving antennas. The signal is detected and demodulated to obtain the message. The communication is usually full duplex. For instance, Figure 59 indicates OSC satellites in space since 2014.

Vendor/Developer	Terminal	Platform	Data Rate	Mass	Power	Wavelength	Modulation	Launch Date
---	---	---	[Mbps]	[kg]	[W]	[nm]	---	---
NICT	SOTA	SOCRATES	10	5.9	16	976/800/1549	OOK	5.2014
DLR	OSIRISv2	BiROS	1000	1.65	37	1550	OOK	6.2016
DLR	OSIRISv1	Flying Laptop	200	1.3	26	1550	OOK	7.2017
Aerospace Corporation	OCSD-B&C	AeroCube-7	200	<2.3	20	1064	OOK	12.2017
NICT	VSOTA	RISESAT	1	<1	4.33	980/1550	OOK/PPM	1.2019
Sony/JAXA	SOLISS	ISS	100	9.8	36	1550	OOK	7.2019
DLR	OSIRIS4CubeSat	PIXL-1	100	0.4	10	1550	OOK	1.2021
MIT Lincoln Labs	TBIRD	PDT-3	200,000	<3	100	1550	QPSK	5.2022
MIT	CLICK-A	CLICK	10	1.2	15	1550	PPM	7.2022
MIT	CLICK-B/C	CLICK	20	1.5	30	1537/1563	PPM	Est. 2023
AAC Clyde Space	CubeCat	---	1000	<1.33	15	1550	OOK	---

FIGURE 59: OSC SYSTEMS IN SPACE [18].

Optical satellite communication can be divided into several categories: Satellite-to-ground communication and Optical ISL (O-ISL) is classified into Inter-ISL defined as Intraplane (containing GEO-GEO, LEO-LEO) and Inter-Orbit Link (IOL) defined as Interplane (containing GEO-LEO) [27] (Figure 60).The high-orbit GEO satellite has wide coverage, making 3 Earth-covering GEO satellites possible. In that way, it is possible to use GEO optical satellite in high orbit as satellite relay of the LEO optical satellite, mainly builds the connection with the Optical Ground Stations (OGS), which finally able to propose an all optical space-earth integration communication network [28].
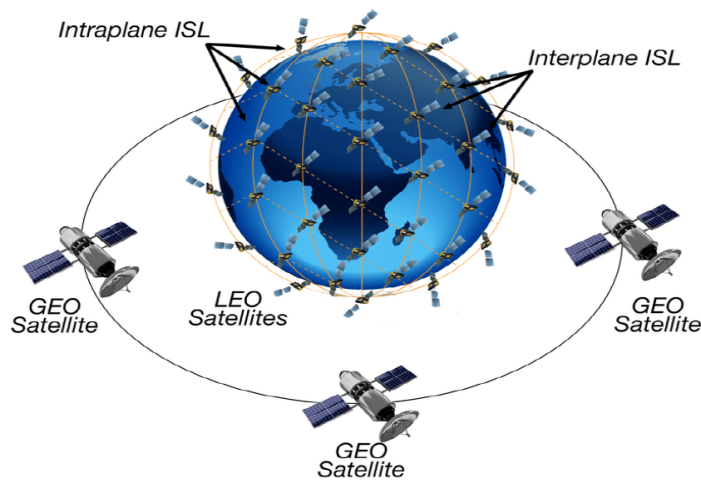
FIGURE 60: GEO & LEO SATELLITES WITH INTRAPLANE AND INTERPLANE ISL [21].

6.2 OSC AND ISL FOR NTN RECENT TRENDS

Constellation programs were planned and then launched to provide global satellite communications services by non-geostationary orbit (NGSO) satellite systems. However, frequency spectra are potentially depleted, additionally spectrum allocation becomes problematic and costly in Radio Frequency (RF) bands as satellite data throughput increases [30].

So, space communication is compelled to investigate higher RF frequencies up to optical frequency bands. Optical communications are used due to high capacity as well as interference tolerance and lack of regulatory restriction which does not require international frequency coordination [31]. For instance, and Proof of Concept (PoC), NASA's Laser Communication Relay Demonstration Satellite (LCRD) was launched on December 7, 2021. Additionally, several OSC satellites were launched as Proof of Concept, and it is possible to have a global view about the history of space laser communication programs in Figure 61.
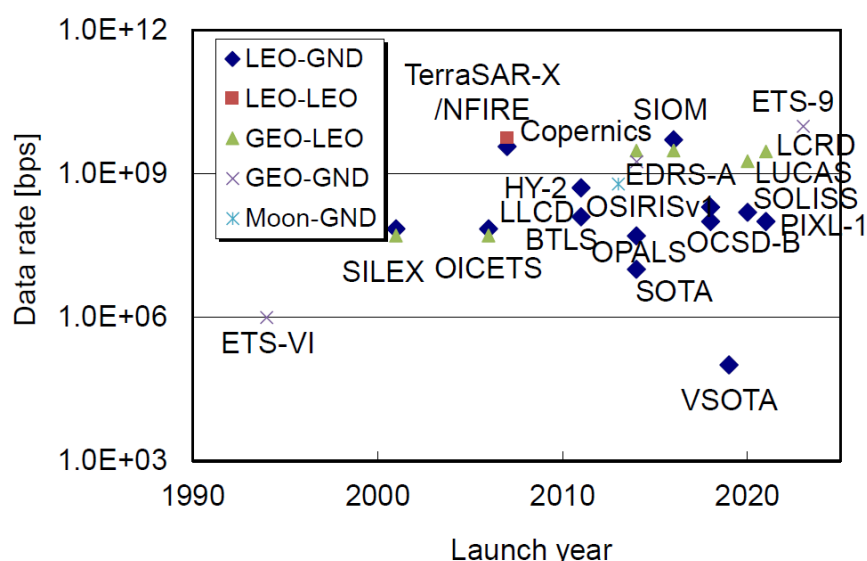
FIGURE 61: SPACE LASER COMMUNICATION: DATA RATE VERSUS YEAR LAUNCH [24].

6.3 KEY SUB SYSTEMS

Optical satellite communication is a multidisciplinary field integrating, at least, optic geometric, atmospheric optic, mechanics, mathematics, and computer science. Figure 62 indicates basic different subsystems constituting an optical transmission satellite.
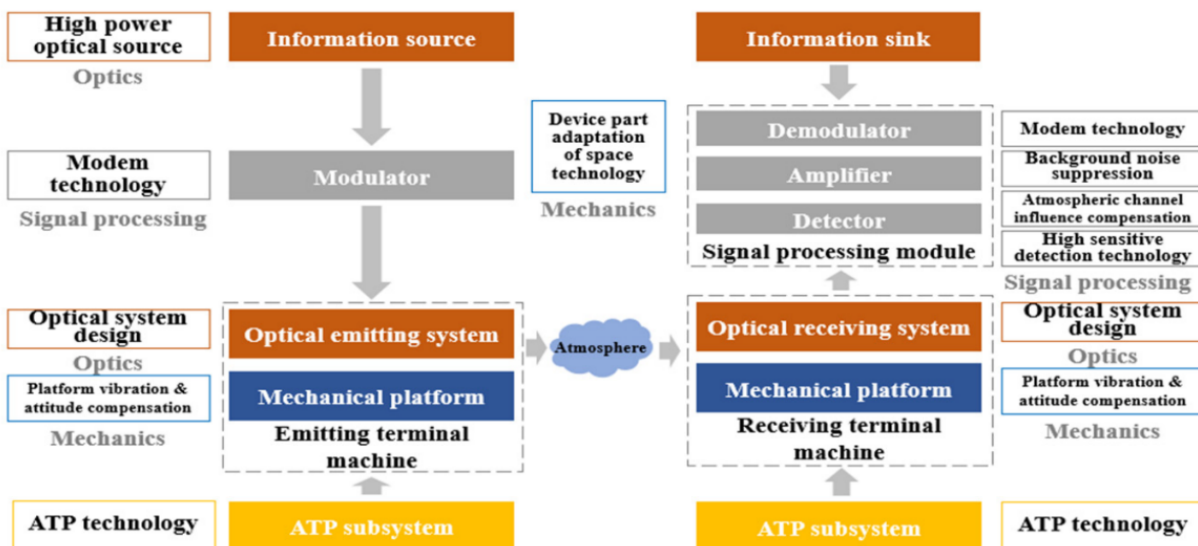

FIGURE 62: SPACE LASER COMMUNICATION: DATA RATE VERSUS YEAR LAUNCH [25].

Like any space device, this one must have specific properties to reduce or cancel the space environment negative effects. It includes, for example, mirror surface performance protection, anti-cold welding of mechanical components, anti-radiation technology of the amplifier, etc.

6.3.1 Optic Layer

6.3.1.1 Optical Emission

The optical sources operate from visible (from 400 nm to 700 nm) to infrared (IR) (up to 10000 nm). In OWC, the two types of sources are LEDs and Laser Diodes.

- ➲ Organic LED (OLED) is intended for flat screens. The modulation bandwidth is around hundreds of kHz.

- ➲ μ-LEDs (≤ 100 μm) can provide modulation bandwidths of hundreds of MHz, thus offering data rates with many sources to provide sufficient illumination for indoor lighting.

- ➲ Phosphor-Converted LEDs (PC-LEDs) are the cheapest with data rate up to few Gbps.

- ➲ Red, Yellow, Green and Blue (RYGB) multi-chip LEDs can offer higher aggregate data rates with Wavelength Division Multiplexing (WDM).

- ➲ Laser Diodes (LDs) are used in high-speed VLC, infrared OWC, and fiber optic communication. LD output is a coherent light and better collimated than LEDs, improving efficiency and point-to-point data transmission. In addition, its narrow optical emission spectrum enables high aggregate data rates with WDM.

Satellite communication has long distance (up to 40,000 kilometers for instance), so ground and satellite stations must use LD (with sometimes, Optic Amplifier – OA) to achieve high enough transmission power to reach other stations. LDs are also chosen to support high bandwidth modulation and high data rate transfer with special amplifier stage to drive low

equivalent impedance. The preferred wavelengths band are around 800nm, 1000nm and 1500nm, corresponding to semiconductor lasers, solid lasers, and fiber lasers applications. In addition, 850nm, 1550nm and 10,000nm are used for ground-satellite links, according to weather conditions, security and atmospheric turbulence.

The signals use to come from Digital to Analog Converter (DAC) stage. For instance, LD with 800 MHz bandwidth of modulated signal can provide up to 8 Gbps throughput with optimal OFDM treatment.

6.3.1.2   Optical Receiver

About the receiver side, photodetectors (PDs) convert light into electricity. Various types of PD are used in OWC, silicon (Si), germanium (Ge), gallium arsenide (GaAs), gallium aluminum arsenide (GaAlAs) and indium and gallium (InGaAs). Each of these detectors has a specific spectral sensitivity, quantum efficiency and strongly depends on the wavelength used.

For instance, silicon PDs have the highest sensitivity in the NIR region (800 nm and 1000 nm) and are cheaper than other PDs. For higher wavelength ranges, other technologies, such as InGaAs and Ge PD are used for Avalanche Photo Diode (APD) for instance.

To achieve a high Signal to Noise Ratio (SNR) and guaranty a long-range link quality, APD photodiode are used with generally two amplifier stage for circuitry conception. Additionally, to avoid interference and improve the SNR, a narrow band optical filter is used in front of APD. Amplification and filtering ensure an optimal signal transfer for Analog to Digital Converter (ADC) stage.

6.3.2   Signal Processing and Modulations

Signal processing technology has two main approaches: modem technology and background noise suppression management. Modem technology includes modulation and demodulation. Modulation uses a baseband signal to control the change of one or more parameters of the carrier signal (amplitude, frequency, phase) and form a modulated signal transmission. Demodulation is the reverse process of modulation, as the original baseband signal will be recovered from the change in parameters of the modulated signal.

Optical satellite communication potentially uses various modulation formats but the simplest and most effective seems to be On-Off Key modulation (OOK) with Intensity Modulation/Direct Detection (IM/DD) to obtain the best efficiency against turbulent atmospheric conditions [34]. The information is encoded with light intensity variation. OOK modulation is simple and robust against the nonlinearity but with spectrum efficiency limitation. Alternatively, Pulse Position Modulation (PPM) and Minimum Shift Keying (MSK) Subcarrier Intensity Modulation (PPM-MSK-SIM) offers advantages of strong anti-interference and high-power ratio. To increase the spectrum efficiency, OFDM modulation is proposed to increase the robustness to multipath propagation (or Interference Inter Symbol - ISI). In addition, the main noise comes from solar radiation and the intensity of the radiation decreases as the wavelength increases. To decrease the background noise, spatial filtering and signal modulation technology is applied. Like radio system, Multi-Input Multi-Output (MIMO) technique is also provided for better bandwidth and throughput. Finally, optical coding division multiple access (OCDMA) technique offer channel allocation flexibility, asynchronously operative ability, privacy enhancement, and network capacity increment but with complexity and cost.

6.3.3   Pointing Acquisition and Tracking (PAT)

Pointing, Acquisition and Tracking (PAT) is the foundation for long-range spatial optical communication and it is the most difficult step since the optical beams are inevitably smaller than the reception estimation area [35]. To precisely point its beam, each satellite terminal

must be able to know the distant satellite exact position or of Optical Ground Station (OGS) terrestrial zone. A first searched area estimation will come from the satellite orbit information. The first terminal points to the supposed position of the remote device using the complete displacement of said satellite or else thanks to a particular pointing unit integrated into the satellite and carrying out a search on two axes. In parallel, a beacon is activated by one or both terminals to inform the remote system of the coarse direction towards which to point the optical beam before starting the communication process. Figure 63 presents different solution for PAT mechanism.
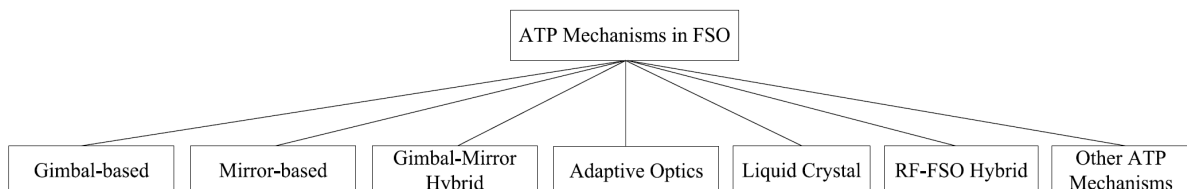
FIGURE 63: CLASSIFICATION OF ACQUISITION, TRACKING, AND POINTING MECHANISMS IN FSO COMMUNICATIONS ACCORDING TO THEIR WORKING PRINCIPLE [28].

For instance, a gimbal-based solution is capable of rotating in most directions to provide a wide pointing range of the incident light beam to the receiving terminal and several alternative technological solutions are provided in ground-to-satellite and satellite-to-satellite communications [35]. Figure 64 shows for instance the gimbal-based solution block diagram of a PAT system.
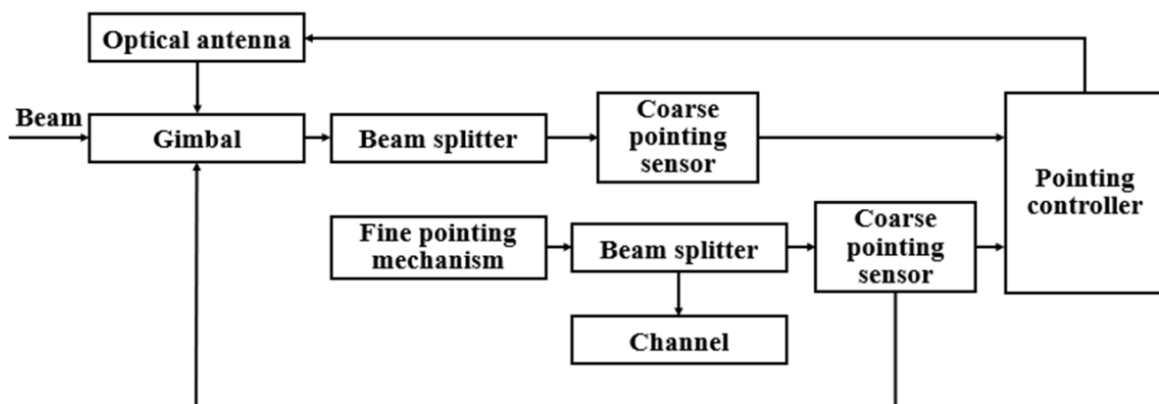

FIGURE 64: PAT BLOCK DIAGRAM [21].

Alternatively, tracking the beacon or the optical communication beam can be done with mirror-based solution as a fast orientation mirror to follow the exact position of the other terminal during their mutual movements.

The main difficulty is an emitted optical beam diameter (beacon) at the receiving terminal much smaller than the reception estimation zone, mainly due to atmospheric disturbances, azimuth or elevation errors, bad mechanical resonances orientation control servo motors, poorly controlled inertial movements, etc. Figure 65 shows an example of an acquisition protocol for a LEO-GEO link.
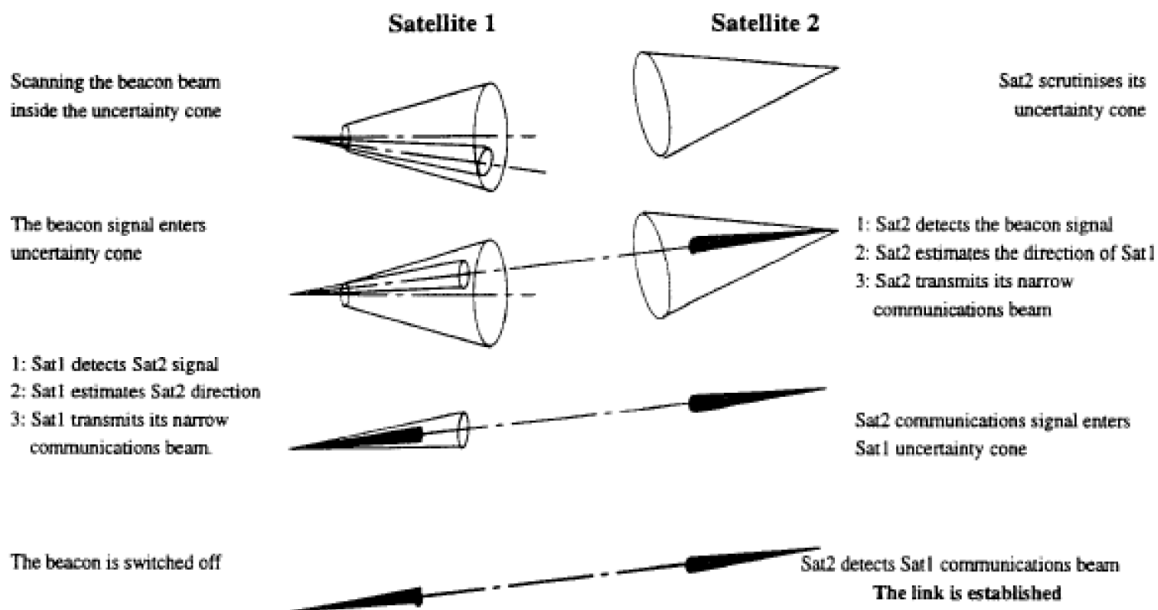
FIGURE 65: EXAMPLE OF THE ACQUISITION PROCEDURE [23].

In this example, a laser emits a beacon to the remote terminal assumed to be in the reception estimation area. It must have a large angular divergence (to minimize the acquisition time) and a high power (from 1 to 20 Watt with Optical Amplifier for instance) to reach large distances. At the same time, the remote terminal uses in reception a detector with a wide Field of View (FoV) whose angle is, in principle, greater than the angle of the estimation zone. This detector can be a CCD camera, for example with a generally low sampling frequency or FPS (Frame Per Second) and high sensitivity to the emitted wavelength spectral band. Generally, this first process for an Optical Inter-Satellite Link (OISL) must be less than 60 seconds including the three phases: Acquisition, Pointing and Tracking (PAT).

For instance, during inter-satellite or inter-orbit optical communication, one scenario considered is that each satellite continuously sends a communication beam to the distant satellite to improve pointing accuracy. This coarse pointing can be performed using a control loop (Frequency around 10 Hz for instance). It is possible to use one or more lasers to generate the signalling beacon, either operating at the communication wavelength, or with different wavelengths. When this acquisition sequence (Acquisition) is finalized, the transmitter switches from coarse pointing mode to fine pointing mode (Pointing). In the case of the fine pointing control loop, the bandwidth should have a higher frequency, order of 1 kHz. This function measures the angular error between the direction of the incoming and outgoing beams and this difference is used as feedback for pointing. There are two types of angle error sensors: CCDs arrays and quadrant photodiodes (QPDs). Depending on the scenario considered, the relative speed of the two terminals which can have very high values, the target is the maximum angular speed that the pointing device is able to reach. When the link is established, the satellites still potentially experience vibrations or misalignments. This leads to a degradation of optical link budget following the elevation and/or azimuth pointing error which is corrected mechanically and/or by software (Tracking). Due to the important role of the PAT system, much work is still undertaken to optimize latency, size, weight, energy consumption and cost.

6.4 STANDARDS

6.4.1 Communication Protocol

First standardized and commercial OWC products was provide thanks to Infrared data association (IrDA) in the 1990s. Then, start in 1997, IEEE 802.11 defined data transmission over infrared spectrum with 2 Mbps data rate but with few commercial products.

In 1999, LEDs interest for communication led to standards in Visible Light Communication (VLC) with IEEE 802.15.7, IEEE 802.15.13, and ITU-T G.9991 (also known as G.vlc). On the other hand, the Japan electronics and information technology industries association (JEITA) published two VLC standards, namely the JEITA CP-1221 and JEITA CP-1222 in 2007. IEEE 802.15.7 2011 revision was proposed by including infrared and near ultraviolet wavelengths (in addition to visible light), and Optical Camera Communications (OCC) specifications for positioning and broadcasting by using led and camera on smartphone.

The IEEE 802.15.7 is an available standard since 2016 with a physical layer (PHY) and medium access control (MAC) sublayer for short-range optical wireless communications (OWC) in optically transparent media using light wavelengths from 190 nanometer (nm) to 10000 nm. The standard can deliver data rates sufficient to support audio and video multimedia services. It also accommodates optical communications for cameras (OCC) where transmitting devices incorporate light-emitting sources and receivers are digital cameras with a lens and image sensor like smartphone device.

The IEEE 802.15.13 Multi-Gigabit/s Optical Wireless Communications Task Group defines a PHY and MAC layer using same wavelengths spectrum band. The standard can deliver data rates up to 10 Gbit/s at distances in the range of 200 meters unrestricted line of sight. It is designed for point-to-point and point-to-multipoint communications. Work on LiFi was continued in 802.15.13 since March 2017. The standard is finalized since 2021, with HHI, pureLifi and ETRI as main actors.

To introduce LiFi to the market, IEEE 802.11 (WiFi) created, in 2017, a new study group, IEEE 802.11bb (TGbb) proposed by HHI, pureLiFi, Oledcomm, Mediopol University and Bims Laboratories. The general scope for this TG is defined by:

- Uplink and downlink operations in 800 nm to 10000 nm band,
- All modes of operation achieve minimum single-link throughput of 10 Mb/s as measured at the MAC data service access point (SAP),
- Interoperability among solid state light sources with different modulation bandwidths.
- Hybrid coordination function (HCF) channel access,
- Overlapping basic service set (OBSS) detection and coexistance,
- Existing power management modes of operation (excluding new modes),
- The project also addresses the security of the transition between the new LC PHY and the existing 802.11 PHYs as well as the security implications in supporting Fast Session Transfer.

In parallel, new products have been proposed based on ITU-T G.vlc standard. This is an high speed indoor communication transceiver with physical layer and data link layer specification. This standard is approved since 2019 and proposed by Huawei, Max linear, Lucibel, Nokia, HHI, CAICT and Signify, mainly for networking wireless indoor communication.

In addition, 6G is currently at the level of discussions by many standardization bodies. Thus, the specification of use cases, technical challenges and potential solutions is not yet finalized. The 3rd Generation Partnership Project (3GPP) has initiated working groups (eg, SA1, SA2, RAN1, RAN2, RAN3) for the integration of satellite access network and Optical Inter satellites Link (O-ISL) into next generation communication technologies. Similarly, the European

Telecommunications Standards Institute (ETSI) has launched a working group named SCN TC-SES which works on the integration of drones and satellites. ITU-R is designing key elements for satellite and NTN integration with 5G.

But currently, there is no specific protocol or standard defined for OSC. Given the early stages of development for optical communication systems, both policy and regulatory approaches are still evolving. In the policy realm, there is an initial draft CCSDS Pink Book in process (CCSDS 141.0-P-1.1) with a goal to facilitate interoperability and cross-support between different communication systems. There is also an optical communication Working Group (WG) with NASA and ESA participation.

6.4.2 Regulatory

Up to now, optical frequencies are unregulated, unlike RF systems which require a licensing process to be able to communicate with a spacecraft. Lasercom interference is not currently coordinated by a regulatory body (like the ITU or NTIA in RF) for two major reasons:

- Laser communications is highly directional, which makes interference unlikely, due to the narrow divergence of the transmitting beam and corresponding small beam footprint at the receiver.
- Up to now, the small number of laser communications systems currently deployed doesn't warrant a complex coordination body like ITU.

6.5 PROPAGATION

The main advantages of OSC links face to microwave/radio links are low gain (telescope) antennas, lightweight terminals, highest data rates with low signal strength, no interference with other transmission systems. Another benefit is a wider bandwidth and narrower beamwidth; with positive and negative aspects: if interference and background noise are reduced, unfortunately the pointing acquisition and tracking (APT) system becomes more complex.

Possible applications of free space optical links are ISL in satellite networks, links for deep space missions, links between UAVs, for HAPs and data links from GEO, MEO, LEO satellites to earth ground stations (OGS).

Space applications are divided into free-space optical links in the troposphere (e.g., uplink and downlink between Earth and satellite) and FSO links above the troposphere (e.g., inter-satellite optical links). Links through the troposphere are primarily influenced by weather conditions similar but not equal to terrestrial FSO links. Inter-satellite optical links are not influenced by weather conditions, as the orbits of the satellites are above the atmosphere.

Compared to the propagation of microwave and RF waves, the transmission of an optical wave through the atmosphere suffers from various negative effects. As shown in Figure 66, atmospheric effects can be divided into two main groups: attenuation effects and refractive index effects.
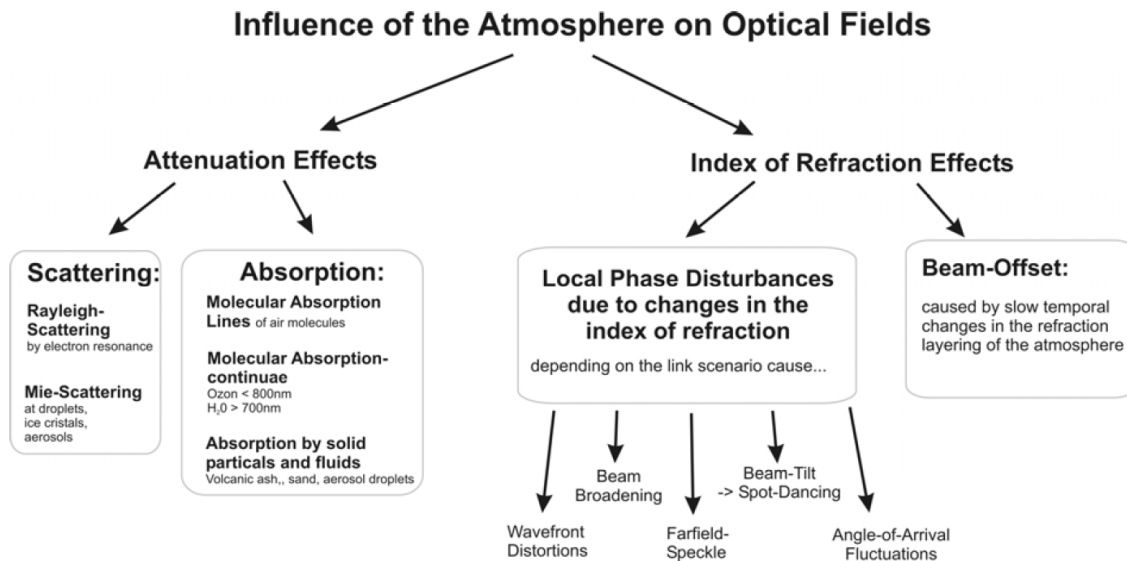
FIGURE 66: OVERVIEW OF ATMOSPHERIC EFFECTS [29].

The level of attenuation effects for a given scenario can be predicted relatively well while variations in refractive index due to turbulence are random and difficult to evaluate. In particular, the different effects of turbulence on the laser beam are:

- Wavefront distortion: successive phase distortions along the path make the beam less and less coherent. Large tilts of the wavefront are called fluctuations in the angle of arrival.

- Beam Broadening: As a result of the deflected light, beam broadening increases the radius of the beam and thus reduces the average intensity.

- Redistribution of the intensity within the beam: the propagation of the deformed wave front leads to destructive and constructive interferences which break the intensity profile of the beam.

- Beam Centroid Wandering: This is caused by turbulent cells larger than the beam radius. The beam is then redirected and drifts on a "medium" optical axis.

Note that for the tropospheric uplink beam, the diameter becomes noticeably wider due to the rapid variation of refractive index with height, causing the optical beam to bend away from the normal. A similar but milder effect is experienced by the tropospheric downlink beam.

Another atmospheric effect related to the refractive index is the beam shift caused by the stratification of the atmosphere. This is especially important for uplinks and downlinks at large zenith angles.

To predict attenuation through the atmosphere, the molecular composition of the atmosphere must be studied and modelled. A strong height dependence of the attenuation can be observed. Regarding the effects of turbulence, several theories have been developed to characterize the distorted beam wave. On the other hand, not all communication systems are equally sensitive to wave distortions. For IM/DD systems, the signal is carried only by optical power and therefore phase distortions are less significant. For coherent systems, however, phase distortions significantly reduce system performance.

Like RF system, the first step is to define a link budget, which determines the quality of the link under certain given weather conditions. For outdoor communication, weather conditions such as fog, clouds, scintillation, snow are more less considering. Due to the distance, atmospheric and molecular attenuations (water, carbon dioxide, ozone molecules) are also having to be

taking account with a better deterministic approach. So, the link margin could be mainly expressed by emitted power (Pe), received sensitivity (Sr), power losses in an optical system (Sl: lens, filter…), geometrical/alignment losses (Al), atmospheric loss, etc.

Figure 67 shows an example of 10 Gbps LEO link budget.
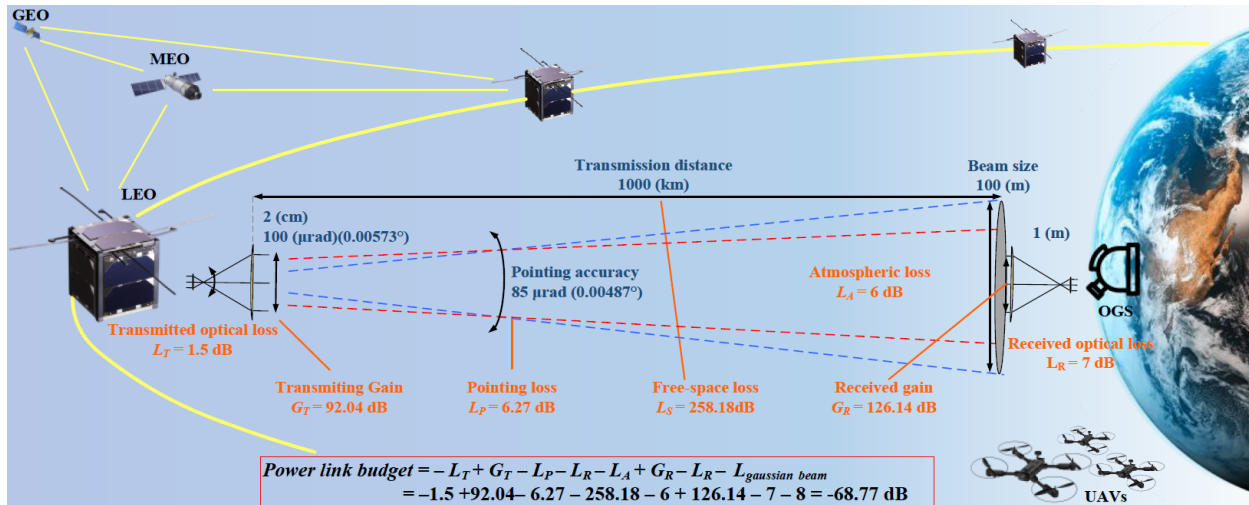
FIGURE 67: LEO LASER OPTICAL COMMUNICATION POWER LINK BUDGET [30].

6.6 QUANTUM COMMUNICATION

Advances in quantum computing offer opportunities far beyond current information and communication technologies, as quantum algorithms could break the security of public-key cryptographic standards currently in use. The operating principle of Quantum Key Distribution (QKD) protocols requires dedicated optical and photonic systems (transmitters and receivers able of generating and measuring quantum states, especially for DV-QKD, Discrete Variable QKD which are very specific). Their technological maturity has steadily increased and continues to increase, and several commercial solutions are available today, at a significant cost. Worldwide efforts are trying to miniaturize this technology to drastically reduce the cost. Currently, quantum communication can be carried out over optical fibers over a distance that, usually, does not exceed a few hundred kilometers because quantum signals cannot be amplified, and their intensity decreases exponentially and is then disturbed by noise. Use of different concepts of quantum repeaters can improve the range.

A conceptual diagram (Figure 68) of quantum technology platform including future quantum networks is proposed by NICT (Japan), Quantum ICT Collaboration Center.

In comparison to fiber links, free-space links are much more interesting for the loss value versus possible range ratio (Figure 69), so the great interest of space quantum communication segments.
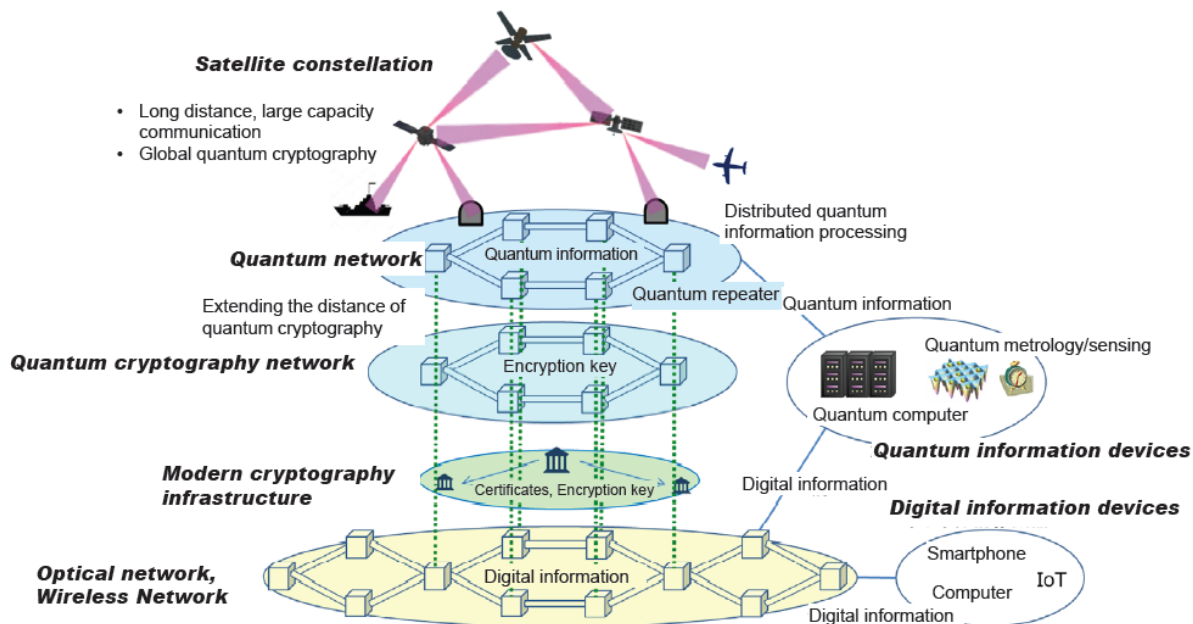
*FIGURE 68: GENERAL VIEW OF FUTURE QUANTUM NETWORKS [31].*
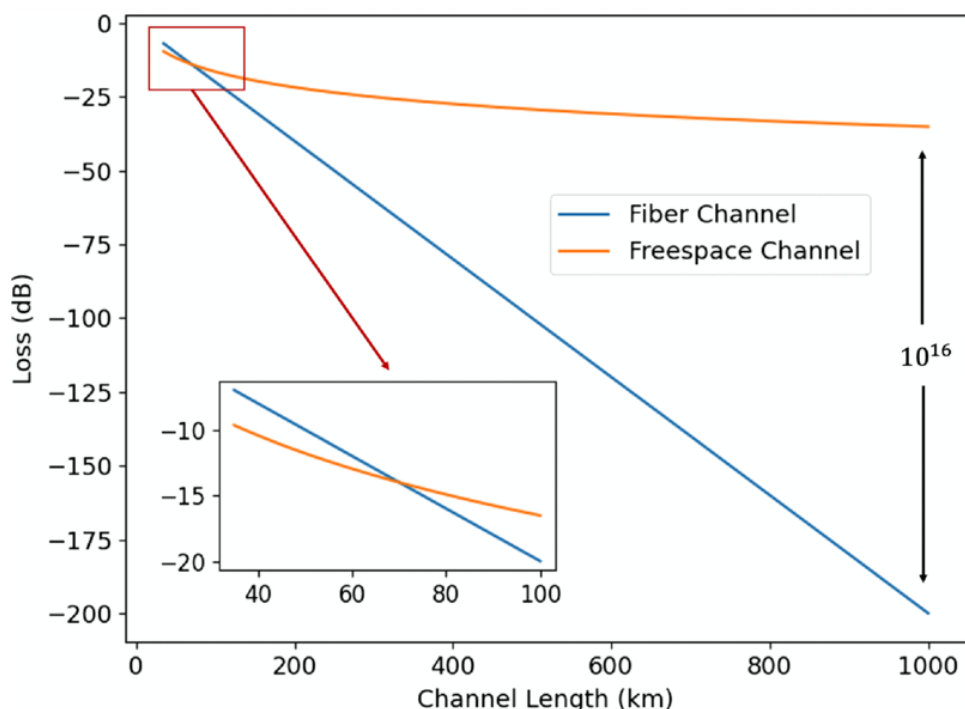
FIGURE 69: TYPICAL LOSSES IN FIBER AND FREE-SPACE CHANNELS [32].

In the field of quantum optical communication by satellite (Sat-QKD), several studies and experiments have been carried out:

➲ The Matera Laser Ranging Observatory demonstrates sensitivity at the single photon level by exploiting corner retroreflectors mounted on a satellite [41].

➲ From a mobile platform, the first experiments were carried out with a quantum transmitter installed in an airplane and the receiver installed in the optical ground station Oberpfaffenhofen of the DLR [42].

➲ Another space-to-ground communication was carried out with SOCRATES satellite (Space Optical Communications Research Advanced Technology Satellite) of NICT (Japan). LEO-to-ground polarization measurements aiming for later space QKD was performed [43].

➲ The Chinese Academy of Sciences has achieved, with Micius satellite, a QKD downlink with different ground stations allowing the exchange of cryptographic keys between Asia and Europe with entanglement based QKD over 1200 km [44].

➲ The European Space Agency (ESA) piloted the launch of the SAGA project to prepare the design of the EAGLE-1 QKD satellite.

➲ And several national aerospace agencies are also undertaking the construction of Sat-QKD demonstrators, for example QUBE (Germany), QEYSSat (Canada), QT Hub (United Kingdom) and SpeQtral (Singapore) [45].

Several protocols exist, such as entanglement based or measurement-device-independent, but the oldest and most widely studied protocol is the BB84 (Prepare-and-Measure - PM) protocol.

However, Sat-QKD terminals must meet the Size, Weight, and Power (SWaP) requirements of satellite platforms. A promising solution for reducing SWaP is the use of integrated photonic chips, which can integrate a complex array of passive and active optical elements (including lasers, phase and amplitude modulators, filters, etc.). A fundamental element is the optic terminal which contains the antenna and the beam steering systems with a modification to accommodate to QKD modules. With respect to the optical budget, the significant transmission loss is related to the divergence of the optical beam (geometric attenuation), then atmospheric scattering and absorption. Coupling, pointing inaccuracy, and internal systems can add losses up to -40dB.

The Sat-QKD operating wavelength should exploit atmospheric transparency windows either in the near infrared band (NIR, around 850 nm), it has slightly higher atmospheric absorption, but with less diffraction losses; or in the C band (around 1550 nm) which makes it possible to use commercial solutions available from conventional fiber optic communication.

Different scenarios are possible for photonic transmission in space constellation configuration (Figure 70).
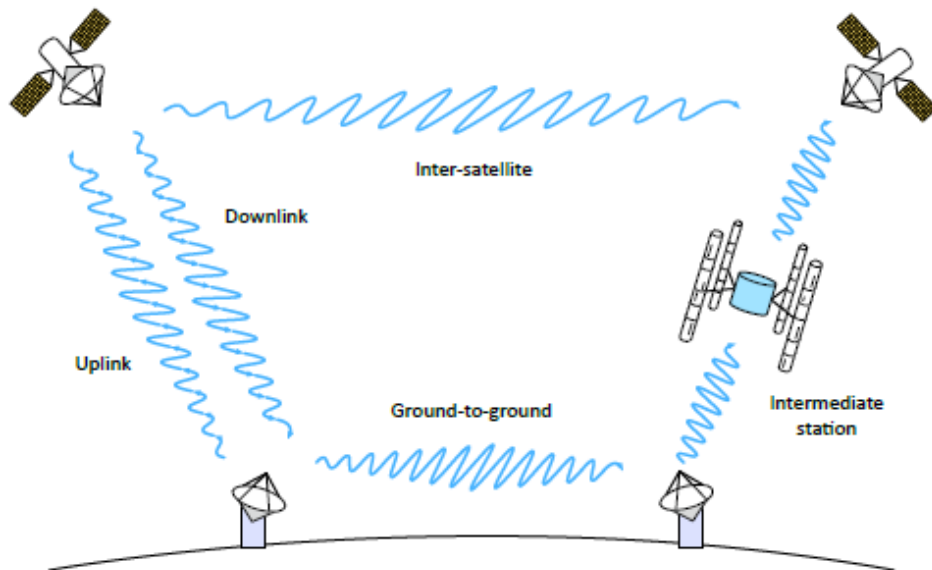

FIGURE 70: OPTICAL QUANTUM COMMUNICATION SCENARIOS [38]

For example, Micius was in downlink scenario and in night-time condition. It is due to lower impact of atmospheric turbulence on the induced broadening and deflection of the light emitted by the satellite at the final part of its path towards receiver. Night operation is preferable to lower background solar light, but is possible only around 30% of the orbit time (around 90 min) for Micius altitude (500 km). Precisely, one-downlink setup was used for QKD and two-downlink setup for entanglement distribution. Moreover, one-uplink setup was tested for quantum teleportation experiment. China also tested QKD from its Tiangong-2 space station [47].

Note that for entangled links between non-line-of-sight ground stations from LEO satellites, a quantum memory will be required, with SwaP requirements especially if cooling is required. Indeed, different quantum memory technologies are already being explored. Terrestrial proof-of-concept tests will be achieved prior to embedded space-qualified modules.

It will be possible to cover different ground stations with inter-linked MEO satellites as depicted in Figure 70.

For use in 5G and beyond NTN situations, the European IRIS^2 project is promising. It will include the EuroQCI initiative space segment with QKD links from specific satellites [48].

6.7 SAFETY

IEC 60825-1 is the main reference applicable for laser safety products (wavelength from 180 nm to 1 mm). In NIR (700 nm − 1400 nm), the predominant consideration is to avoid retinal damage. For wavelengths longer than 1400 nm, the main consideration is to avoid damaging the cornea and the skin, as radiation at those wavelengths is absorbed by water, and the vitreous humor of the eye protects the retina from damage [49]. Several decades of testing and experimentation have made it possible to define several laser classes (from 1 to 4) depending on the uses and applications. The telecommunication products for satellite use cases have no specific restrictions except information class on product.

However, in the US there are three regulatory entities that are concerned with aspects of outdoor laser operations: The FAA, DoD Laser Clearing House (for DoD missions) and the NASA Laser Safety Review Board (for NASA missions).

➱ FAA coordination is required if potentially harmful laser irradiance is transmitted through navigable airspace. This includes prevention of injury as well as potential distraction of pilots by visible lasers. The FAA will most likely only be concerned about transmitters at ground stations because transmitters on spacecraft are hundreds of miles above the highest-flying aircraft and beam dispersion is large enough that there are usually no safety implications. Missions should coordinate with their local FAA service center to get approval, documented with a "letter of non-objection."

➱ The DoD Laser Clearinghouse (LCH) works to ensure that DoD and DoD-sponsored outdoor laser use does not impact orbiting spacecraft or their sensors. That includes both US DoD and foreign assets. LCH and mission operators might enter close cooperation where LCH permits specific laser engagements. The process of coordinating with LCH to get to that point can take many months and should be started as early as possible. However, currently LCH will only engage DoD and DOD-sponsored missions.

➱ NASA's Laser Safety Review Board (LSRB) is focused on personnel safety for all outdoor laser operations. NASA missions prepare safety documentation and submit to LSRB for review before launch. LSRB will also verify FAA concurrence. Further information on

regulations can be found in ANSI Z136.6 "American National Standard for Safe Use of Lasers Outdoors".

6.8 OPTIC VERSUS RADIO (RF)

Optical communication by satellite is of increasing interest to researchers and industrials, probably due to several following advantages. Figure 71 seems to indicate the distinctive elements of optical communication compared to RF, i.e., smaller antennas, lighter mass, and lower power.

Link senario	Data rate	Frequency band					
		Optical		Ka-band		Millimeter-band	
GEO-LEO							
Antenna dia.	2.5 Gbps	10.2 cm	(1.0)	2.2 m	(21.6)	1.9 m	(18.6)
Mass		65.3 kg	(1.0)	152.8 kg	(2.3)	131.9 kg	(2.0)
Power		93.8 W	(1.0)	213.9 W	(2.3)	184.7 W	(2.0)
GEO-GEO							
Antenna dia.	2.5 Gbps	13.5 cm	(1.0)	2.1 m	(15.6)	1.8 m	(13.3)
Mass		86.4 kg	(1.0)	145.8 kg	(1.7)	125.0 kg	(1.4)
Power		124.2 W	(1.0)	204.2 W	(1.6)	175.0 W	(1.4)
LEO-LEO							
Antenna dia.	2.5 Gbps	3.6 cm	(1.0)	0.8 m	(22.2)	0.7 m	(19.4)
Mass		23.0 kg	(1.0)	55.6 kg	(2.4)	48.6 kg	(2.1)
Power		33.1 W	(1.0)	77.8 W	(2.3)	68.1 W	(2.1)
Moon-satellite							
Antenna dia.	155 Mbps	15.7 cm	(1.0)	3.5 m	(22.3)	3.2 m	(20.4)
Mass		100.5 kg	(1.0)	243.1 kg	(2.4)	222.2 kg	(2.2)
Power		144.4 W	(1.0)	340.3 W	(2.4)	311.1 W	(2.2)

FIGURE 71: OSC AND RF COMMUNICATION SYSTEMS WITH TRANSMIT POWER OF 10, 50, AND 20 W FOR OPTICAL, KA AND MILLIMETER BAND SYSTEMS, RESPECTIVELY (VALUES IN PARENTHESES ARE NORMALIZED TO OPTICAL PARAMETERS) [42].

6.9 OSC USE CASE

6.9.1 Use Case Example

There are many constellations project and programs mainly in Medium Earth Orbit (MEO) and Low Earth Orbit (LEO) which have the advantage of low latency and lower power possibility due to the shorter distance compares to orbiting satellites geostationary terrestrial (GEO). Space-X has launched more than 1,892 LEO satellites since May 2019 to establish a global network of broadband satellites under the Starlink program [51]. Amazon has announced its intention to launch more than 3236 LEO satellites, called Kuiper Systems [52]. Laser Light Communications plans to create a 12-MEO constellation satellite network to reach a total capacity of 7.2 Tbps [53]. Analytical Space uses hybrid RF and optical downlinks to provide high-speed, low-latency data transmissions via the LEO data relay network of nanosatellites [54]. BridgeCom intends to create laser communication services based on a worldwide network of optical earth stations [55]. Kaskilo will create a LEO constellation of 288 satellites and will mainly provide Internet of Things (IoT) service for Industry 4.0 [56]. Huawei plans to build a LEO constellation of 10,000 satellites called Massive VLEO for 6G [57]. Many other missions

are planned for CubeSats and micro-satellites like Transcelestial Technologies [58] or Golbriak Space [59].

Applications of space laser communications can be classified into five categories:

1. data download for Earth Orbital missions based on ground-to-satellite links,

GEO data relay,

wideband satcom using 10 thousand class satellites,

all-optical high-speed communications

cybersecurity guaranteed by Quantum Key Distribution (QKD) technologies.

Figure 72 shows a summary of OSC link applications.
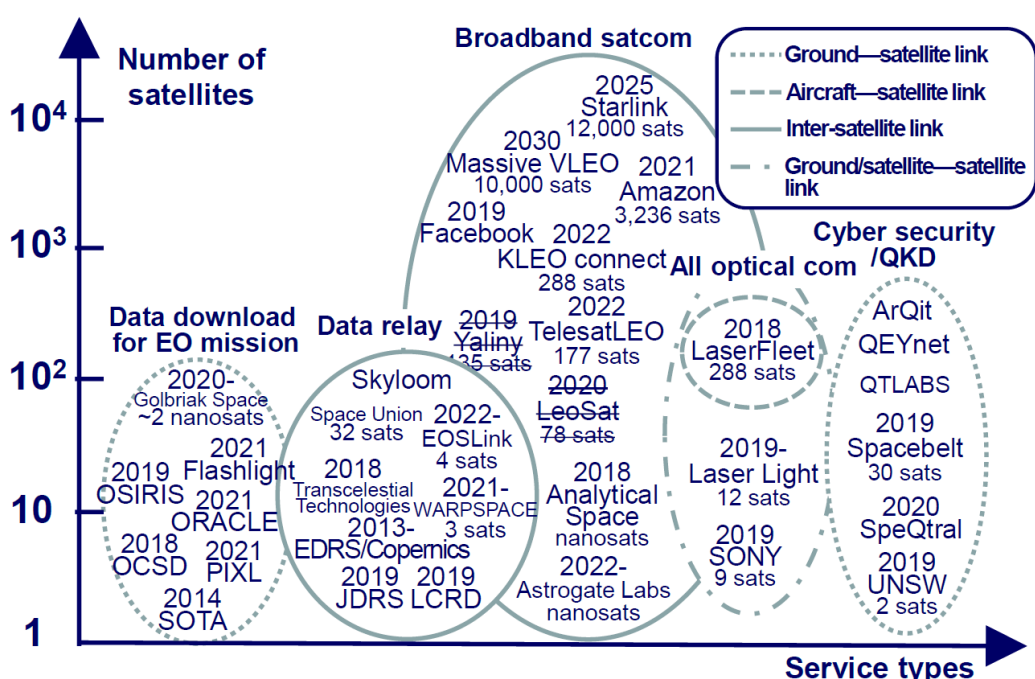
FIGURE 72: APPLICATIONS FOR OSC [17].

6.9.2 Optical Satellite Network

GEO satellites appear stationary to observers on the ground because the satellite rotates synchronously with the Earth. This property makes GEO satellites particularly suitable for communications, streaming or weather monitoring. GEO satellites are attractive because of their coverage as only three satellites can provide global coverage. Optical communications in GEO were primarily developed for data relay from LEO (prime example with ESA EDRS system). New communications satellites may require data rates up to Tbit/s and more for the uplink. Optical links offer this potential throughput with global coverage.

Optical satellite communication has mainly been developed for point-to-point transmission, by LEO links or GEO relays. Radiofrequency satellite networks have been studied for a long time with different constellations in GEO, MEO and LEO [60]. Routing process manages constellation traffic, notifying gateways of traffic congestion or inter-satellite link failures. The design of the switching and monitoring approach between the layers to guarantee a desired QoS (Quality of Service) depends on the number of layers (constellations and satellites per

orbit), the number of inter-satellite links and the available throughput. It is now possible to envisage a combination of radiofrequency and optical links to deal with all possible applications.

Optical LEO satellite constellations are available due to short lead times, optimized power budgets and closer distances to MEO and GEO. But the satellite-to-ground pointing accuracy is limited due to the larger pointing angles. Typically, 5 to 10 times greater beam divergence is expected for LEO communications than for GEO. The main disadvantage is therefore a decrease in received power, leading to similar transmitted power requirements for LEO and GEO, with current technologies. This constraint is less during inter-satellite optical communication, but the APT device must be more precise and faster. GEO satellites are more expensive to develop and deploy, due to the greater launch distance and higher radiation requirements. On the other hand, the advantage is wide coverage but less availability due to the properties of the atmosphere.

An optical global network would be a combination of the three orbits (as shown in Figure 73), optimizing QoS and combining several applications.
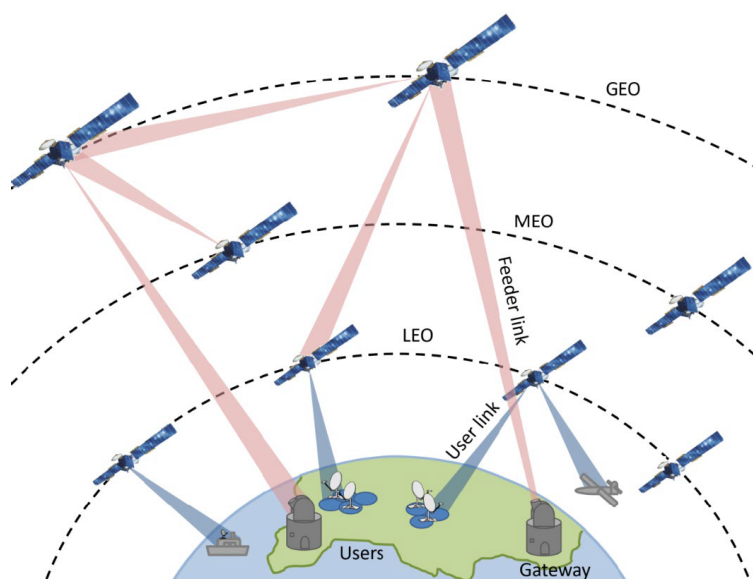

FIGURE 73: OPTICAL SATELLITE-COMMUNICATIONS NETWORK [53].

A system combining variety of applications may need to combine a mesh configuration with constellations of satellites. Figure 74 shows a satellite network concept. The development of ad hoc satellite platforms, for backhauling and switching between the ground and the GEO for example, would make it possible to increase the data rate of the feeder links. In this case, the GEO platform could integrate signal regeneration (error correction algorithms protecting the data through atmospheric turbulence.) and optical switching to other application-oriented satellites (MEO or LEO).

Satellites at shorter distances can be easily connected to optical links with limited power requirements and carrying high data volumes. Other dedicated platforms can connect other GEO nodes over large distances, for instance between Europe and Asia or to LEO constellations. Optical frequencies could be best candidates for such networks because they are more mass and power efficient, also more resistant to interference and this give alternative solution face to RF spectrum bottleneck. However, a combination of optical and RF technologies is required to meet the requirements of such a variety of applications.
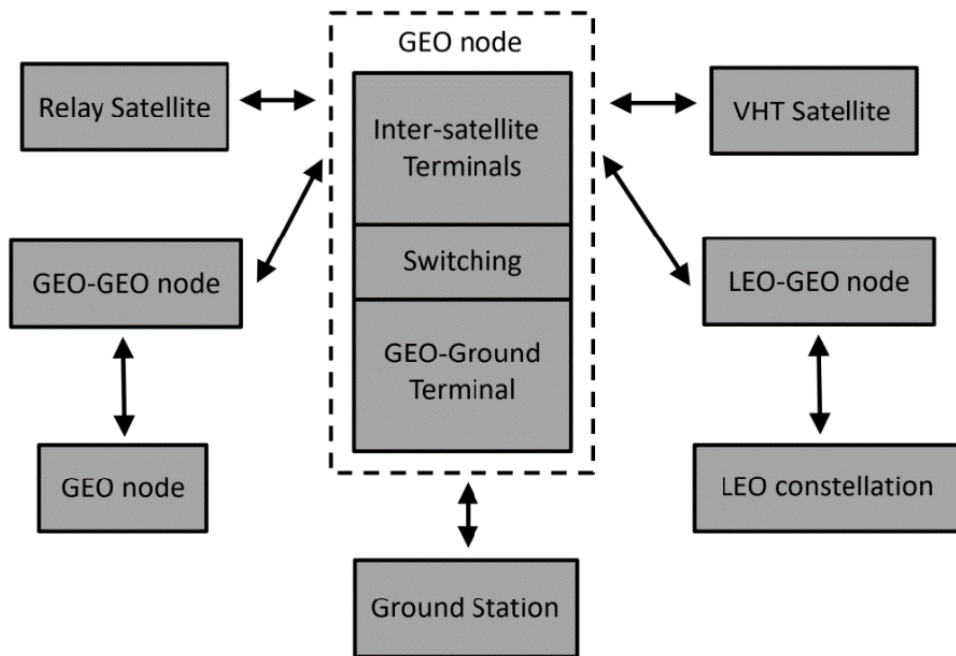
FIGURE 74: CONCEPTUAL BLOCK DIAGRAM FOR AN OPTICAL SATELLITE NETWORK [54].

6.9.3 Space Air Ground Integration Network (SAGIN)

SAGIN concept integrated satellite links, aviation system and ground communication network. SAGIN's vision requires a multi-level approach and includes space, air and ground network elements: a) ground center design, (b) air center design, (c) satellite center design, (d) and SAGIN communication global control center. As shown in Figure 75 this network (or network of networks) is consisting of GEO, MEO, LEO, aerial (airships, UAVs, HAVs) and ground devices (WLAN, LoRan, WiMAX, 4G, 5G…), which makes the integration of whole communication networks possible. Future communication networks target is to build an integrated network framework (SAGIN) and realize the interconnection, complementarity and efficient coordination between Space, Aerial, and ground Network.

➲ Satellites: It is very likely that several satellites (GEO, MEO and LEO) will use optical beam. Multi-layer satellite (intraplane and interplane) communication must improve service availability and therefore resilience. For this, Acquisition, Pointing, Tracking (APT) functions still need research and study work.

➲ Aerial: High Altitude Platforms (HAPs) can have an intermediate role and operate seamlessly in continuous collaboration with Low Altitude Platforms (LAPs) such as drones to provide improved latency.

➲ Ground: Ground communication system is mainly defined by LoRaWan, Wi-Fi and 2G, 3G, 4G, 5G technologies and 6G technology before 2030. Device-to-device connectivity, IoT and peer-to-peer networking are the basis of these solutions.

This integrated network includes the integration of system, terminal, and application, and it help the network layer protocol realize the interconnection (or Interplane and Intraplane switching – for instance by using protocol IEEE 1905 [63] or Ethernet) of the whole network and achieve compatibility between systems. An efficient routing process is essential to achieve effective and low latency communication and work has been done to integrate FSO and optical communication [64] and [65].
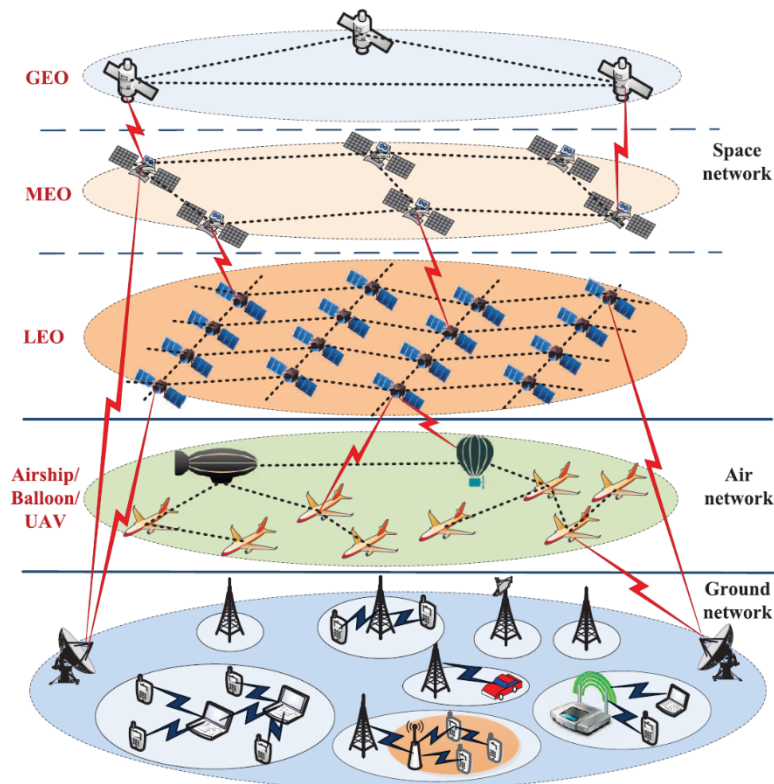
FIGURE 75: SAGIN EXAMPLE [51].

6.10 OSC AND FUTURE TREND

OSC technology development is now on operational phase and due to the laser beam small divergence angle, the current satellite optical communication links are point-to point transmission. Space optical communication, with its advantages of high speed, small size, lightweight and low power consumption, has become an effective approach to high-speed communication between satellites, especially in the application of small satellites. Face to limited onboard resources (payload) for satellite communication systems, optical solutions offer an attractive approach as shown in Figure 76 these potentialities are a low onboard resource need, including energy consumption, in relation to the potential throughput.

Additionally new research area is explored. Such as Quantum key Distribution, QKD is a protocol that shares a secret cryptographic key through entangled photons. Sources and optical front ends have been development for transmitting these keys from small satellite spaceborne platforms [67] and [68].

Deployable Optical Receiver Aperture (DORA) project is developing a OSC 1 Gbps full duplex [69] large apertures in space. The inter-spacecraft optical communicator (ISOC), which includes arrays of fast photodetectors and transmit telescopes to provide full-sky coverage, gigabit data rates and multiple simultaneous links, was initially developed at NASA's Jet Propulsion Laboratory with funding from NASA's Small Spacecraft Technology (SST) program from 2018 to 2020.

There are also currently several (Inter satellites Optical Communications (ISOC) for short-, mid-, and long-range applications that use appropriate levels of power and aperture size,

respectively, to achieve Gb/s data rate [70]. A new O-ISC version is currently developed by Chascii Inc. for cislunar applications. Major programs, such as European Data Relay System use small satellites in low-Earth orbit is to form an intersatellite link to geosynchronous orbit. NICT (Japan) is looking to establish this type of link with a CubeSat through the CubeSOTA program [71].

In addition to CubeSat terminals, larger terminals for larger SmallSats are under development by Tesat, Mynaric [72], SpaceMicro [73], and SA Photonics.

DARPA has funded the Space-BACN program that seeks to develop a reconfigurable and multi-protocol inter-satellite OSC that can be supported on small satellites.

The use of WDM and coherent detection paves the way for an explosion of capabilities. Thus, to further expand the satellite network with optic solution, it is judicious to look after point-to multipoint or multi point to point solutions with one global protocol and more advanced technologies.

Operator needs will be sensitive to transparent services as envisaged in a SAGIN solution. Services centered around Extremely Enhanced Mobile Broadband (eeMBB), Extremely Reliable Low Latency Communications (eRLLC), and Ultra-Massive Machine Type Communications (umMTC) need to be improved. Augmented Reality (AR) and Virtual Reality (VR) sensitive broadcasts must contend with proactive content caching or high throughput techniques. OSC solution has a card to play.
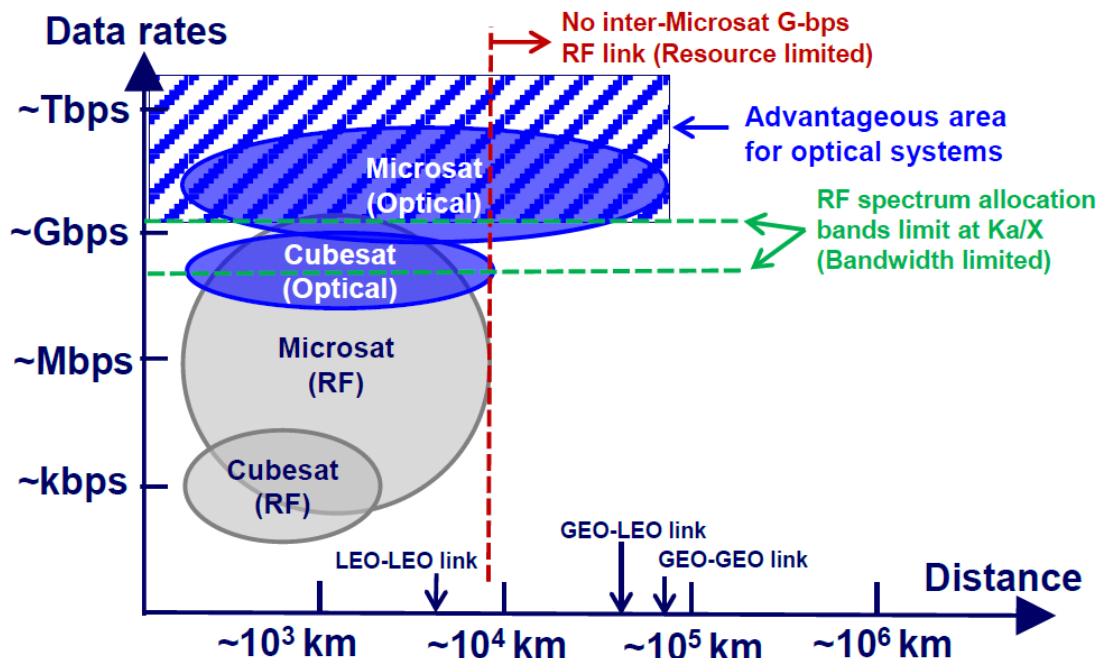

FIGURE 76: OSC POTENTIAL DATA RATE AREA (FOR MICRO-SATELLITES) [17].